# PETROLOGY OF ULTRAMAFIC ROCKS FROM CONICAL SEAMOUNT BASED ON *ALVIN* SUBMERSIBLE AND OCEAN DRILLING PROGRAM STUDIES

A THESIS SUBMITTED TO THE GRADUATE DIVISION OF THE UNIVERSITY OF HAWAII IN PARTIAL FULFILLMENT OF THE REQUIREMENTS FOR THE DEGREE OF

MASTER OF SCIENCE

IN

GEOLOGY AND GEOPHYSICS

MAY 1991

By Kristine L. Saboda

Thesis Committee:

Patricia Fryer, Chairperson
Kost Pankiwskyj
Mike Mottl

We certify that we have read this thesis and that, in our opinion, it is satisfactory in scope and quality as a thesis for the degree of Master of Science in Geology and Geophysics.

THESIS COMMITTEE

Patricia Fryer
Chairperson

Michael J. Mottl

Kostantin Wawinsky

## ACKNOWLEDGMENTS

I would especially like to thank Dr. Patricia Fryer for providing moral and financial support during the course of this project. Patty's "pep" talks kept me going many, many times when I seemed to hit the "brick wall". Thanks are also due to the various members of my ever changing committee over the past years---Mike Mottl, Kost Pankiwskyj, John Mahoney, Gerard Fryer, Paul Lucey, B. Ray Hawke.

Thanks also to the scientists and crews of the various cruises that collected the data used in this project---*R/V Atlantis II, R/V Fred Moore, R/V Sonne, R/V Resolution*, and most especially Laura Stokking, Peter Stoffers, and Janet Haggerty. Neverending moral support was provided by fellow graduate students ---Wendy, Beth, Ron, Gerald, Martha, Nancy and Sylvia.

This project could not have been completed without the help and support of Karl, Joan, Karen, David, Kathylynn, Dave, Kirk, Kathy, Erik, Brian, Elizabeth, Kevin, Christopher, Emily, Vivian, and most especially Dad.

This research was supported by NSF Grants OCE8411717 and OCE8614191 and a grant for shore-based science related to ODP 125 from USSAC.

". . . AND THERE WAS MUCH REJOICING------yeaaaaaaaaa. . ."

## ABSTRACT

The ultramafic rocks recovered from *Alvin* and Ocean Drilling Program studies on Conical Seamount are clasts of variably alteration and metamorphosed harzburgite and dunite, both of which exhibit little original compositional variation. Stratigraphic relationships among the rocks within the drill holes are subtle and mainly reflect variations between the degree of alteration and metamorphism of the rocks within each hole. Examinations of fluid compositions and serpentine muds in which the ultramafic clasts are entrained provide strong evidence that serpentinization reactions are occurring *in situ* in the seamount.

The ultramafic rocks that form the clasts in the serpentine muds of Conical Seamount represent a depleted supra-subduction-zone mantle affected by very low- to medium-grade metamorphism. Metamorphism took place as a consequence of interaction with fluids generated by dehydration of the subducted slab, both in the source region and in the body of the edifice. Subtle variations in mineral content of the rocks are consistent with interpretations of periodicity of activity associated with formation of serpentine mudflows on the flanks of Conical Seamount.

# TABLE OF CONTENTS

# LIST OF TABLES

## LIST OF ILLUSTRATIONS

# INTRODUCTION

The Mariana arc-trench system, the easternmost of a series of backarc basins and intervening remnant arcs that form the eastern edge of the Philippine Sea Plate (Figure 1), is well known as a classic example of an intraoceanic convergence zone. Its evolution has been studied by numerous investigators over nearly two decades (e.g. Karig, 1971; Uyeda and Kanamori, 1979; LaTraille and Hussong, 1980; Fryer and Hussong, 1982; Mrosowski et al., 1982; Hussong and Uyeda, 1981; Bloomer and Hawkins, 1983; Karig and Ranken, 1983; McCabe and Uyeda, 1983; Hsui and Youngquist, 1985; Fryer and Fryer, 1987; Johnson and Fryer, 1988). The Mariana forearc has undergone extensive vertical uplift and subsidence in response to seamount collision, as well as tensional and rotational fracturing associated with adjustments to plate subduction and to changes in the configuration of the arc (Hussong and Uyeda, 1982; Fryer, et al., 1985). Serpentine seamounts, up to 2500 m high and 30 km in diameter, occur in a broad zone along the outer-arc high (Fryer, et al., 1985, Fryer and Fryer, 1987). These seamounts may be horsts of serpentinized ultramafic rocks or may have been formed by the extrusion and buildup of serpentine muds. Conical Seamount, one of these serpentine seamounts, is located within this broad zone of forearc seamounts, about 80 km from the trench axis, at about 19$^{o}$30'N (Figure 2). The seamount is approximately 20 km in diameter and rises 1500 m above the surrounding seafloor. *Alvin* submersible, *R/V Sonne* bottom photography, seismic reflection, and SeaMARC II studies indicate that this seamount is composed of unconsolidated serpentine muds that contain clasts of serpentinized ultramafic and metamorphosed mafic rocks, and authigenic carbonate and silicate minerals (Saboda, et al., 1987;

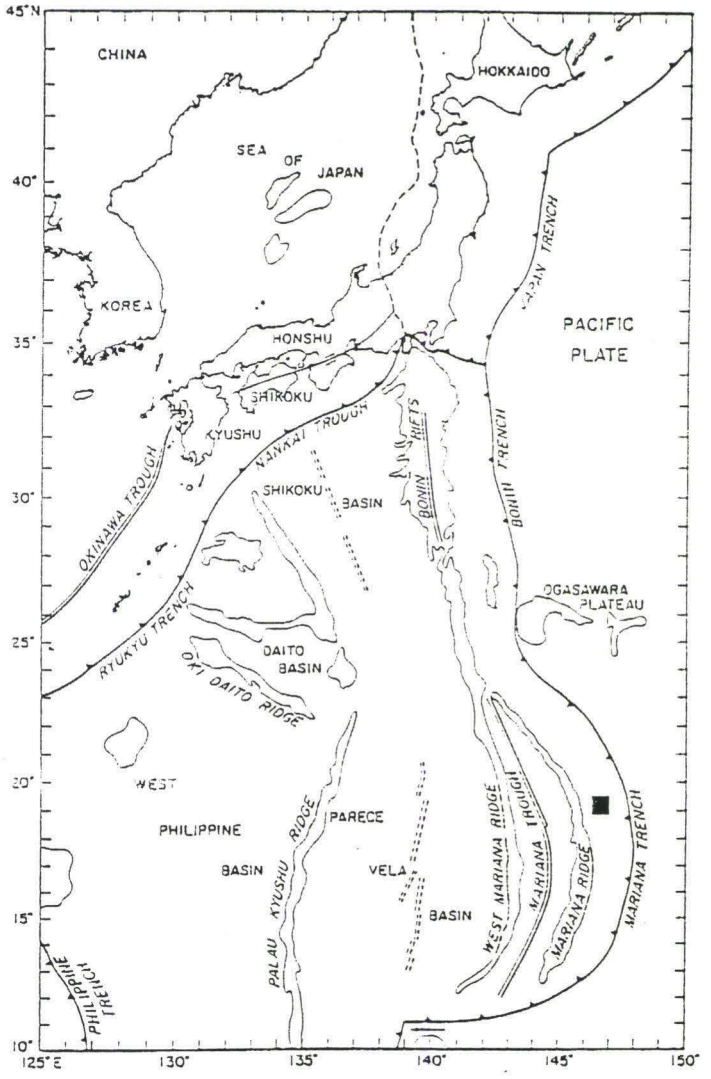


Figure 1. Bathymetry and geologic features in the Philippine Sea region. Basins and ridges are outlined by the 4 km bathymetric contour, except for the Izu-Bonin arc, West Mariana Ridge, and Mariana arc, which are outlined by the 3 km contour. Barbed lines locate subduction zones; medium double lines locate active spreading centers; dashed double lines locate relict spreading centers; solid square locates Conical Seamount (Fryer, et al., 1990).

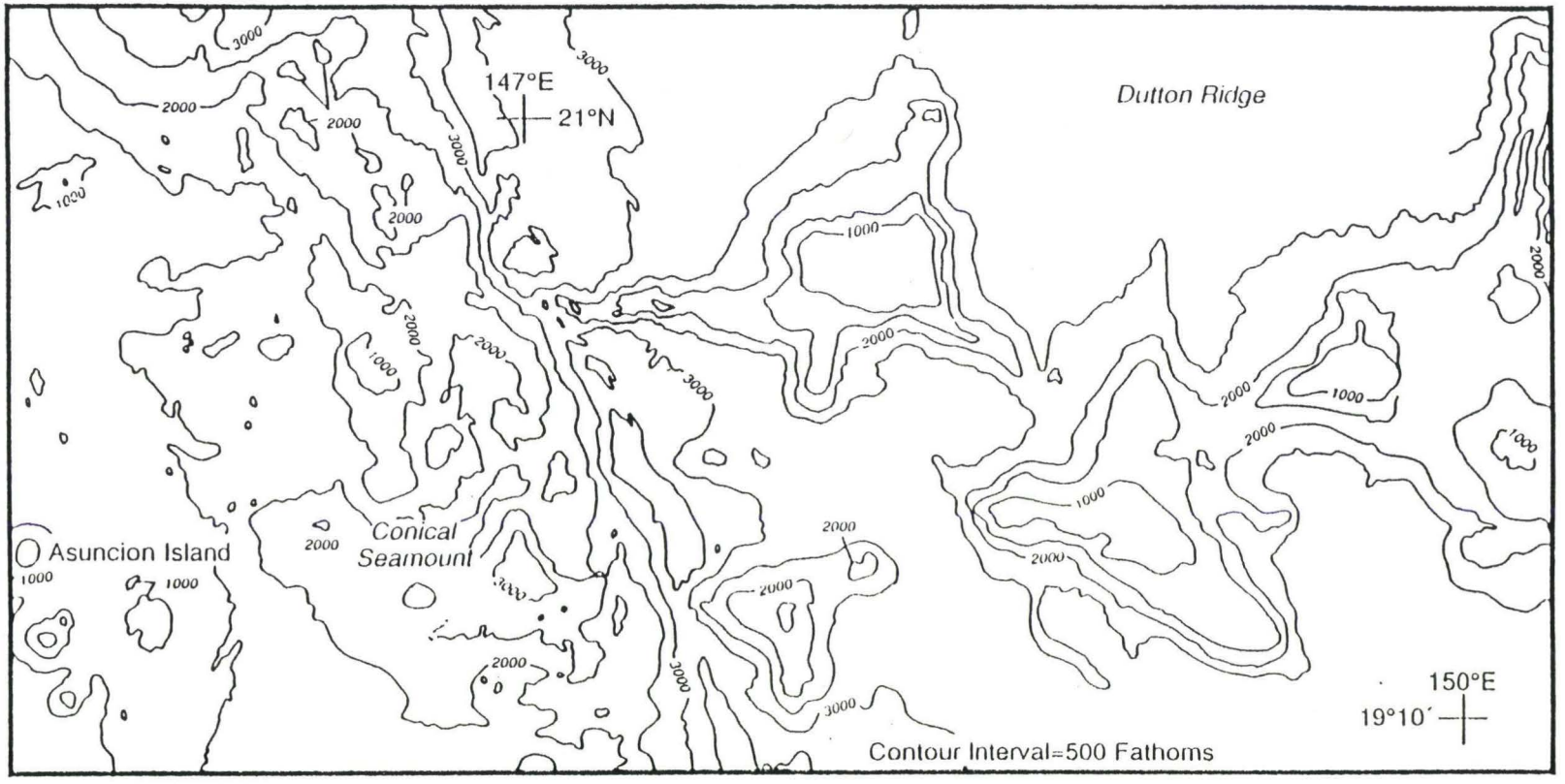


Figure 2. Map of Mariana outer forearc showing nearby regional bathymetry, from U.S. Navy SASS data. Contour interval is 500 fathoms (Fryer and Smoot, 1985).

Haggerty, 1987b; Fryer, et al. 1990). During Leg 125, scientists drilled three sites (two flank sites and one summit site) on Conical Seamount to investigate the origin and evolution of the seamount. This was accomplished directly by studying the composition and structure of the muds of which it is composed and indirectly by studying the composition and textures of the ultramafic rocks from which the muds most likely were derived.

The following thesis is a synthesis of work done on Conical Seamount on board the *R/V Atlantis II* (summer 1987), the *R/V Sonne* (summer 1988), and the *R/V Resolution* (spring 1989). This study presents the petrology and geochemistry of the ultramafic clasts recovered from this seamount in addition to a brief summary of the various cruise results. An analysis of serpentine flow types and features based on bottom camera photography is also presented.

## BACKGROUND

Studies of the origin of serpentine seamounts in the Mariana forearc region have direct application to interpretation of subaerial exposures of serpentine in former convergent margin terrains. Deposits of "sedimentary" serpentine similar to the deposits formed on the flanks of the Mariana serpentine seamounts have been described from numerous locations on land in former convergent margins (Lockwood, 1971; Phipps, 1984; Lagabrielle, et al., 1986). The mechanism of emplacement of some of these subaerially exposed deposits has been compared with that of the Mariana seamounts (Carlson, 1984).

Several of the seamounts on the outer half of the Mariana forearc that have been sampled consist of serpentinized ultramafic rocks and minor amounts of metagabbros, metabasalts, and metasediment (Bloomer 1982; Bloomer and Hawkins, 1983; Fryer, et al., 1985; Fryer and Fryer, 1987; Saboda and Fryer, 1987; Johnson and Fryer, 1987; Fryer, et al., 1990; Johnson, 1990). These results indicate that the seamounts were formed by diapiric intrusion of serpentinized ultramafic rocks into crustal levels within the eastern half of the forearc (Hussong and Fryer, 1981; Bloomer, 1982; Bloomer and Hawkins, 1983). A diapiric origin of these seamounts implies that the rocks represent materials entrained within a rising serpentine body. The metamorphic processes occurring both at depth and within the individual edifices can be investigated by examining the rocks. These rocks also give an indication of the nature of the mantle and crust through which they rise.

The best studied of the Mariana seamounts are those near 19$^{o}$30'N (Figures 3A and 3B). Dredging at the summit of these seamounts yielded

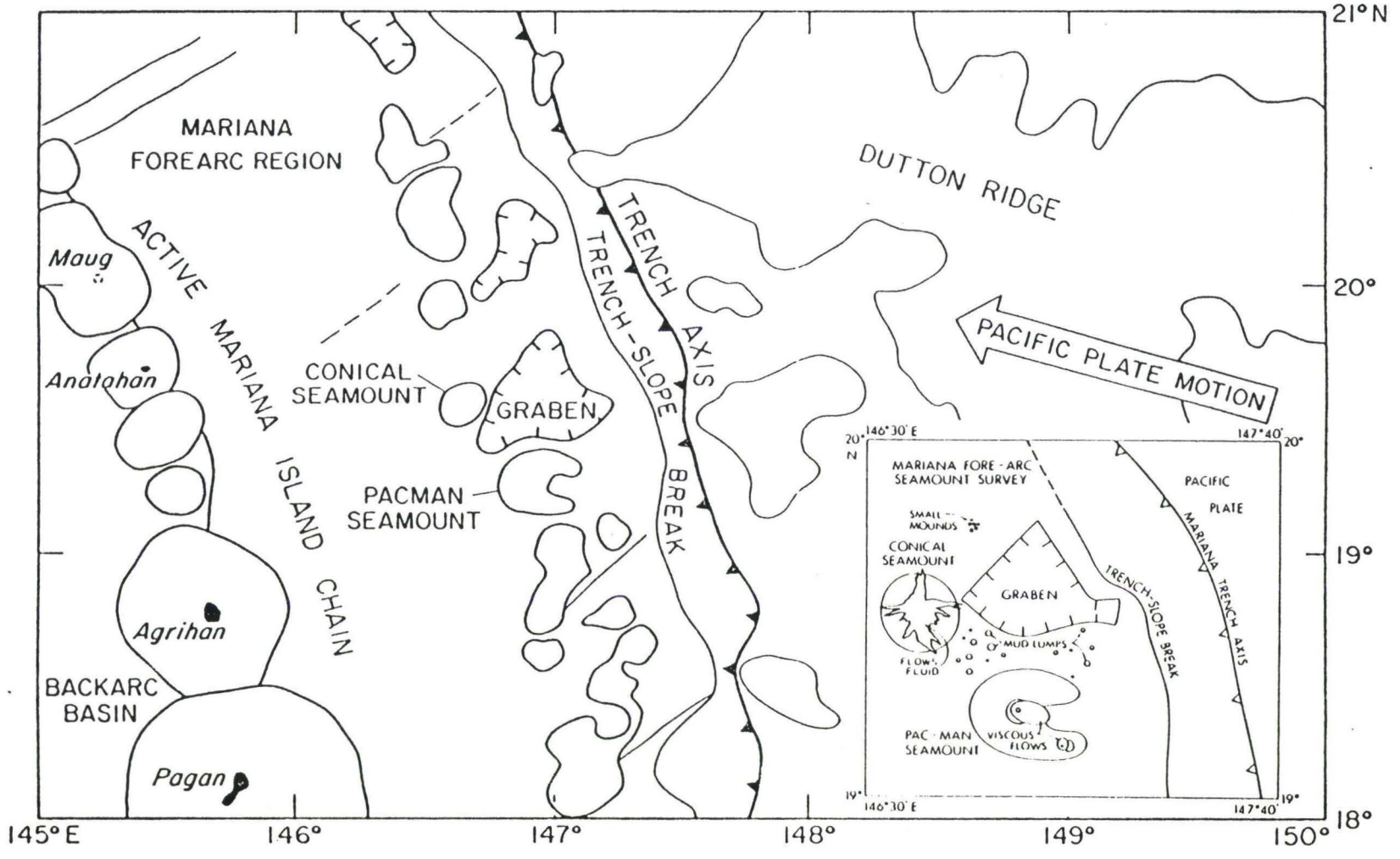


Figure 3A. Geologic sketch showing the disposition of serpentine seamounts and a large graben in the Mariana forearc (Fryer, et al., in press).

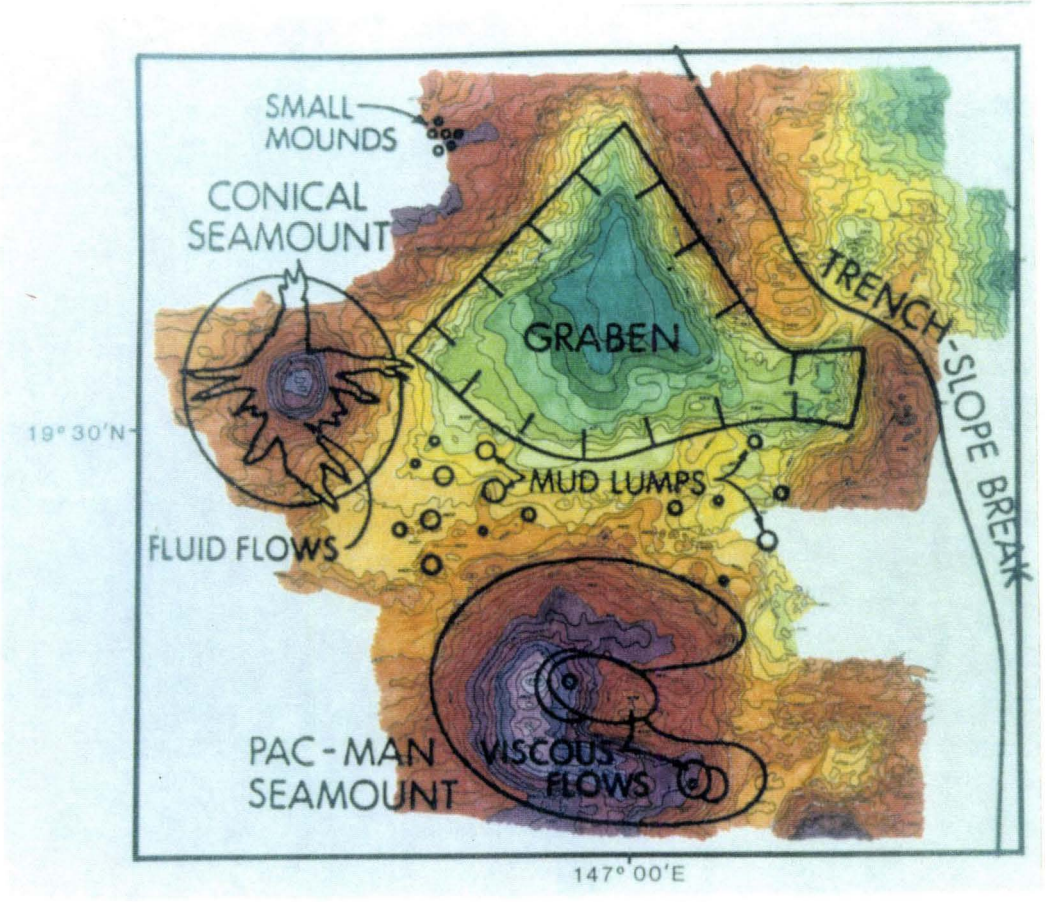


Figure 3B. Geologic sketch of serpentine seamounts at 19°30'N overlain on SeaMARC II bathymetry contoured in 100 m intervals, colored in 200 m intervals with lightest purple being less than 2800 m and darkest green being greater than 5800 m.

serpentinized ultramafic materials, metamorphosed mafic rocks, manganese crusts with adhering pelagic sediment, serpentine muds, and some semilithified, vitric siltstones. SeaMARC II side-scanning sonar images and bathymetry of the two seamounts in this region show flow features of the various types on their flanks (Hussong and Fryer, 1985; Fryer, et al., 1985; Fryer and Fryer, 1987; Fryer, et al., 1990). The lower flanks of Conical Seamount show concentric, long-wavelength ridges, especially on the southeast side (Figure 4). All flanks of the seamount are mantled with long sinuous flows. The flows extend for a maximum distance of up to 18 km from the summit and cover an area of ~ 700 $km^2$. Their sinuous morphology indicates that they are composed of low viscosity material. Conical Seamount was initially interpreted to be a large serpentine mud volcano (Fryer, et al., 1987; Fryer and Fryer, 1987; Fryer, et al., in press).

One example of a subaerial exposure of serpentine possibly analogous to Conical Seamount is within the New Idria, California, serpentine mass (19 km x 6 km), that lies between the San Andreas fault on the west and Great Valley on the east (Coleman, 1957; 1986). The serpentinite body is surrounded by the Franciscan formation of Cretaceous age and the Great Valley Sequence of Late Cretaceous age. Together, the flanking sediments and serpentine mass comprise an asymmetric anticlinal dome that is the northern extension of the Coalinga anticline (Figure 5) (Coleman, 1980). The contact between the sediments and serpentinite consists of high angle faults and shear zones that indicate upward movement of the serpentinite mass (Coleman, 1961). Within the mass is a serpentinite body that consists of highly sheared and crushed incoherent fragments of chrysotile asbestiform that has little strength (Figure 6). This serpentine body has a circular surface expression and may represent a

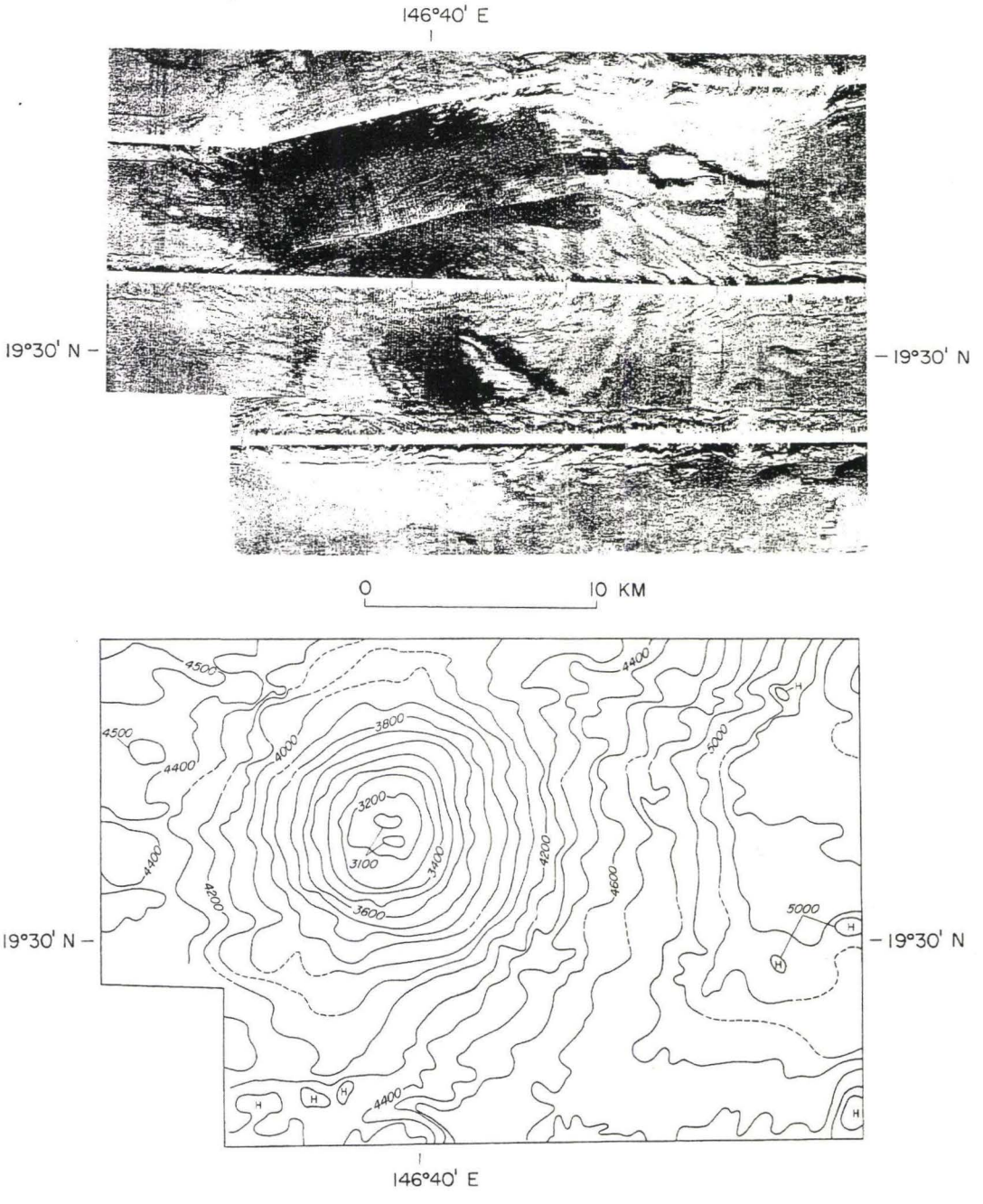


Figure 4. SeaMARC II side-scanning sonar image and bathymetry of Conical Seamount. The dark regions are areas of high backscatter (Fryer, et al., 1990).

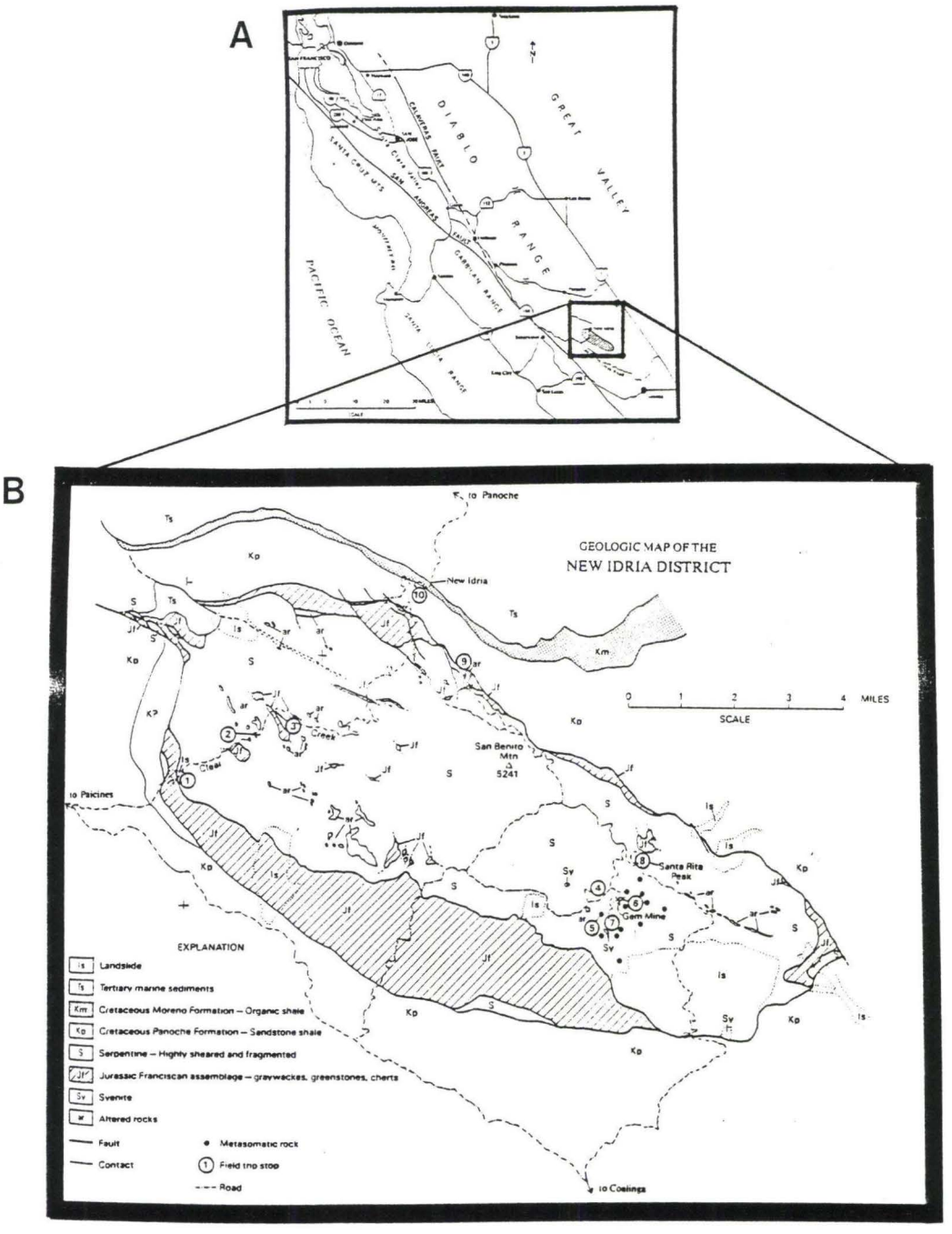


Figure 5. A: Index map of central California showing some of the major highways and secondary roads along with important geologic features.

B: Geologic sketch map of the New Idria district showing major units. Roads are indicated and field trip stops are numbered (Coleman, 1986).

Figure 6. Photograph of Union Carbide Company mine (UCC) in New Idria serpentine mass. This mine is located approximately near field stop #4 on figure 5B.

conduit for an edifice similar to Conical Seamount. The original protolith is believed to be tectonized harzburgites and dunites based on examination of the extant olivine and orthopyroxene (Coleman, 1986). Layering, which probably represents flow features, is found in parts of the exposed serpentine body in the potential conduit feature (Figure 7). Alteration rims are also visible around serpentinized ultramafic clasts enclosed within the serpentine mud (Figure 8). Both these features are also present in Conical Seamount deposits.

Figure 7. Photograph of layering (possible flow feature) in serpentine of UCC mine.

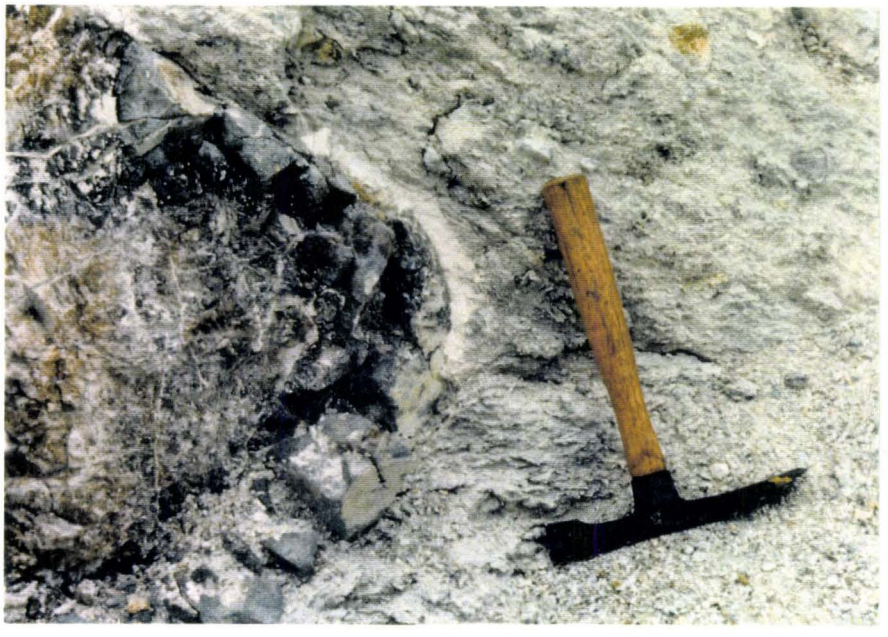

Figure 8. Photograph of serpentinized ultramafic rock contained within the serpentine matrix. Note the presence of the alteration rind.

## SUBMERSIBLE OBSERVATONS AND BOTTOM PHOTOGRAPHY

### *ALVIN* SUBMERSIBLE STUDIES

The results of the nine dives on Conical Seamount, by the *R/V Atlantis II* in the summer of 1987, provided the first comprehensive look at an active serpentine mud volcano. These dives were designed to characterize and sample the flow features on the flanks of the edifice, to investigate the faults and deformation of the flanks of the seamount, and to study the summit region of the seamount (Fryer, et al., 1987; Fryer, et al., 1990; Fryer, et al., in press). Five flank dives (1851-1855, Figure 9.) investigated the flow composition and morphology. Four summit dives (1859-1862, Figure 10) studied chimney structures and vent morphology.

During dives 1854, 1855, and 1859 through 1862, at depths less than 3200 m, columnar to irregularly shaped, vertical projections of serpentine mud were noted. These structures are veined with and partially cemented by carbonate (Figures 11 and 12), and some are topped with cobbles. The structures range from a few centimeters to about 1.5 m high. In several cases, the structures provide a pedestal for the growth of chimneys. Escaping fluids probably precipitate carbonate, not only forming chimneys, but also cementing the matrix of the flow below the surface. Fluids rise from within the serpentine flow and may be concentrated in one locality or disseminated throughout the flow. Where concentrated, or where impeded from escaping locally because of surface "caprocks", the precipitating carbonates might form a fortified column. The chimney pedestals probably were exposed either as the surrounding serpentine flow receded , by current

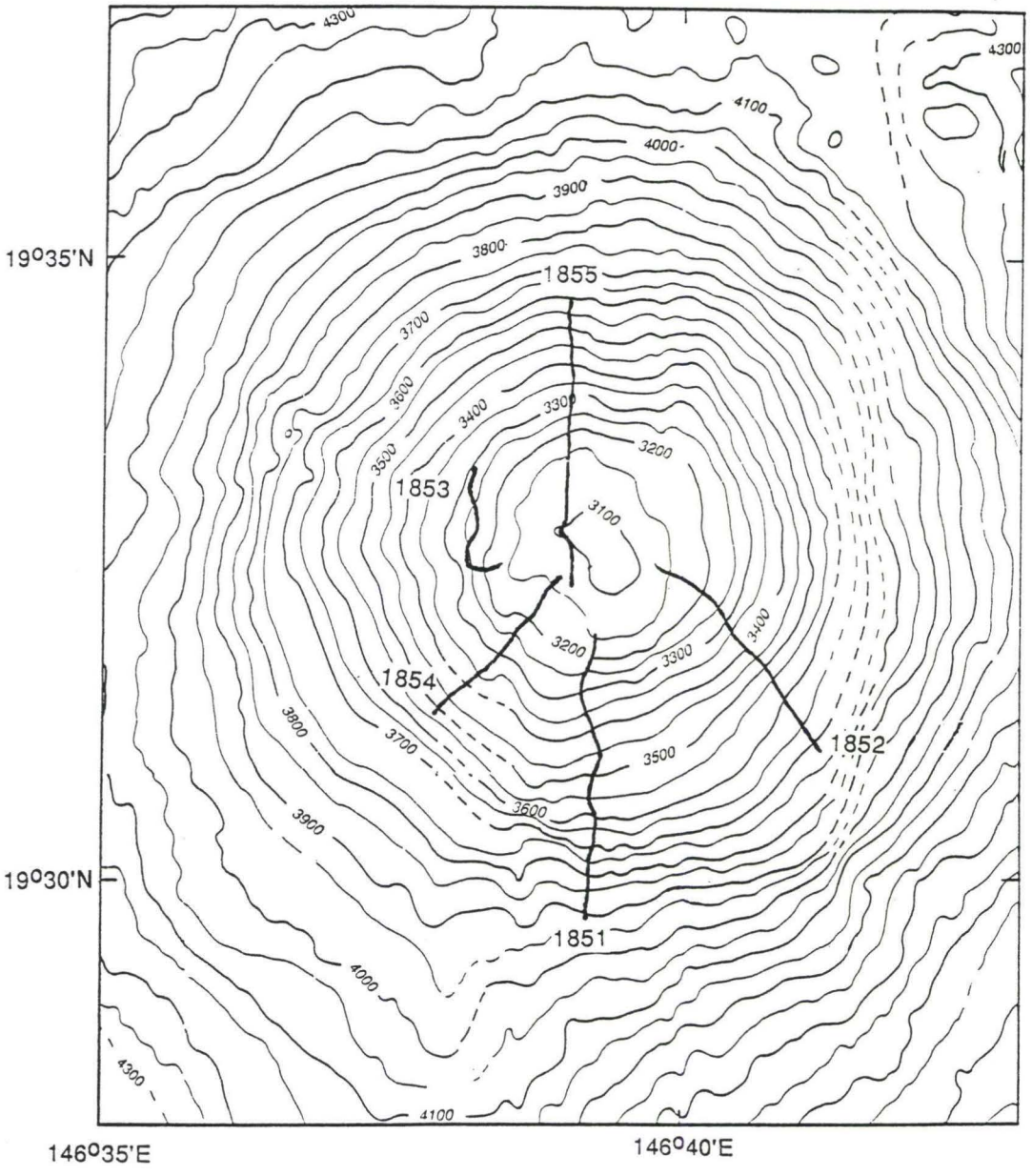


Figure 9. SeaBeam bathymetric contour map (in meters), (collected on *R/V Sonne* cruise), of Conical Seamount showing *Alvin* dive tracks 1851, 1852, 1853, 1854, and 1855 on the upper flanks.

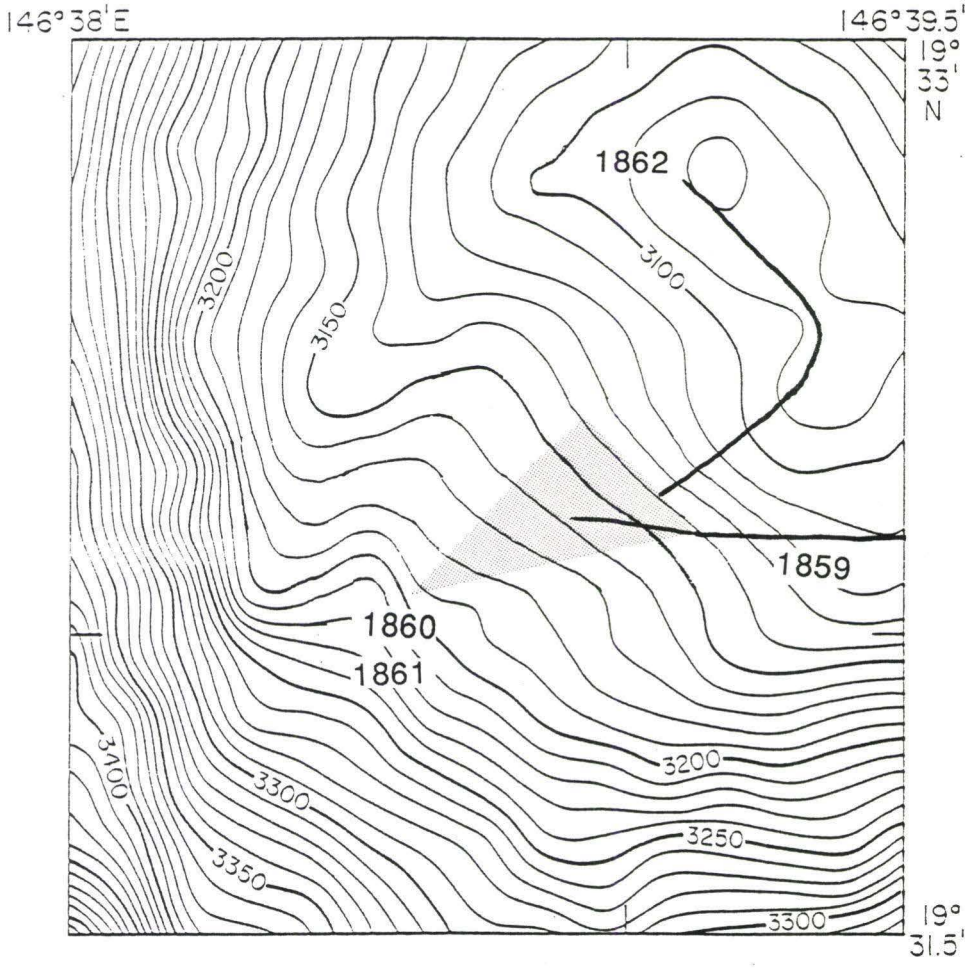


Figure 10. SeaBeam bathymetric contour map (in meters), (collected on *R/V Sonne* cruise), of Conical Seamount showing *Alvin* dive tracks 1859, 1860, 1861, and 1862 on the summit region. The shaded area represents the chimney and vent region of the seamount. Dive 1859 started on the eastern summit flank and proceeded toward the vent area. Dives 1860 and 1861 plot within the shaded area. Dive 1862 started in the vent region and proceeded north over the summit knolls.

Figure 11. *Alvin* bottom photograph of a serpentine pedestal cemented by carbonate

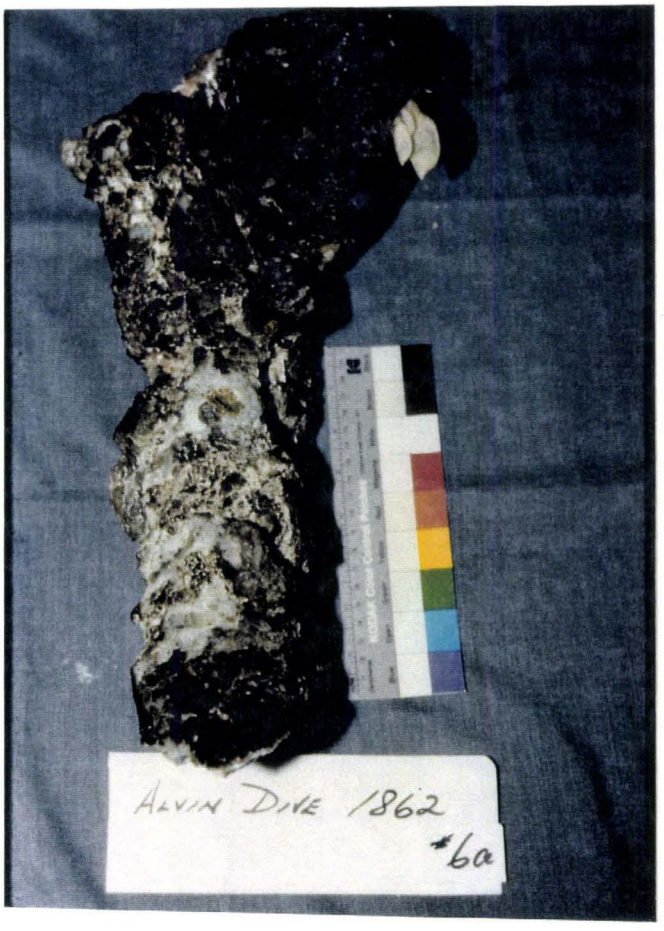


Figure 12. Shipboard photograph of a serpentine pedestal cemented by carbonate (A87-1862-2a). Note the presence of a large ultramafic "cap" rock on top of pedestal. (J. Haggerty, pers. comm.).

erosion, by deflation of the flow as fluid escaped, or by slumping and sliding downslope of uncemented serpentine mud (Fryer, et al., in press).

Two types of chimney structures were discovered on the dives. One type found at the end of dive 1854 and near dives 1859 through 1862 (Haggerty, 1987b; Fryer, et al., in press) is composed of carbonate, is 0.5 to 1.5 m high (Figure 13), and is found in a small field (about 250 m by 350 m) at a depth of about 3140 m to 3160 m, west of the southern summit knoll. The carbonate chimneys are composed of varying proportions of aragonite and calcite. A sample from one of these corroded-looking chimneys contains excess 210Pb, indicating that it is less than 150 yr old (Fryer, et al., in press). None of these chimneys exhibit signs of active venting.

A second type of chimney, composed of silicate, was also discovered near the summit of Conical Seamount in the same region as the carbonate chimneys (Figure 14). This type contained only trace amounts of carbonate and did not appear corroded. Most of these chimneys are taller, ranging from 2 to 3.5 m high, and thicker, up to 2 m at the base, than the carbonate chimneys and are uniformly coated with a thin black layer of ferromanganese oxide. The top of one of the larger chimneys has a smooth, white to pale golden-brown surface. When the surface of this chimney was scraped a slow seeping of vent fluid was observed to emanate from orifices in the chimney. Analysis of the vent fluids collected show a highly unusual high pH, low alkalinity, high methane, high sulfate composition (Fryer, et al., in press). The material forming this type of chimney is a magnesium silicate, analogous to the aluminum silicate, allophane, and has the same composition as that of the silicate found in vugs within the carbonate chimneys (Haggerty, 1987b; Fryer, et al., in press).

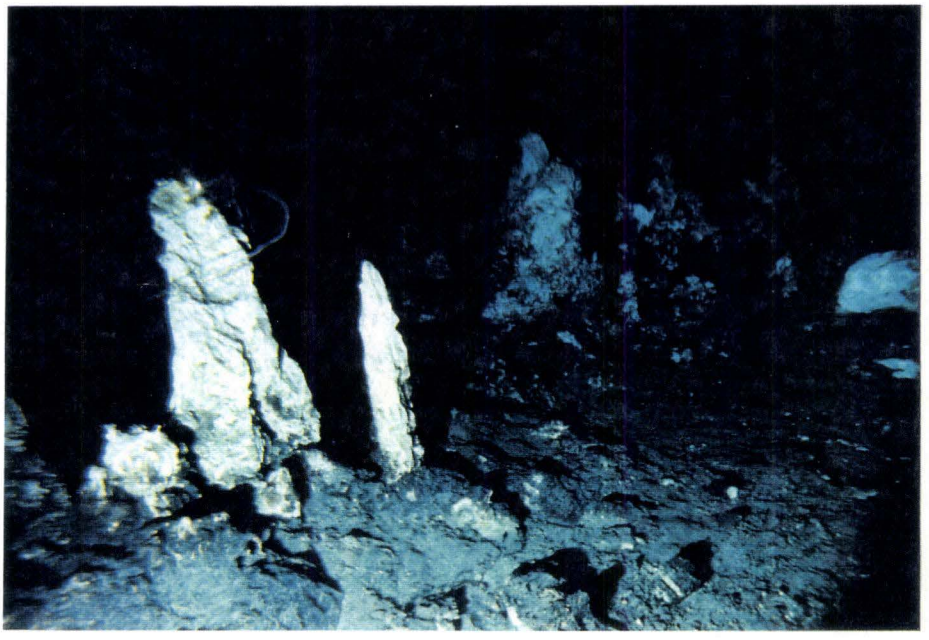

Figure 13. *Alvin* bottom photograph of carbonate chimneys near the summit of Conical Seamount. Left hand chimney is approximately 1.5 m tall. Note the corroded appearance of the structure

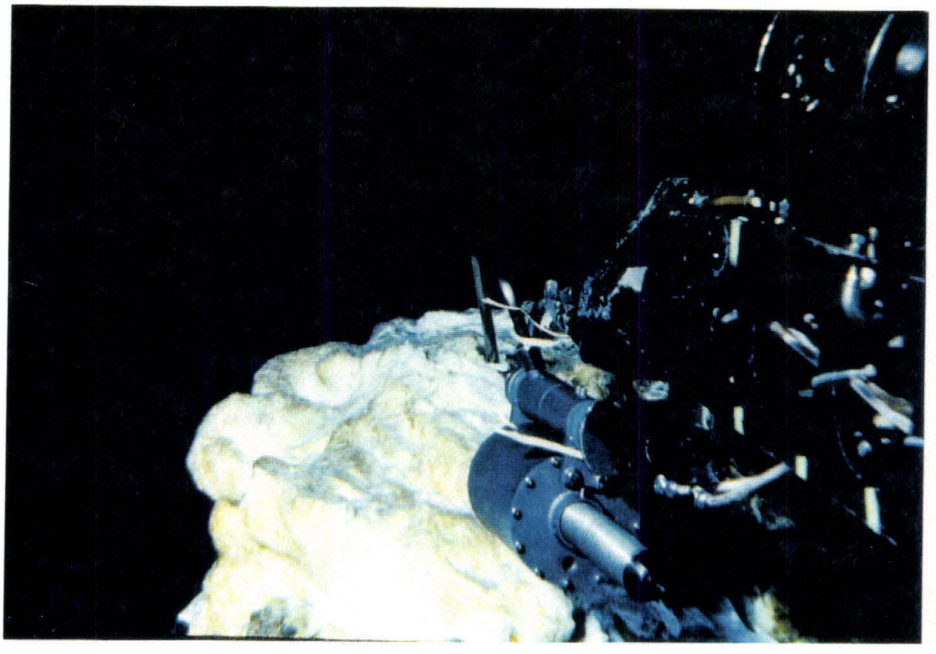

Figure 14. *Alvin* bottom photograph of the top of an actively forming silicate chimney near the summit of Conical seamount

Clasts of serpentinized ultramafic rocks were recovered from the dives and in dredges from Conical Seamount (Fryer and Fryer, 1987). The ultramafic samples are primarily harzburgite (Saboda, et al., 1987). The harzburgites are 27% to 99% serpentinized and contain 1% to 15% clays, up to 7% carbonate, up to 4% iron oxide, up to 5% chlorite, and up to 1% brucite as secondary phases (Table 1). All modal mineralogy presented in this thesis is based on modal estimates and not point counts. However, five samples were chosen at random and point counted (500 total counts each) in order to compare with the modal estimates. The resulting discrepancy between the two techniques is within 2% for most of the minerals except for olivine (3.8%), orthopyroxene (5.5%), and serpentine (4.7%). The low percentage of brucite in the table may be due to the difficulty of identifying it optically. Fine-grained brucite is usually intergrown with the serpentine and their distinguishing features (low-moderate relief and birefringence) are very similar. Brucite is usually identified optically when it occurs as veins crosscutting the serpentine and showing characteristic first order yellow interference colors. Brucite identification determined by x-ray diffraction is presented in the the section on drilling results.

The distinction between the serpentine phases in thin section is based on the morphologic characteristics. Antigorite is the most easily identified phase. In monomineralic samples it forms a flame-like or radiating bladed texture. In contact with olivine it generally forms lepidioblastic fabric of anhedral blades intergrown with relict olivine grains. Chrysotile is the next most easily distinguished serpentine phase. It generally forms in veins developed in fractures as cross-fiber veins with fibers oriented near $90^{o}$ to the vein margins or in micro-shear zones as slip-fiber veins with fibers parallel to the shear planes. Lizardite is difficult to distinguish because it is

Table 1.

Modal mineralogy of ultramafic rocks from Conical Seamount, Alvin dive samples

| Sample | ol ext | ol orig | opx ext | opx orig | sp ext | sp orig | cpx ext | cpx orig | clays | chl | br | mt | serp | other | total sec |
|---|---|---|---|---|---|---|---|---|---|---|---|---|---|---|---|
| A87-1851-5a | 2 | 78 | 7 | 20 | <1 | 1 | <1 | <1 | 8 | 1 | 0 | 2 | 80 | | 91 |
| A87-1851-5b | 0 | 88 | 2 | 12 | <1 | <1 | 0 | 0 | 8 | 4 | 0 | 2 | 83 | tr? | 97 |
| A87-1851-6 | 7 | 84 | 5 | 15 | 1 | 1 | <1 | <1 | 7 | 1 | 0 | 3 | 76 | | 87 |
| A87-1852-1 | tr | 79 | 7 | 20 | 1 | 1 | <1 | <1 | 3 | tr | 0 | 3 | 83 | 2 talc? | 91 |
| A87-1852-2 | 0 | 73 | 5 | 25 | 2 | 2 | 0 | 0 | 15 | 0 | 0 | 2 | 76 | | 93 |
| A87-1852-8 | 10 | 72 | 15 | 25 | 1 | 1 | 2 | 2 | 7 | 3 | 0 | 4 | 58 | | 72 |
| A87-1852-9 | 0 | 84 | 4 | 15 | 1 | 1 | 0 | 0 | 4 | 2 | ? | 4 | 85 | | 95 |
| A87-1853-2 | 0 | 84 | 5 | 15 | <1 | 1 | 0 | 0 | 15 | 5 | 0 | 15 | 50 | 10 hem | 95 |
| A87-1853-4b | tr | 79 | 5 | 20 | 1 | 1 | <1 | <1 | 10 | 0 | <1? | 2 | 81 | tr? (vein) | 93 |
| A87-1853-5a | 3 | 84 | 7 | 15 | 1 | 1 | <1 | <1 | 3 | tr | 0 | 1 | 84 | <1carb | 88 |
| A87-1854-6 | 4 | 79 | 7 | 20 | 1 | 1 | 0 | 0 | 3 | 2 | 0 | 3 | 80 | tr carb | 88 |
| A87-1855-1 | 30 | 73 | 15 | 25 | 1 | 2 | 0 | 0 | 2 | 1 | 0 | 3 | 48 | tr? (vein) | 54 |
| A87-1855-2 | 3 | 84 | 7 | 15 | 1 | 1 | tr | tr | 5 | 1 | 0 | 4 | 79 | | 89 |
| A87-1855-4 | 0 | 87 | 1 | 12 | 1 | 1 | 0 | 0 | 10 | 0 | 0 | 2 | 86 | | 98 |

Table 1. (continued)

**Modal mineralogy of ultramafic rocks from Conical Seamount, Alvin dive samples**

| Sample | ol ext | ol orig | opx ext | opx orig | sp ext | sp orig | cpx ext | cpx orig | clays | chl | br | mt | serp | other | total sec |
|---|---|---|---|---|---|---|---|---|---|---|---|---|---|---|---|
| A87-1859-2a | 25 | 74 | 15 | 25 | <1 | 1 | 0 | 0 | 8 | 0 | 0 | 2 | 50 | <1carb | 60 |
| A87-1859-2b | 32 | 69 | 25 | 30 | <1 | 1 | <1 | <1 | 8 | 1 | 0 | 3 | 30 | <1carb | 42 |
| A87-1859-2c | 24 | 85 | 12 | 15 | <1 | <1 | 0 | 0 | 4 | 1 | 0 | 2 | 55 | 1carb | 63 |
| A87-1859-2e | 0 | 54 | 7 | 45 | 1 | 1 | <<1 | <<1 | 5 | 0 | 0 | 2 | 85 | | 92 |
| A87-1860-5 | tr | 84? | 0 | 15? | 1 | 1 | 0 | 0 | 7 | 0 | 1 | 0 | 90 | 1carb | 99 |
| A87-1860-6 | 40 | 62 | 30 | 35 | 2 | 2 | 1 | 1 | 2 | <1 | 0 | 1 | 24 | | 27 |
| A87-1861-4 | 0 | 77.5 | 10 | 20 | 2 | 2.5 | 0 | 0 | 8 | <1 | <1?? | 4 | 68 | 7carb | 88 |
| A87-1861-5 | 39 | 63 | 27 | 35 | 1 | 1 | 1 | 1 | 5 | 0 | 0 | 2 | 25 | <1carb | 32 |
| A87-1862-3a | 15 | 73 | 10 | 25 | 1 | 1 | 1 | 1 | 3 | 0 | 0 | 2 | 65 | <4 (vein) | 74 |
| A87-1862-3b | 0 | 73 | 4 | 25 | 1 | 2 | 0 | 0 | 6 | 0 | 1?? | 2 | 85 | <1hem | 95 |
| A87-1862-3c | 30 | 79 | 12 | 20 | 1 | 1 | 0 | 0 | 0 | 0 | <1? | 2 | 55 | | 57 |
| A87-1862-3d | 40 | 75 | 14 | 22 | 1 | 1 | 2 | 2 | 1 | <1 | 0 | 2 | 40 | | 43 |
| A87-1862-3g | 40 | 87 | 5 | 12 | <1 | 1 | 0 | 0 | 2 | 0 | 0 | 2 | 50 | | 54 |

ol ext=olivine extant; ol orig=olivine original; opx ext=orthopyroxene extant; opx orig=orthopyroxene original; spinel ext=spinel extant; sp orig=spinel original; cpx ext=clinopyroxene extant; cpx orig=clinopyroxene original; clays=clay minerals; chl=chlorite; br=brucite; mt=magnetite; serp=serpentine; tr?=trace amount of an unknown; hem=hematite; carb=carbonate; total sec=total amount of secondary minerals.

usually much finer-grained and is often intimately intergrown with the other serpentine phases and with brucite. It can form a platey texture, however, it generally forms pseudomorphic mesh or hour-glass textures after olivine or antigorite in the rocks we studied. Mesh textures in serpentine are the result of retrograde conditions, whereas hourglass textures are indicative of mild prograde (Wicks, 1979). In mild retrograde conditions, where temperature decreases during the reaction, the reaction rates are reduced, stopping the formation of platey lizardite in the mesh rims and producing fine-grained, poorly crystallized mesh centers (Wicks, 1979). The most common texture observed in the rocks studied is mesh texture with fine-grained poorly crystallized mesh centers.

Although much of the original mineralogy has been obscured, the modal percentages of the original minerals may be estimated by examining the serpentine textures, the interrelationships among the various serpentine phases, and the relationships between the serpentine phases and the extant mafic minerals in the rocks. The harzburgite samples are estimated to have contained originally from 62% to 88% olivine, 12% to 45% orthopyroxene, 1% to 2% spinel, and up to 2% clinopyroxene.

In addition to the characteristic high relief and high birefringence, the pale-green to colorless extant olivine is highly fractured and mostly anhedral. Extant orthopyroxene has straight extinction and lower birefringence than olivine. The orthopyroxene grains are sub-anhedral, kink-banded, have exsolution lamellae, and are generally more resistant to alteration and metamorphism than the olivine (Figure 15), except for A87-1862-3d and 3g which show orthopyroxene altered more than olivine. The extant clinopyroxene has oblique extinction and is generally found in small sub-anhedral grains near the margins of and as exsolution lamellae within

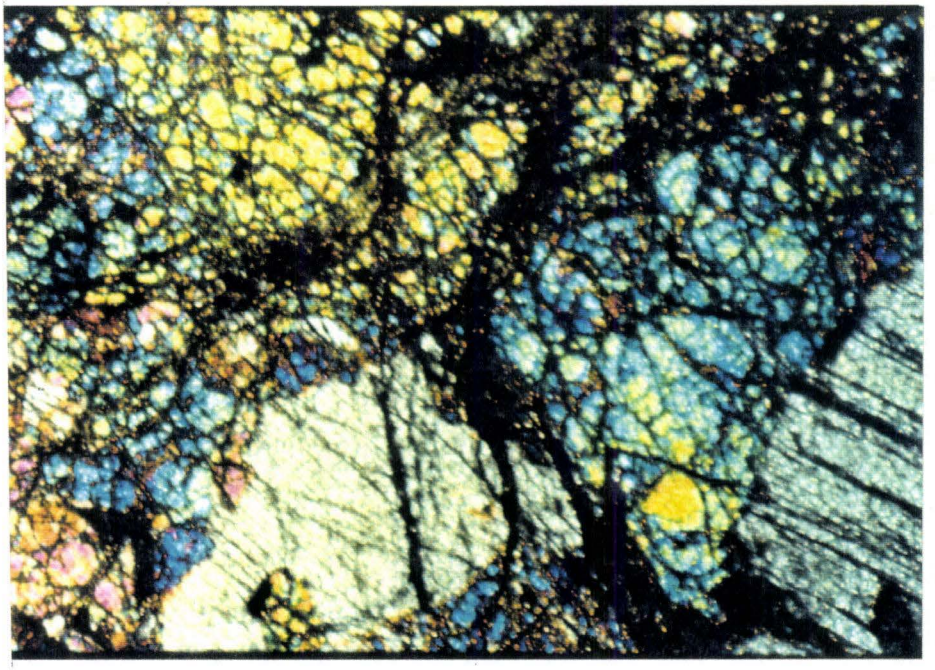

Figure 15. Photomicrograph of sample A87-1859-2b, (42% altered/metamorphosed harzburgite), showing typical ultramafic mineralogy consisting of olivine and orthopyroxene with minor magnetite, clays, and serpentine. Photomicrograph is taken with crossed polars and the field of view is 5 mm.

the orthopyroxene. Spinels are elongate to equant and usually form characteristic raggedy trains. Some are fractured and are filled with an anomalous blue-brown chlorite mineral (probably penninite) (Figure 16).

As is commonly observed the serpentinization proceeds differently in the olivine and orthopyroxene crystals of the rocks studied. In the olivine the serpentine forms along the fractures and growth of the serpentine veins gradually causes expansion of the rock. This metamorphism forms a characteristic mesh or hourglass texture. In the orthopyroxene the serpentine forms along the cleavage planes and then expands throughout the grain, forming a bastitic texture that may later alter to chlorite and other secondary phases (Figure 17). Numerous veins of serpentine (mostly chrysotile?) with associated magnetite, brucite, chlorite, clays and carbonate are also present up to 2 mm in size (Figure 18).

The temperature and pressure constraints of the type of very low- to medium-grade of metamorphism represented by the Alvin samples from Conical Seamount are described by Wicks (1979). He also notes that metastability of serpentine phases within broad temperature/pressure ranges can occur. Thus, although these criteria (Wicks, 1979) can help determine the grade of metamorphism of the rocks in this study, without further, detailed analysis the metamorphic grade of the rocks can only be constrained to very low- to medium-grade .

None of the *Alvin* dive samples show tectonized fabrics and all analyses of ultramafic rocks have shown island arc affinities (Bloomer, 1982). The *Alvin* samples are probably upper mantle rocks of arc affinity that were metamorphosed as a consequence of the flux of fluids derived from dehydration reactions within the downgoing Pacific plate. These rocks were probably plucked from the walls of a deep-seated conduit and

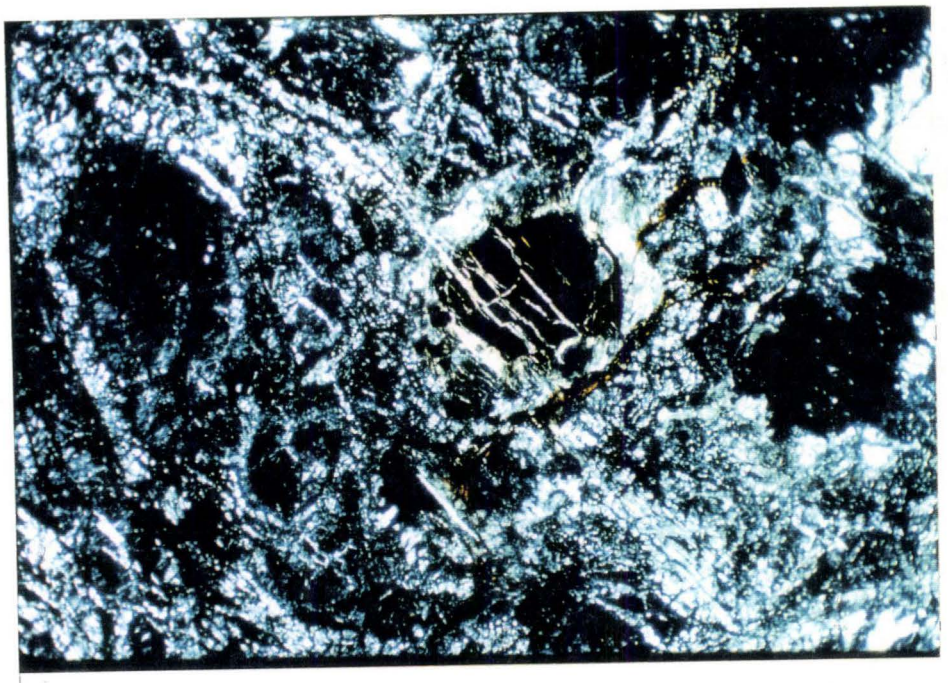

Figure 16. Photomicrograph of sample A87-1853-2, (95% altered/metamorphosed harzburgite), showing fractured spinels. The fractures are filled with anomalous blue-brown chlorite material believed to be penninite. Upper photomicrograph field of view is 9 mm and lower photomicrograph field of view is 2 mm. Both are taken with crossed polars.

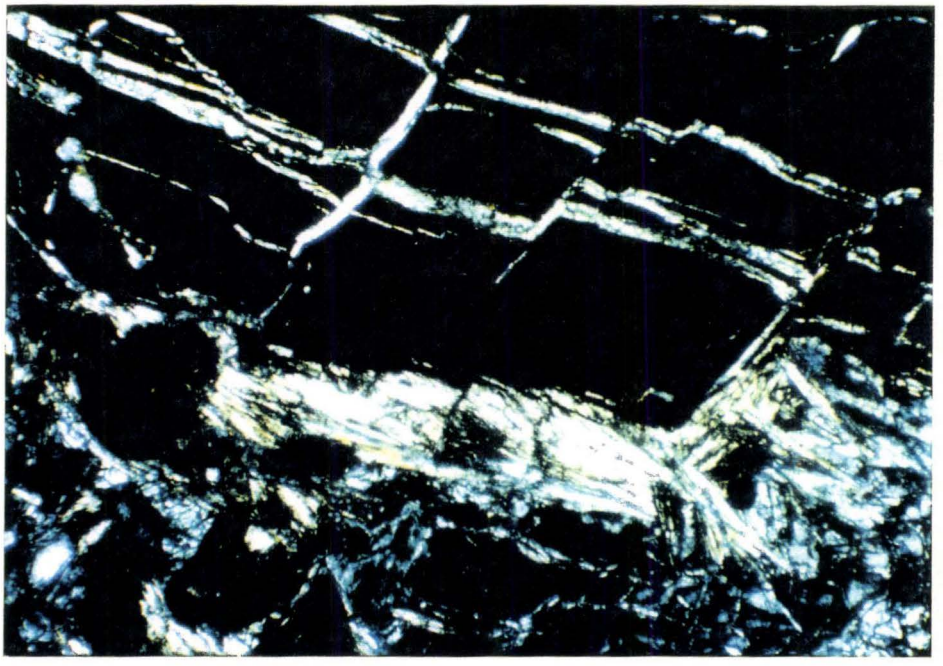

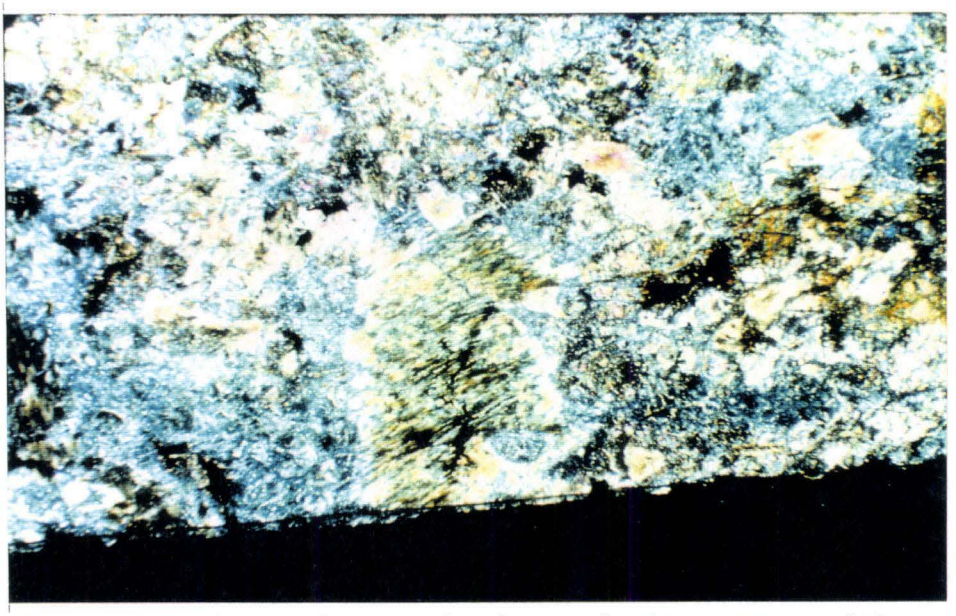

Figure 17. Photomicrograph of sample A87-1854-6, (88% altered/metamorphosed harzburgite), showing bastitic orthopyroxene altering to chlorite in the center of the picture. Upper photomicrograph is taken with crossed polars and lower photomicrograph is taken under plane light. The field of view is 9 mm.

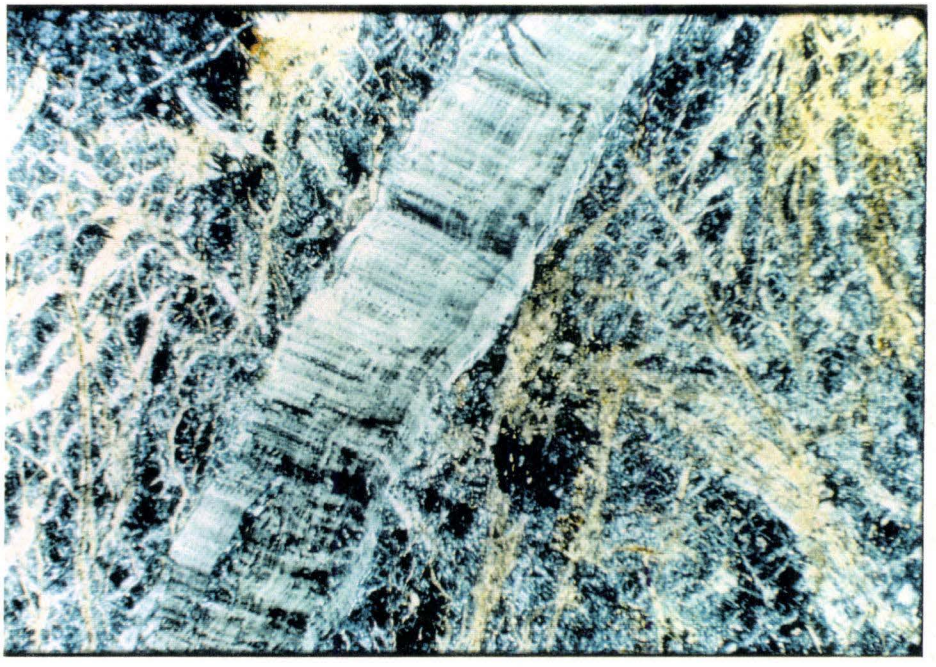

Figure 18. Photomicrograph of sample A87-1862-3a (74% altered/metamorphosed harzburgite) showing veins consisting of serpentine, magnetite, clays, and chlorite. The field of view is 9 mm.

entrained within rising pulses of fluid-charged serpentine muds that erupt slowly from the summit of the seamount.

The mud flows were observed in all dives on Conical Seamount. Based on the *Alvin* observation the flows on Conical Seamount have a variety of surface textures and structures (Fryer, et al., in press). A relative age discrimination was applied, based on the degree of sediment cover on the flows, on the amount of manganese encrustation on the flow surface, and the degree of contortion of the flow surface, in an attempt to map regions of recent flow activity (Fryer, et al., in press). The *Alvin* observations showed that the youngest flows are light green, have contorted surfaces, and lack a sediment cover. These flows have numerous cobbles and boulders, (1 mm to 20 cm in size), consisting primarily of serpentinized peridotites and dunites, with small amounts of metabasalts and metagabbros scattered over their surfaces. The older flows have a smoother surface, are covered with sediment and, in places, have ferromanganese and/or carbonate encrustations. Some old flows have well-developed current lineations and minor bioturbation visible.

## *R/V SONNE* BOTTOM PHOTOGRAPHY STUDIES

The *R/V Sonne* bottom photography track map (Figure 19) shows the region of the summit surveyed in a 1988 effort to investigate the potential for finding sites suitable for ODP advanced piston coring. Attempts to piston core the region failed. However, photographs collected serve to augment the *Alvin* data and further document the structure of the summit region. Flows with contorted surfaces, numerous boulders scattered over the surface, and little sediment cover are considered relatively young (Figure

20). Older flows have sediment covered surfaces (Figure 21). There are regions of fractured terrain and carbonate precipitates (Figure 22 and 23).

The northern and southern flanks of the summit knolls are primarily unfractured flows (Figures 24A thru 24D). However, in the notch between the two summit knolls there are fractured and sheared flows (Figures 25E thru 25H). The fractured terrain is consistent with the suggestion that the summit is in extension (Fryer, et al., 1990). The flows apparently originate from near the western side of the two summit knolls, in the vent region of the seamount (Fryer, et al., in press).

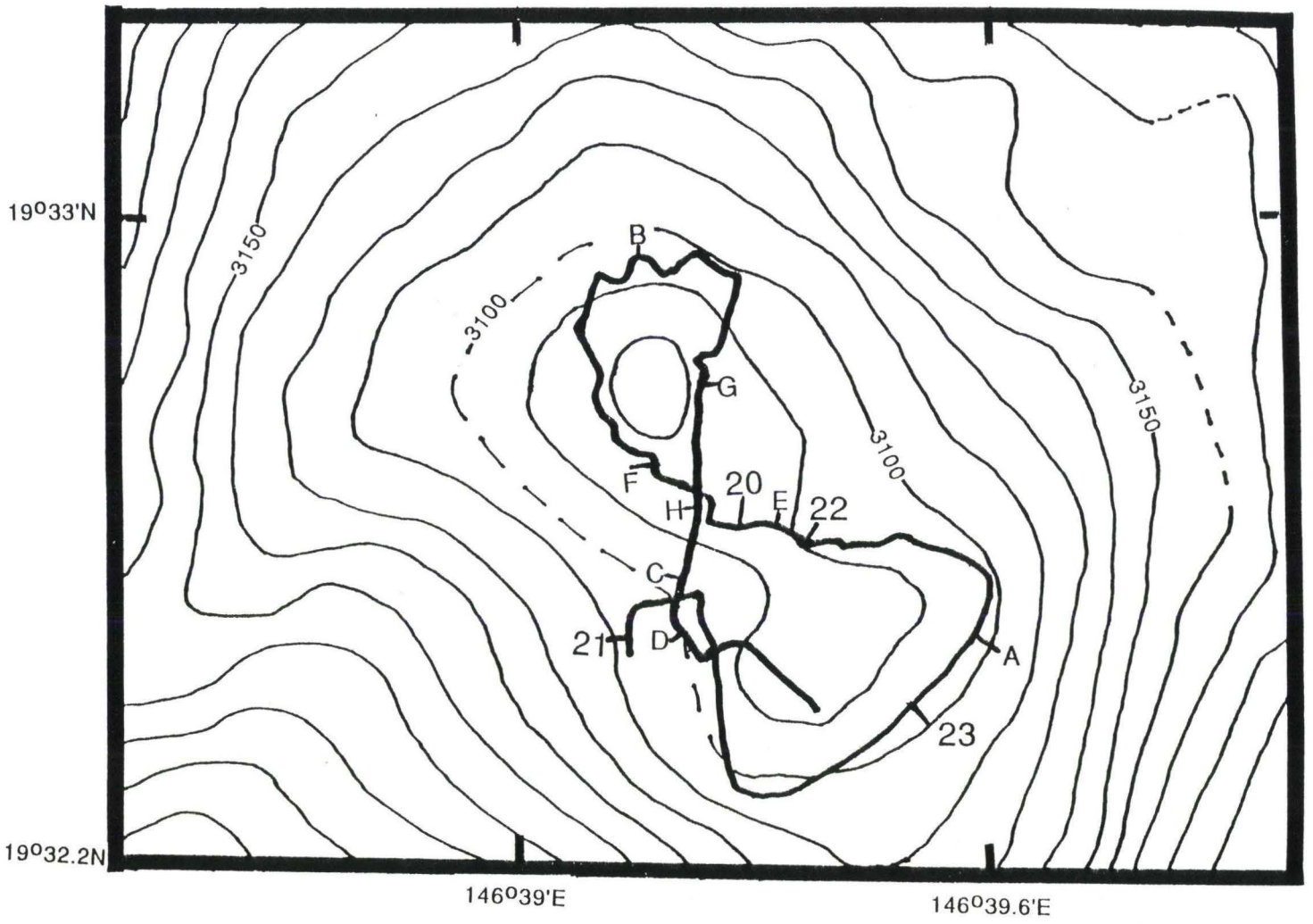


Figure 19. *R/V Sonne* SeaBeam bathymetry map of Conical Seamount summit area showing camera sled track and locations of bottom photographs shown in figures 20 thru 25.

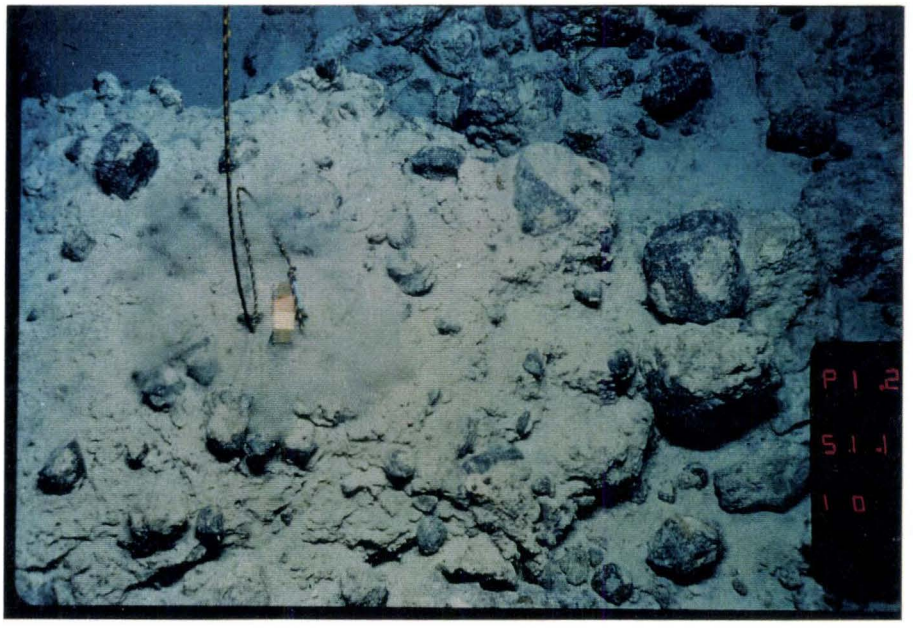

Figure 20. *R/V Sonne* bottom photograph of young serpentine flow showing a contorted surface and abundance of clasts. The rope hanging down through the center of the photograph has a 10 cm block attached to it for scale.

Figure 21. *R/V Sonne* bottom photograph of an old serpentine flow showing a smooth sediment covered surface and lack of clasts. The rope hanging down through the center of the photograph has a 10 cm block attached to it for scale.

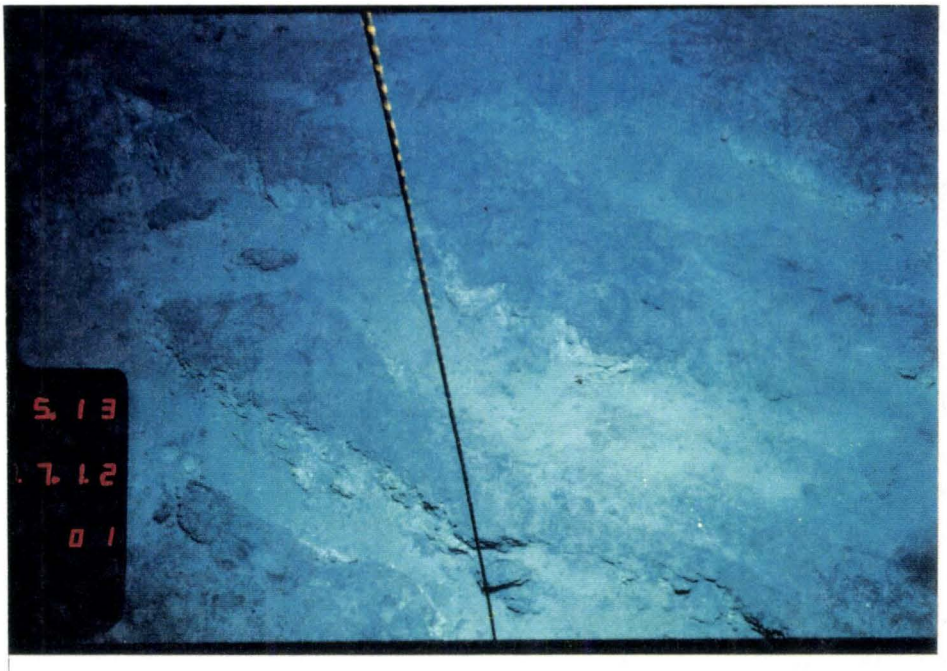

Figure 22. *R/V Sonne* bottom photograph of parallel fissures approximately 10-20 cm wide and rimmed with carbonate-rich material. The rope hanging down through the center of the photograph has a 10 cm block attached to it for scale.

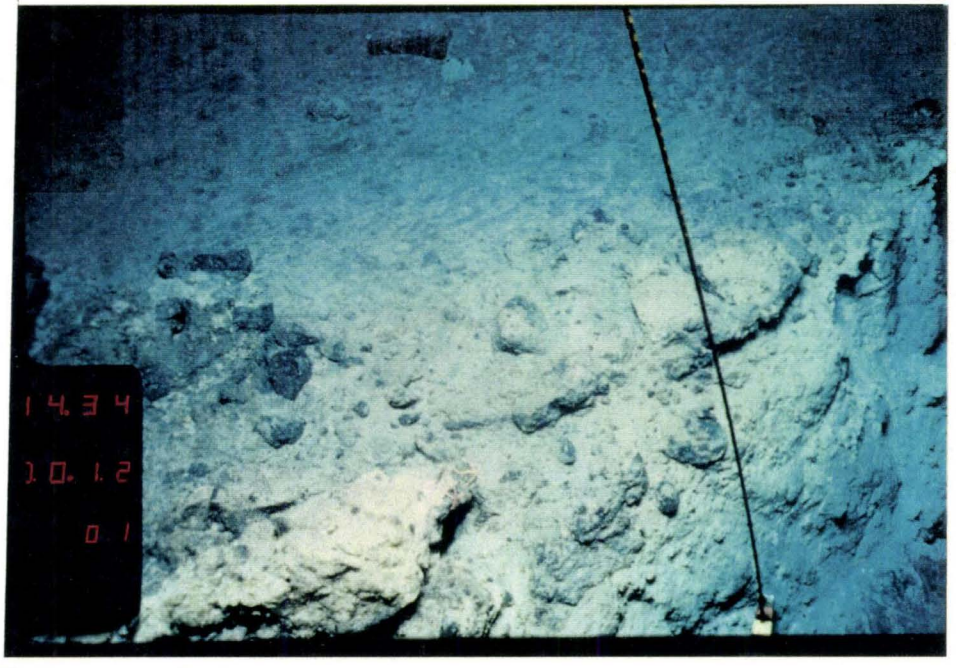

Figure 23. *R/V Sonne* bottom photograph of a fault scarp approximately 1.5 m high. Note the nature of the flow interior. The rope hanging down through the center of the photograph has a 10 cm block attached to it for scale.

A

B

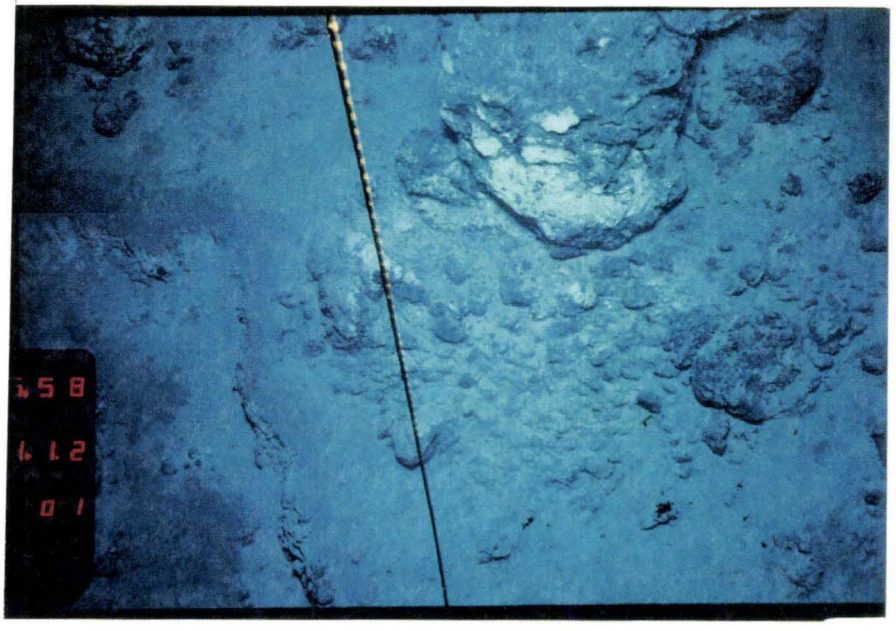

Figure 24: A, B, C, D. *R/V Sonne* bottom photographs of unfractured serpentine flows. The rope hanging down through the center of the photograph has a 10 cm block attached to it for scale.

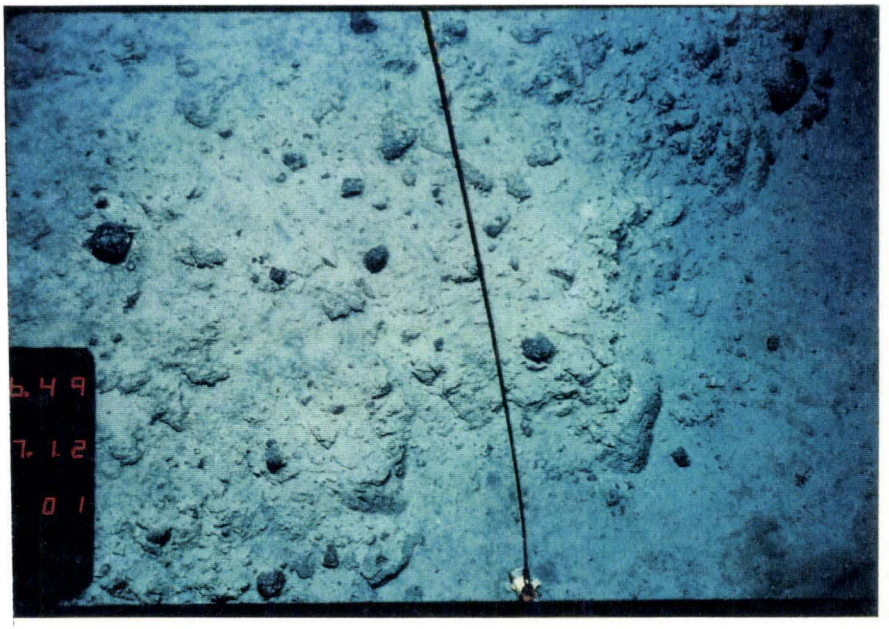

C

D


E

F

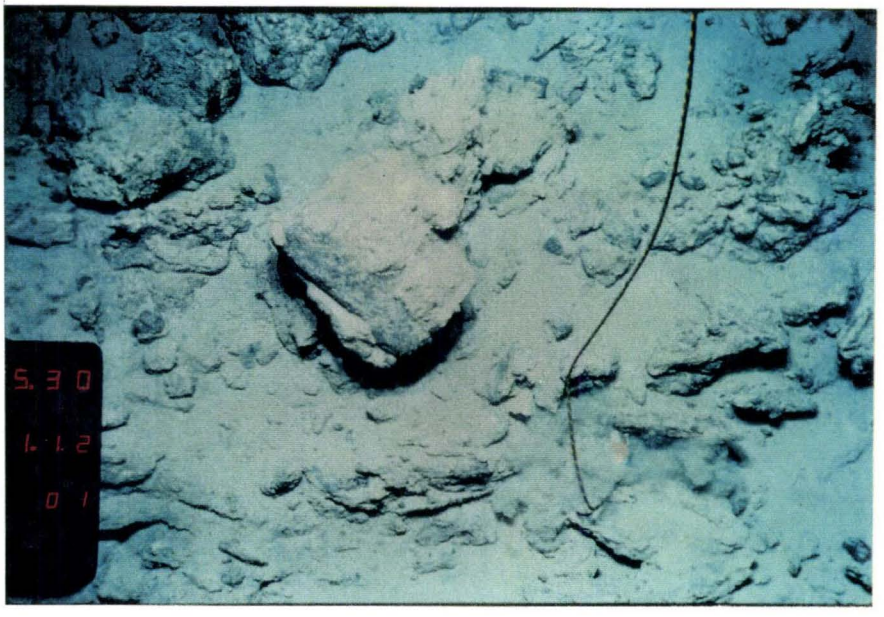


Figure 25: E, F, G, H. *R/V Sonne* bottom photographs of fractured serpentine flows. The rope hanging down through the center of the photograph has a 10 cm block attached to it for scale.


G

H

# ODP DRILLING RESULTS

Leg 125 of the Ocean Drilling Program drilled three sites (two flank sites and one summit site, Figure 26) on Conical Seamount in order to investigate directly the origin and evolution of the seamount by studying the composition and structure of the muds of which it is comprised and indirectly by studying the composition and textures of the ultramafic rocks from which the muds most likely were derived.

## SHIPBOARD STUDIES

The following is a synthesis of work done on the *R/V Resolution* by the author in collaboration with other shipboard scientists (Fryer, Pearce, Stokking, et al., 1990).

### 1) SITE 778------CONICAL SEAMOUNT SOUTH FLANK SITE

#### Principal Results

Site 778 (19$^{o}$29.93'N, 146$^{o}$39.94'E) is located in the midflank region of the southern quadrant of Conical Seamount at a depth of 3913.7 meters below sea level (mbsl), (Figure 26). The objective of this site was to penetrate the flank of the seamount about 5.5 km due south of its summit. Side-scan sonar and *Alvin* submersible studies had indicated this area is covered by recent, unconsolidated, flows of serpentine muds (Fryer, et al., 1985; Fryer, et al., 1990). This site is located in the center of a major region of serpentine flows. The chemical effects of serpentinization on the oceanic lithosphere and its sedimentary cover can be investigated by examining the mineralogy and composition of both the clasts, veins, and matrix within the

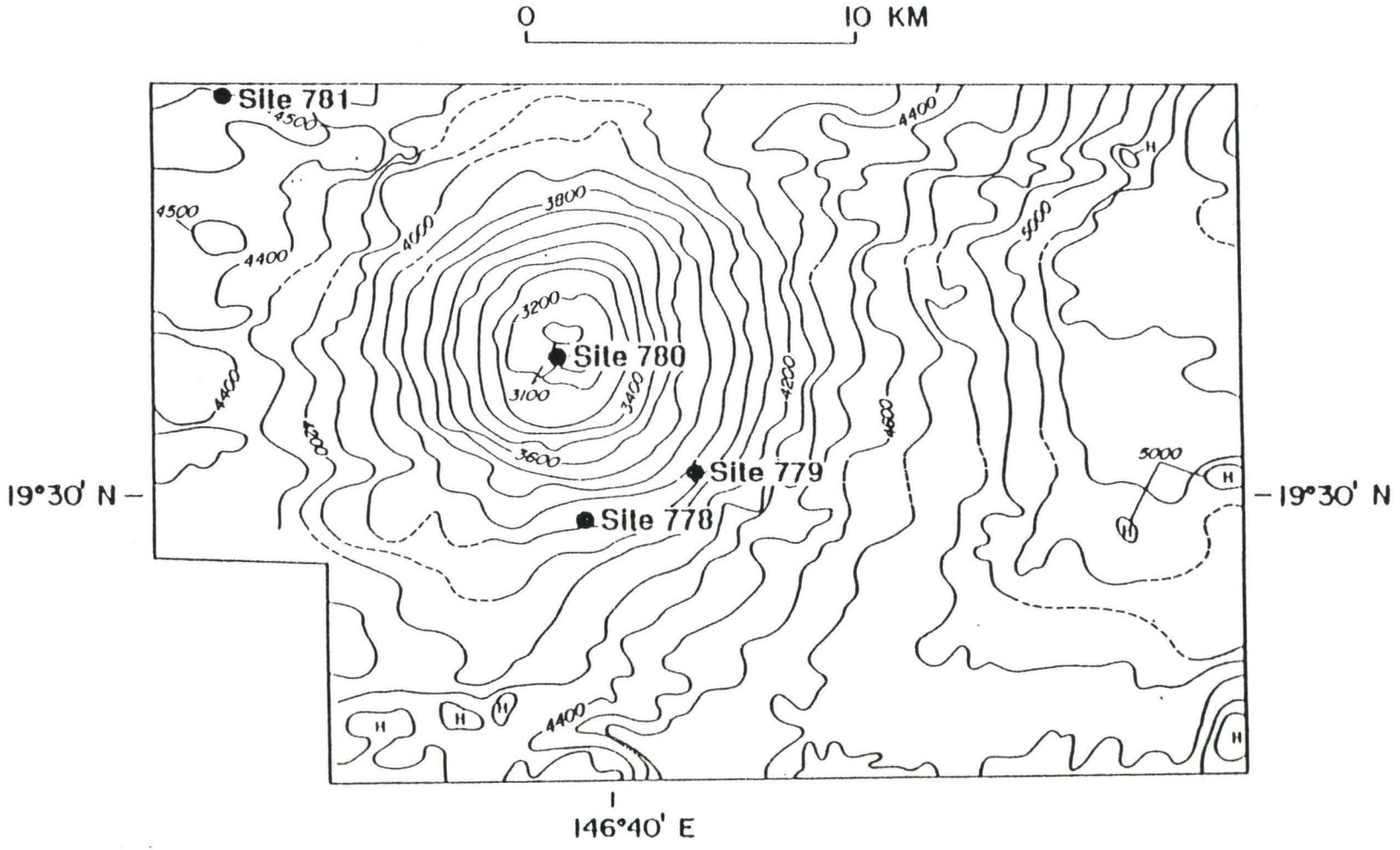


Figure 26. Locations of Leg 125 drill sites on Conical Seamount in the Mariana forearc using SeaMARC II bathymetry.

serpentine flows. The principal conclusions of Site 778 investigations based on shipboard observations are that very low- to medium-grade metamorphism characterizes the source region of the serpentine flows that make up the seamount. Dehydration of the subducted lithosphere may have played an important part in the serpentinization of the source (Fryer, et al., 1987; Haggerty, 1987b; Fryer, et al., 1990; Fryer, Pearce, Stokking, et al., 1990). The primary mantle material in the seamount is harzburgite with subordinate dunite which show evidence of melt extraction in an island arc environment (Fryer, Pearce, Stokking, et al., 1990; Ishii, et al., in press). The composition of the dominant harzburgite is remarkably uniform.

## Petrography

The serpentinized, tectonized harzburgites range in color from a deep blackish-green to a light dun. Many exhibit small-scale color variations caused by veining of serpentine and carbonate. Although most clasts are massive, some show small-scale foliation caused by alignment of bastitic orthopyroxene. Chromium-spinels are sometimes dumbbell-shaped and occasionally form stringers defining a lineation.

Shipboard thin section examination shows the primary minerals have been altered pervasively to serpentine. The texture of the serpentine phases present and their interrelationships throughout clasts recovered in all of the drillholes on this seamount fall within the range observed in the dredge and *Alvin* samples. Thus, the suite of clasts recovered attests to a general uniformity in very low- to medium-grade of metamorphism. Original orthopyroxene, olivine, clinopyroxene, and apparently fresh chrome-spinel are still preserved (Table 2). Serpentinized olivine (about 80-95 modal % of the rock) forms a massive mesh-textured fabric, having no obvious crystal

Table 2.

Modal mineralogy of ultramafic rocks from Conical Seamount, Leg 125 samples

| Sample site-core | interval (cm) | p # | rock name | ol ext | ol orig | opx ext | opx orig | cpx ext | cpx orig | sp ext | sp orig | clays | chl | br | mt | serp | other | total sec |
|---|---|---|---|---|---|---|---|---|---|---|---|---|---|---|---|---|---|---|
| 125-778A-2R-1 | 57-59 | 2 | SH | <0.1 | 85 | 5 | 15 | .2-.3 | .2-.3 | .5-1 | .5-1 | 15 | 0 | 0 | 1 | 78 | <1 carb | 95 |
| 125-778A-2R-1 | 74-75 | 5 | SH | 8 | 90 | 8 | 10 | <0.1 | <0.1 | 0.5 | 0.5 | 25.5 | tr | 1 | 3 | 50 | | 79.5 |
| 125-778A-2R-1 | 78-81 | 6 | SH | 10 | 80 | 15 | 20 | <0.1 | <0.1 | 0.5 | 0.5 | 20 | 0 | 0 | 2 | 52.5 | ~1 carb | 74.5 |
| 125-778A-7R-1 | 12- 16 | | SH | 0 | 70 | 1 | 29 | 0 | 0 | 1 | 1 | 0 | 0 | 0 | 2 | 96 | | 98 |
| 125-778A-7R-1 | 13- 16 | | SH | 0 | 80 | <1 | 19 | 0 | 0 | <1 | 1 | 2 | 0 | 0 | 2 | 95 | | 99 |
| 125-778A-7R-1 | 25-28 | | SH | 0 | 85-90 | 0 | 10- 15 | 0 | 0 | <1 | 1 | 3 | 0 | 0 | 0 | 95-97 | | 98-100 |
| 125-778A-7R-2 | 55-60 | | SH | <0.1 | 85? | <1 | 15? | 0 | 0 | <1 | <1 | 10 | 0 | 0 | 2 | 87 | | 99 |
| 125-778A-7R-2 | 74-75 | | SH | 0 | 72-77 | 0 | 20-25 | 0 | 0 | <1 | 3 | <1 | <1 | 5? | 2 | 92 | | 99 |
| 125-778A-7R-CC | 0- 2 | | SH | 0 | 77-82 | 0 | 15-20 | 0 | 0 | 2 | 3 | 5 | 0 | 0 | 3 | 90 | | 98 |
| 125-778A-7R-CC | 0- 3 | | SH | 0 | 70-80 | 0 | 20-25 | 0 | 0 | 2- 3 | 3 | 10 | 2 | 0 | 2 | 83-84 | | 97-98 |
| 125-778A-8R-1 | 39-40 | 7 | SH | 0 | 75-82 | 1- 2 | 15-20 | tr | 1- 2 | 2- 3 | 2- 3 | 5- 10 | 2- 3 | 2 | 1 | 79-87 | tr sph? | 95-97 |
| 125-778A-8R-1 | 47-48 | 8 | SH | 0 | 85 | 0 | 14 | 0 | 0 | 1 | 1 | 5 | tr | tr? | 1- 2 | 92-93 | | 99 |
| 125-778A-9R-1 | 57-58 | | ASH | 0 | 90 | 0 | 10 | 0 | 0? | 1 | 1 | 10- 20 | 0 | 0 | 0 | 80-90 | | 99 |
| 125-778A-12R-2 | 43-45 | | SH | 0 | 75-80 | 0 | 18-23 | 0 | 0 | 2 | 2 | 0 | <1 | 0 | 1- 2 | 85-87 | 10 thu? | 98 |
| 125-778A-12R-2 | 73-75 | | SH | 0 | 73-78 | <1 | 20-25 | 0 | 0 | 1 | 2 | 0 | 2- 4 | 0 | 2 | 93-95 | | 99 |

Table 2. (continued)

Modal mineralogy of ultramafic rocks from Conical Seamount, Leg 125 samples

| Sample site-core | interval (cm) | p # | rock name | ol ext | ol orig | opx ext | opx orig | cpx ext | cpx orig | sp ext | sp orig | clays | chl | br | mt | serp | other | total sec |
|---|---|---|---|---|---|---|---|---|---|---|---|---|---|---|---|---|---|---|
| 125-779A-3R-CC | 13-15 | 2 | SD | 20 | 94 | 0 | 5 | 0 | 0 | 0.1 | 1 | 0 | 5- 10 | 0 | 1 | 70-75 | | 80 |
| 125-779A-4R-1 | 27-30 | 3 | SH | 0 | 78.5 | <1 | 20 | tr | tr | 1.5 | 1.5 | 10 | 0 | 0 | 1 | 87 | | 98 |
| 125-779A-4R-1 | 42-44 | 5 | SH | 0 | 83-88 | 0 | 10- 15 | 0 | 0 | 2 | 2 | 10 | 0 | 0 | <1 | 88 | | 98 |
| 125-779A-5R-1 | 108-109 | 12 | SD | 10 | 88 | 5 | 10 | <1 | 1 | 0.5 | 1.5 | 0 | 5- 10 | <1 | 2 | 72-77 | | 84.5 |
| 125-779A-5R-2 | 14-15 | 3 | ASH | 0 | 83-89 | 0 | 10- 15 | 0 | 0 | 1- 2 | 1- 2 | 50-60 | 0 | 0 | <1 | 38-49 | | 98-99 |
| 125-779A-5R-2 | 34-37 | 3 | STH | 15-20 | 84-89 | 3- 5 | 10- 15 | tr | tr | 0.5 | 1 | 0 | 5 | 0 | 1 | 69-76 | | 74-81 |
| 125-779A-5R-2 | 40-43 | 3 | SH | <1 | 83-88 | 1- 2 | 10- 15 | <1 | <1 | 2 | 2 | 0 | 2 | 2 | 1 | 91 | | 96 |
| 125-779A-5R-2 | 65-69 | 4 | SD | 0 | 99 | 0 | 0 | 0 | 0 | 1 | 1 | 0 | 0 | 1 | 1 - 2 | 97-98 | | 99 |
| 125-779A-5R-2 | 116-120 | 10a | SH | 8- 10 | 78-83 | 2 | 15-20 | tr | tr | 1- 2 | 2 | 3 | 5 | tr? | 1 | 79-81 | | 86-89 |
| 125-779A-6R-1 | 18-20 | 2 | SH | 15-20 | 77-82 | 10- 15 | 15-20 | 1 | 1? | 2 | 2 | <1 | 3 | 0 | 1 | 58-68 | | 62-72 |
| 125-779A-8R-1 | 27-29 | 5a | ASH | 0 | 84-89 | 0 | 10- 15 | 0 | 0 | 0.5 | 1 | 20 | 0 | 0 | 2 | 77 | | 99.5 |
| 125-779A-8R-1 | 57-60 | 5b | SH | 0 | 78 | 0 | 20 | 0 | 0 | 2 | 2 | 10 | 1 | 20-30 | 0 | 57-67 | | 98 |
| 125-779A-8R-1 | 82-83 | 8a | STD | 45-50 | 93 | 4 | 5 | tr | tr | 2 | 2 | 0 | 0 | 0 | 2 | 44-49 | | 46-51 |
| 125-779A-8R-1 | 90-93 | 8b | STD | 40-50 | 96 | 2 | 3 | 0 | 0 | 0.5 | 1 | 5 | 0 | 0 | <1 | 42-52 | | 47-57 |
| 125-779A-9R-2 | 52-54 | 4b | STH | 25 | 85-87 | 10 | 10- 12 | 1 | 1 | 1.5 | 1.5 | 2 | 1 | 0 | 1 | 68.5 | | 72.5 |
| 125-779A-10R-1 | 26-29 | 3 | STD | 55 | 94 | 1 | 5 | <0.1 | <0.1 | 0.5 | 1 | 0 | 3 | tr | 3 | 37 | | 43 |
| 125-779A-10R-1 | 39-43 | 5 | STD | 40 | 97 | 2 | 3 | 0 | 0 | 0.5 | 1 | 0 | 0 | 3 | 2 | 51 | 1 carb | 57.5 |
| 125-779A-10R-1 | 54-57 | 6 | STD | 50 | 97 | 2 | 3 | 0 | 0 | 0.5 | 1 | 0 | 0 | 3 | 2 | 42 | | 47.5 |
| 125-779A-10R-2 | 28-31 | 1 | SH | 0 | 88 | 0 | 12 | 0 | 0 | tr | <1 | 0 | 0 | 3? | <1 | 96 | | 99 |
| 125-779A-11R-1 | 6 - 9 | 2 | SH | <1 | 87 | 0 | 12 | tr | tr | 1 | 1 | 0 | 0 | <1 | <1 | 98 | | 99 |
| 125-779A-11R-1 | 14-18 | 3 | SH | tr? | 82 | 0 | 15 | 1.5 | 1.5 | 1.5 | 1.5 | 0 | 0 | 0 | <1 | 97 | | 97 |
| 125-779A-11R-1 | 34-36 | 5 | SD | 0 | 99 | 0 | 0 | 0 | 0 | tr | 1 | 0 | 0 | 0 | tr | 100 | | 100 |

Table 2. (continued)

Modal mineralogy of ultramafic rocks from Conical Seamount, Leg 125 samples

| Sample site-core | interval (cm) | p # | rock name | ol ext | ol orig | opx ext | opx orig | cpx ext | cpx orig | sp ext | sp orig | clays | chl | br | mt | serp | other | total sec |
|---|---|---|---|---|---|---|---|---|---|---|---|---|---|---|---|---|---|---|
| 125-779A-12R-1 | 38-42 | 6 | SH | 10 | 86 | 8 | 12 | 1 | 1 | 1 | 1 | 0 | 2 | 0 | <1 | 78 | | 80 |
| 125-779A-13R-1 | 2- 5 | 1 | SH | 0 | 87 | 0 | 12 | 0 | 0 | <1 | 1 | <1 | 2 | 0 | <1 | 95 | | 99 |
| 125-779A-13R-2 | 50-54 | 1 | SH | 20-25 | 79-84 | 10- 15 | 15-20 | <1 | <1 | <1 | 1 | 0 | 2 | 0 | 2 | 54-64 | | 58-68 |
| 125-779A-13R-3 | 9 - 11 | 1 | SH | 50 | 86 | 5 | 12 | tr | tr | 1 | 2 | 0 | 1 | 0 | 1 | 42 | | 44 |
| 125-779A-14R-1 | 74-77 | 5a | SD | 40 | 91 | 2 | 8 | <1 | <1 | 1 | 1 | 0 | 2 | 0 | 1 | 54 | | 57 |
| 125-779A-14R-2 | 21-24 | 3 | SD | 20-25 | 95 | 1 | 3 | <0.1 | <0.1 | 1 | 2 | 2 | 3 | 0 | 1 | 67-72 | | 73-78 |
| 125-779A-14R-2 | 77-79 | 8 | SH | 40-50 | 80-85 | 10- 15 | 15-20 | 3 | 3 | 2 | 2 | 0 | 0 | 0 | <1 | 30-45 | | 30-45 |
| 125-779A-14R-2 | 139-141 | 16 | SH | 40 | 78-83 | 10 | 15-20 | <1 | <1 | 1 | 1.5 | 0 | 3 | 0 | 1 | 45 | | 49 |
| 125-779A-15R-1 | 15-17 | 4 | SH | 33 | 83-85 | 12 | 12 | 3 | 3 | 1 | 2 | 0 | 0 | 0 | 1 | 50 | | 51 |
| 125-779A-15R-2 | 18-20 | 3 | SH | 21 | 87 | 7 | 12 | <1 | <1 | 1 | 1 | 0 | 0 | 0 | 1 | 70 | | 71 |
| 125-779A-15R-2 | 24-27 | 3 | SD | 10 | 94-97 | 0 | 2- 5 | 0 | 0 | 0.3 | 1 | 0 | <1 | 5? | 2 | 82 | | 89.7 |
| 125-779A-15R-2 | 37-40 | 5 | SH | 40 | 81 | 10 | 15 | 1 | 1 | 3 | 3 | 0 | 0 | 0 | 1 | 45 | | 46 |
| 125-779A-15R-2 | 110-111 | 17 | SD | 54 | 97 | tr | tr | 0 | 0 | 1 | 2 | 2 | <1 | 0 | 2 | 40 | | 45 |
| 125-779A-16R-1 | 16-19 | 3 | SH | 50 | 86 | 7 | 12 | 0 | 0 | 1 | 2 | 0 | <1 | 0 | 2 | 40 | | 42 |
| 125-779A-16R-1 | 19-23 | 3 | D | 76-81 | 95 | 2 | 3 | <1 | <1 | 0.5 | 1.5 | 0 | 0 | 0 | 1 | 15-20 | | 16-21 |
| 125-779A-16R-1 | 37-40 | 6 | H | 69 | 83 | 7 | 15 | <1 | <1 | <1 | 2 | 0 | 0 | 0 | 2 | 25 | 4 talc? | 31 |
| 125-779A-16R-1 | 50-52 | 8 | H | 68 | 84 | 7 | 15 | <1 | <1 | <1 | 1 | tr | 0 | 0 | 1 | 20 | 3 talc? | 24 |
| 125-779A-16R-1 | 127-129 | 19 | SD | 52 | 90 | 3 | 8 | tr | tr | 1 | 2 | 1 | 0 | 0 | 1 | 40 | 2 talc? | 44 |
| 125-779A-16R-2 | 44-47 | 6 | SH | 18 | 81 | 5 | 12 | 5 | 5 | 1 | 2 | 0 | 0 | 0 | 1 | 70 | | 71 |
| 125-779A-16R-2 | 61-64 | 9 | SH | 20 | 85 | 10 | 12 | 2 | 2 | 1 | 1 | 0 | 1 | 0 | 1 | 65 | | 67 |
| 125-779A-16R-2 | 74-77 | 9 | H | 48 | 76.5 | 12 | 20 | 2 | 2 | 1 | 1.5 | 0 | 1 | 0 | 1 | 35 | | 37 |
| 125-779A-16R-2 | 117-120 | 11 | SH | 12 | 83 | 10 | 15 | 1 | 1 | 1 | 1 | 0 | tr | 0 | 1 | 75 | | 76 |
| 125-779A-17R-1 | 144-145 | 17 | SD | 31 | 98 | 0 | 0 | 0 | 0 | 1 | 2 | 2 | 0 | 0 | 1 | 65 | | 68 |

Table 2. (continued)

Modal mineralogy of ultramafic rocks from Conical Seamount, Leg 125 samples

| Sample site-core | interval (cm) | p # | rock name | ol ext | ol orig | opx ext | opx orig | cpx ext | cpx orig | sp ext | sp orig | clays | chl | br | mt | serp | other | total sec |
|---|---|---|---|---|---|---|---|---|---|---|---|---|---|---|---|---|---|---|
| 125-779A-17R-2 | 17-20 | 3 | H | 48 | 73 | 15 | 25 | tr | tr | 1 | 2 | 0 | <1 | 0 | 1 | 35 | | 36 |
| 125-779A-17R-2 | 21-24 | 3 | H | 47 | 74 | 20 | 25 | tr | tr | 1 | 1 | 0 | tr | 0 | 2 | 30 | | 32 |
| 125-779A-17R-3 | 77-80 | 8b | H | 53 | 83 | 10 | 15 | tr | tr | 1 | 2 | 0 | 0 | 0 | 1 | 35 | | 36 |
| 125-779A-17R-3 | 80-83 | 8b | H | 43 | 83 | 10 | 15 | <1 | <1 | 1 | 2 | 0 | tr | 0 | 1 | 45 | | 46 |
| 125-779A-17R-4 | 44-47 | 4 | SH | 27.5 | 87 | 7 | 12 | tr | tr | 0.5 | 1 | 0 | 0 | 0 | 1 | 65 | | 66 |
| 125-779A-19R-2 | 97-99 | 13 | D | 61.5 | 99 | 0 | 0 | 0 | 0 | 0.5 | 1 | 0 | 0 | 1? | 2 | 35 | | 38 |
| 125-779A-22R-1 | 58-60 | 11 | ASH | tr | 84 | 1 | 15 | 0 | 0 | 1 | 1 | 25 | 0 | 2 | 1 | 70 | | 98 |
| 125-779A-22R-1 | 63-65 | 11 | SH | 35 | 79 | 12 | 20 | 0 | 0 | <1 | 1 | 0 | 1 | <1? | 1 | 50 | | 53 |
| 125-779A-22R-2 | 18-20 | 2 | SD | 15 | 99 | 0 | 0 | 0 | 0 | 0.5 | 1 | 5 | 0 | 0 | 2 | 77.5 | | 84.5 |
| 125-779A-22R-3 | 55-57 | 7 | SD | 35 | 91 | 3 | 7 | 0 | 0 | 1 | 2 | 0 | 0 | 0 | 1 | 60 | | 61 |
| 125-779A-24R-1 | 36-38 | 6 | SD | 0 | 93 | 0 | 7 | 0 | 0 | <1 | <1 | 7 | 0 | 0 | tr | 93 | | 100 |
| 125-779A-25R-1 | 85-87 | 10b | SD | 20 | 99 | 0 | tr | 0 | 0 | 0.5 | 1 | 0 | 0 | 0 | 1 | 78 | | 79 |
| 125-779A-26R-2 | 50-52 | 2b | H | 48 | 81 | 15 | 18 | <1 | <1 | 1 | 1.5 | 0 | 0 | 0 | 1 | 35 | | 36 |
| 125-779A-26R-2 | 71-75 | 2c | ASH | 2 | 86 | 2 | 12 | tr | tr | 1 | 2 | 30 | 0 | tr | 2 | 63 | | 95 |
| 125-779A-26R-3 | 101-103 | 3b | SH | 21.5 | 62.5 | 25 | 35 | 1 | 1 | 1.5 | 1.5 | 0 | 0 | 0 | 1 | 50 | | 51 |
| 125-779A-28R-2 | 109-113 | | ASD | 0 | 100 | 0 | 0 | 0 | 0 | tr | tr | 15-20 | 0 | <1? | 1 | 78-83 | | 100 |
| 125-779A-28R-3 | 26-28 | 2a | SH | tr | 83.5 | 0 | 15 | 0 | 0 | 1 | 1.5 | 5 | 0 | 0 | <1 | 93 | | 99 |

Table 2. (continued)

**Modal mineralogy of ultramafic rocks from Conical Seamount, Leg 125 samples**

| Sample site-core | interval (cm) | p # | rock name | ol ext | ol orig | opx ext | opx orig | cpx ext | cpx orig | sp ext | sp orig | clays | chl | br | mt | serp | other | total sec |
|---|---|---|---|---|---|---|---|---|---|---|---|---|---|---|---|---|---|---|
| 125-780C-6R-1 | 61-62 | 7a | SH | 21 | 78 | 15 | 20 | 1 | 1 | 1 | 1 | 0 | 2 | 0 | 1 | 60 | | 63 |
| 125-780C-8R-1 | 98-101 | 10 | SD | 38.5 | 92 | 0 | 7 | 0 | 0 | 0.5 | 1 | 0 | 2 | 0 | 1 | 55 | 3 talc | 61 |
| 125-780C-10R-1 | 13-16 | 2 | STH | 15 | 76 | 20 | 22 | 0.5 | 0.5 | 1.5 | 1.5 | 0 | <1? | 0 | <1 | 62 | | 63 |
| 125-780C-10R-1 | 36-37 | 6 | SD | 0 | 96 | 0.5 | 3 | 0 | 0 | 0.5 | 1 | 0 | 0.2 | 0.2? | 8 | 90.6 | | 99 |
| 125-780C-10R-1 | 36-37 | 6 | SD | 0 | 89.5 | 0 | 9 | 0 | 0 | 1.5 | 1.5 | 0 | 0 | 0.5 | 1.5 | 96.5 | | 98.5 |
| 125-780C-16R-1 | 53-59 | 7 | SH | 20 | 74 | 15 | 24.5 | tr | tr | 0.5 | 0.5 | 0 | 0 | tr | 1 | 63.5 | | 64.5 |
| 125-780C-18R-1 | 60-61 | 2a | SH | 15 | 76.5 | 12 | 20 | 1.5 | 1.5 | 1.5 | 2 | <1 | <1? | 0 | 1 | 67 | 1 talc | 70 |
| 125-780D-7X-1 | 25-26 | | S | 0 | ? | 0 | ? | 0 | 0 | 0 | ? | 0 | 0 | 3? | 3 | 94 | | 100 |
| 125-780D-7X-5 | 94-96 | | SH | 0 | 79 | 0 | 20 | 0 | 0 | 0.5 | 1 | 0 | 0 | 0 | <1 | 99 | | 99.5 |

SD=serpentinized dunite; SH=serpentinized harzburgite; H=harzburgite; D=dunite; S=serpentinite; ASD=altered serpentinized dunite; ASH=altered serpentinized harzburgite; STD=serpentinized tectonized dunite; STH=serpentinized tectonized harzburgite; ol ext=olivine extant; ol orig=olivine original; opx ext=orthopyroxene extant; opx orig=orthopyroxene original; spinel ext=spinel extant; sp orig=spinel original; cpx ext=clinopyroxene extant; cpx orig=clinopyroxene original; clays=clay minerals; chl=chlorite; br=brucite; mt=magnetite; serp=serpentine; tr?=trace amount of an unknown; hem=hematite; carb=carbonate; thu=thulite; sph=sphene; total sec=total amount of secondary minerals.

outlines. Bastitic orthopyroxene (5-20 modal %; less than 10 mm in dimension) is typically kink-banded and sometimes elongate. Clinopyroxene occurs as exsolution lamellae along the (100) plane of orthopyroxene and usually displays undulose extinction. Relict clinopyroxene (less than 1 mm in size) is also present in the margins of some orthopyroxene crystals. Chromium-spinel (less than 1 mm in size) occurs as disseminated and isolated anhedral grains.

Serpentine comprises from 40% to 100% of the secondary mineralogy. Shipboard petrographic identifications indicate that the serpentine phases are primarily mesh-textured lizardite and bladed antigorite. The rocks are variably veined with serpentine and carbonate. Veins are 0.1 to 1 mm-wide and up to 2 cm-long. Vein serpentine is fibrous, oriented orthogonal to vein walls, and is probably chrysotile. Vein carbonate is microcrystalline, whitish-green, and may include subordinate brucite.

The serpentinized dunites vary from black to dun, with some local mottling where veined. The primary mineralogy consists of 95% serpentinized olivine, with about 5% orthopyroxene and up to 1% chromium-spinel (Table 2). A mesh texture characterizes these clasts. Bastite pseudomorphs of orthopyroxene are apparently undeformed and are up to 5 mm in size. Spinel is euhedral, less than 1 mm in size, and forms local bands (up to 10 mm wide) of disseminated grains.

Two clasts of talc bearing serpentine were recovered. They are light greenish-white, have a soapy feel, and are very soft (Mohs' scale hardness of 2). The mineralogy is essentially talc and serpentine, with trace amounts of chromium-spinel.

## Geochemistry

Shipboard X-ray fluorescence (XRF) analyses were carried out on 10 samples of serpentinized, tectonized harzburgite clasts from Site 778. Prior to analysis, samples were crushed in a Spex 8510 shatterbox using a tungsten carbide barrel. This produced some Ta and massive W contamination of the sample. A fully automated wavelength-dispersive ARL8420 XRF (3 kW) system equipped with a Rh target X-ray tube was used to determine the abundance of major oxides and trace elements in whole-rock samples. Systematic errors resulting from short-term or long-term fluctuations in X-ray tube intensity were corrected by normalizing the measured intensities of the samples to those of a standard that is always run with a set of six samples. Loss on ignition (LOI) values were determined by drying the sample at 110$^{o}$C for 8 hours, and then by weighing before and after ignition at 1030$^{o}$C. There is very little variation in the major and trace element composition of the ultramafic rocks analyzed (Fryer, Pearce, Stokking, et al., 1990).

### Major Elements

Volatile loss on ignition (LOI) is high in these samples (Table 3), ranging from 5.53 to 16.06 weight % (wt%), and clearly results from serpentinization. LOI only includes volatile loss between 110$^{o}$C and 1030$^{o}$C and thus represents $H_2O^+$ and $CO_2$. The upper range of LOI values is similar to values reported from numerous serpentinized peridotites (e. g. Michael and Bonatti, 1985), however, the lower values (5.53 and 6.01) are significantly smaller. Total major element percentages are typically 98 to 100 wt%, (including $Cr_2O_3$ and NiO). MgO ranges from 27.30 to 39.61 wt%, and $SiO_2$ ranges from 34.14 to 41.52 wt%. Total iron, calculated as $Fe_2O_3$,

## Table 3.

### Major-element data for ultramafic rocks from Hole 778A

| Core: | 2R-1 | 2R-1 | 3R-CC | 7R-2 | 7R-CC | 8R-1 | 12R-2 | 12R-2 |
|---|---|---|---|---|---|---|---|---|
| Interval (cm): | 53 - 56 | 89 - 92 | 1 - 7 | 73 - 78 | 7 - 13 | 36 - 44 | 43 - 45 | 73 - 75 |
| SiO2 | 38.17 | 35.69 | 40.93 | 34.14 | 37.46 | 34.61 | 41.52 | 39.29 |
| TiO2 | 0.00 | 0.00 | 0.00 | 0.00 | 0.00 | 0.00 | 0.00 | 0.00 |
| Al2O3 | 0.74 | 0.00 | 1.09 | 0.85 | 0.76 | 0.68 | 0.71 | 1.01 |
| Fe2O3 | 6.73 | 6.77 | 7.21 | 8.66 | 7.86 | 8.00 | 8.95 | 7.64 |
| MnO | 0.10 | 0.10 | 0.10 | 0.14 | 0.13 | 0.16 | 0.08 | 0.06 |
| MgO | 36.59 | 35.88 | 36.85 | 39.32 | 39.15 | 39.21 | 39.61 | 37.04 |
| CaO | 0.07 | 3.52 | 0.74 | 0.02 | 0.03 | 0.08 | 0.06 | 0.07 |
| Na2O | 0.09 | 0.09 | 0.00 | 0.09 | 0.00 | 0.00 | 0.00 | 0.00 |
| K2O | 0.01 | 0.00 | 0.01 | 0.01 | 0.05 | 0.00 | 0.00 | 0.00 |
| P2O5 | 0.00 | 0.01 | 0.00 | 0.00 | 0.00 | 0.00 | 0.00 | 0.00 |
| LOI | 15.06 | 15.55 | 11.49 | 14.76 | 13.66 | 16.06 | 6.01 | 11.99 |
| NiO | 0.29 | 0.39 | 0.28 | 0.39 | 0.36 | 0.33 | 0.36 | 0.37 |
| Cr2O3 | 0.36 | 0.07 | 0.37 | 0.41 | 0.33 | 0.37 | 0.42 | 0.53 |
| Total | 98.20 | 98.08 | 99.08 | 98.79 | 99.79 | 99.50 | 97.70 | 98.00 |

Data (in wt% oxides) are for whole-rock analyses by XRF;
LOI is loss on ignition between 150 deg. C and 1030 deg. C.

ranges from 6.73 to 8.95 wt% and $Al_2O_3$ typically ranges from 0.47 to 1.09 wt%. These are within the range of values reported from serpentinized ultramafic samples elsewhere (e. g. Michael and Bonatti, 1985). Other major elements have predictably low abundances: CaO is typically less than 0.10 wt%, although two samples reach 0.78 wt% (Table 3), MnO ranges from 0.08 to 0.16 wt% in all samples, and the usual ranges for $TiO_2$, $Na_2O$, $K_2O$, and $P_2O_5$ are near the detection limit (less than 0.02 wt%). One sample, 125-778A-2R-1, 89 to 92 cm, falls outside some of the typical ranges of major element concentrations with no $Al_2O_3$ (0.00 wt%) and high CaO (3.52 wt%) (Fryer, Pearce, Stokking, et al., 1990).

Trace Elements

The compatible elements are predictably quite high in concentration (Table 4). Typical values for Ni range from 2173 to 3039 ppm, while Cr is more restricted ranging from 2260 to 2785 ppm. As expected for residual mantle material, abundances of incompatible elements (Nb, Zr, Sr, Rb) are low, ranging from none detected (nd) to 2 ppm (near the detection limit). Transition elements each fall within a restricted range: Zn from 28 to 64 ppm; V from 22 to 62 ppm; and Cu from 2 to 14 ppm. Ce and Ba are typically below the detection limit of 10 ppm. There are no significant correlations between trace element concentrations and depth.

Sample 125-778A-2R-1, 89 to 92 cm, does not follow the patterns described above and has very low Cr (501 ppm), very high Sr (595 ppm) and CaO (3.52 wt%), and falls at the low end of the ranges for V (22 ppm) and Zn (28 ppm) and the high end of the Ni range (3039 ppm). With the exception of Sr, this sample is indistinguishable from the other samples on the basis of the more incompatible elements. High Sr and CaO may be

**Table 4.**

**Trace-element data for ultramafic rocks from Hole 778A**

| Core: | 2R-1 | 2R-1 | 3R-CC | 7R-2 | 7R-CC | 8R-1 | 12R-2 | 12R-2 |
|---|---|---|---|---|---|---|---|---|
| Interval (cm): | 53 - 56 | 89 - 92 | 1 - 7 | 73 - 78 | 7 - 13 | 36 - 44 | 43 - 45 | 73 - 75 |
| Nb | tr | tr | tr | tr | tr | tr | tr | tr |
| Zr | 1 | 2 | 0 | 1 | 1 | 1 | 0 | 1 |
| Y | 0 | nd | 1 | nd | nd | nd | 1 | nd |
| Sr | 9 | 595 | 5 | 2 | 3 | 8 | 9 | 12 |
| Rb | 0 | nd | 1 | nd | 1 | 1 | nd | 0 |
| Zn | 52 | 28 | 36 | 39 | 42 | 64 | 42 | 40 |
| Cu | 3 | 3 | 11 | 2 | 2 | 4 | 8 | 2 |
| Ni | 2281 | 3039 | 2173 | 3034 | 2818 | 2638 | 2813 | 2905 |
| Cr | 2496 | 501 | 2523 | 2786 | 2261 | 2510 | 2866 | 3603 |
| V | 46 | 22 | 40 | 38 | 41 | 48 | 48 | 62 |
| Ti | 0 | 0 | 0 | 0 | 0 | 0 | 0 | 0 |
| Ce | tr | tr | nd | tr | nd | nd | tr | nd |
| Ba | tr | nd | tr | nd | nd | 10 | nd | nd |

Data (in ppm) are for whole-rock analyses by XRF;
tr=below detection limits (<5 ppm for Nb; <10 ppm for Ba and Ce);
nd = not detected (background count was greater than sample count).

accommodated in secondary minerals, such as carbonates, which are found within the veins. The low Cr may indicate significant alteration of chromite to magnetite or reflect a low initial chromite content in the sample (Fryer, Pearce, and Stokking, et al., 1990).

## 2) SITE 779-----CONICAL SEAMOUNT SOUTHEAST FLANK SITE

### Principal Results

Site 779 (19°30.75'N, 146°41.75'E), about 3.5 km northeast of Site 778, is located approximately in the midflank region of the southeast quadrant of Conical Seamount at a depth of 3947.2 mbsl (Figure 26). The scientific objectives of Site 779 were identical to those for Site 778. Side-scan sonar and *Alvin* submersible studies indicated that this area is mantled by a pelagic sediment cover, overlying exposures of unconsolidated serpentine muds, containing serpentinized clasts of mafic and ultramafic rocks (Fryer, et al, 1985, Fryer, et al., 1990). The ultramafic clasts recovered are similar to those from Site 778, mostly harzburgites and subordinate dunite. Thus, the rocks from this site provide further evidence for the refractory nature of the peridotite as a consequence of partial melting in a supra-subduction zone environment. The degree of serpentinization varies, but generally decreases downhole to a depth of ~125 meters below seafloor (mbsf) (core 16). It increases again from about 170 mbsf (core 22) to at least 235 mbsf (core 28). Thus, the freshest samples are from cores 16-19 (135-170 mbsf).

Shipboard petrographic observations indicate that medium-grade metamorphism is characteristic of the source region.

## Petrography

The serpentinized and tectonized harzburgites are massive and vary from light to dark gray (where relatively fresh) to dark gray-green (where serpentinized). The primary minerals in these rocks are olivine, orthopyroxene, chromium-spinel, and subordinate clinopyroxene (Table 2). Orthopyroxene varies from about 10 to 40 modal %, with olivine forming most of the remainder. Clinopyroxene (1-3 modal %) is present as exsolution lamellae in orthopyroxene and as anhedral crystals less than 1 mm in diameter, typically situated near the margins of the orthopyroxene. Chromium-spinel exists in trace amounts to about 2 modal % and contains rare, brightly reflective grains that may be a sulfide mineral or a metallic alloy (rich in platinum-group elements).

These harzburgites have experienced penetrative deformation. Typically, orthopyroxene crystal morphologies range from equant to raggedly elongate with wavy cleavage surfaces and extinction. Kink-banding is also very common in these rocks and thin clinopyroxene lamellae are bent, probably the result of metamorphicly induced stress. Chromium-spinel crystals range from equant (less than 0.2 mm in size) to disrupted dumbbell-type shapes. Stringers of these elongate spinels define a crude lineation parallel to elongate olivine and orthopyroxene. In the orthopyroxene-rich types, rounded olivines are sometimes found within orthopyroxene.

The degree of serpentinization is extremely variable. In some samples, most of the olivine and orthopyroxene have been replaced by the mesh-textured serpentine and relict bastite, respectively. In these strongly serpentinized rocks, all of the original chromium-spinel (translucent in shades of deep reddish-brown/green when fresh) has been replaced by an

opaque oxide mineral, probably magnetite. In some samples, this transformation process is incomplete. These partially altered spinels have original chromium-rich translucent cores, rims of magnetite, and radially arranged halos of microcrystalline chlorite (probably penninite). This type of alteration also has penetrated cracks in the original spinel grains.

There are numerous veins of serpentine (up to about 40-mm wide) cutting the harzburgites, many of which record a multistage history of filling. The degree of serpentinization of the harzburgite is usually greater near the veins. Antigorite or lizardite fills most of these veins. Some veins contain chrysotile that has grown both parallel to the original fracture walls and as discontinuous, crosscutting subsets. Subordinate brucite also is present. Some spinel trains are dislocated during the formation of serpentine veins. Orthopyroxenes, adjacent to the veins in some samples, have been altered to chlorite. Typically, serpentinization affected olivine the most, orthopyroxene less, and clinopyroxene the least. However, in several samples, serpentinization may have affected orthopyroxene more than olivine.

The serpentinized and tectonized dunites are generally massive, vary from deep greenish-black to black, and sometimes grade to harzburgite over distances of a few millimeters. The primary mineralogy consists of 90%-99% olivine, 1%-9% orthopyroxene, and up to 1% chromium-spinel (Table 2). Most dunites have been extensively serpentinized and exhibit mesh texture and splays of antigorite. They are also cut by numerous serpentine-rich veins. Some samples contain crudely-aligned, elongate (less than 15 mm), and irregularly-shaped olivine that tends to form a sheared fabric. Micro-granulation of olivine, kink-banding in bastite, elongation of spinel, and deformation of clinopyroxene exsolution lamellae in orthopyroxene all

provide evidence of penetrative tectonism. An unusually large amount of fresh olivine persists in a few samples, despite transformation of almost all of the orthopyroxene to serpentine. Spinel is completely altered to magnetite in the serpentinized portions. Other secondary minerals include chlorite and brucite (Fryer, Pearce, Stokking, et al., 1990).

## Geochemistry

Shipboard geochemical (XRF) analyses of clasts entrained within the serpentine mud at Site 779 were carried out on 32 samples of serpentinized, tectonized ultramafics, both harzburgites (21 samples) and dunites (11 samples). All ultramafic samples are remarkably homogeneous chemically and deviate very little from average values (Tables 5 and 6) (Fryer, Pearce, Stokking, et al., 1990).

### Major Elements

LOI of these samples ranges from 4.77 to 17.41 wt%, and correlates positively with percent serpentinization. Although ranges of major element concentrations are similar in dunite and harzburgite samples, some small distinctions exist. (Table 5). $SiO_2$ ranges from 29.39 to 40.80 wt% in both harzburgite and dunite samples, and MgO is slightly higher in the dunite samples (38.94-43.43 wt%) than in the harzburgite samples (37.34-42.69 wt%). $Al_2O_3$ is slightly lower in the dunites (0.07-0.60 wt%) than the harzburgites (0.21-0.88 wt%); $Fe_2O_3$ is also lower in the dunites (5.66-8.05 wt%) than in the harzburgites (7.00-9.04 wt%). Mg# [Mg= Mg/(Mg+Fe) x 100] is high in all rocks, ranging from 89.84 to 93.65. $Na_2O$ and $P_2O_5$ are not detected, and $K_2O$ 0 to 0.3 wt% with one exception: sample 125-779A-24-1, 36-38 cm, dunite has 4.00 wt% $K_2O$. In all rocks, $SiO_2$ and MgO are

Table 5.

Major-element data for ultramafic rocks from Hole 779A

Dunites

| Core: | 3R-CC | 8R-1 | 10R-1 | 14R-1 | 14R-2 | 15R-2 | 16R-1 | 19R-2 | 22R-2 | 22R-3 | 24R-1 | 25R-1 | average |
|---|---|---|---|---|---|---|---|---|---|---|---|---|---|
| Interval (cm): | 13 - 15 | 90 - 93 | 40 - 43 | 74 - 77 | 21 - 24 | 24 - 27 | 19 - 23 | 97 - 99 | 18 - 20 | 55 - 57 | 36 - 38 | 85 - 87 | Dunite |
| SiO2 | 36.74 | 39.47 | 38.14 | 38.30 | 35.25 | 35.54 | 40.80 | 39.21 | 39.47 | 38.09 | 34.50 | 34.44 | 37.50 |
| TiO2 | 0.00 | 0.00 | 0.00 | 0.00 | 0.00 | 0.00 | 0.00 | 0.00 | 0.00 | 0.00 | 0.00 | 0.00 | 0.00 |
| Al2O3 | 0.39 | 0.28 | 0.63 | 0.38 | 0.07 | 0.07 | 0.60 | 0.19 | 0.40 | 0.10 | 0.46 | 0.12 | 0.31 |
| Fe2O3 | 7.38 | 7.63 | 8.08 | 7.33 | 7.14 | 5.66 | 8.05 | 8.15 | 7.36 | 7.76 | 7.31 | 7.02 | 7.41 |
| MnO | 0.10 | 0.11 | 0.12 | 0.10 | 0.09 | 0.08 | 0.10 | 0.12 | 0.10 | 0.11 | 0.11 | 0.09 | 0.10 |
| MgO | 40.31 | 41.21 | 41.19 | 41.71 | 41.35 | 42.14 | 43.43 | 44.36 | 40.95 | 42.96 | 38.94 | 43.40 | 41.83 |
| CaO | 0.14 | 0.15 | 0.60 | 0.44 | 0.10 | 0.21 | 0.54 | 0.25 | 0.15 | 0.13 | 0.37 | 0.20 | 0.27 |
| Na2O | 0.00 | 0.00 | 0.00 | 0.00 | 0.00 | 0.00 | 0.00 | 0.00 | 0.00 | 0.00 | 0.00 | 0.00 | 0.00 |
| K2O | 0.02 | 0.00 | 0.00 | 0.01 | 0.00 | 0.02 | 0.01 | 0.00 | 0.00 | 0.00 | 4.00 | 0.00 | 0.34 |
| P2O5 | 0.00 | 0.00 | 0.00 | 0.00 | 0.00 | 0.00 | 0.00 | 0.00 | 0.00 | 0.00 | 0.00 | 0.00 | 0.00 |
| NiO | 0.28 | 0.28 | 0.30 | 0.31 | 0.30 | 0.45 | 0.32 | 0.32 | 0.27 | 0.30 | 0.29 | 0.34 | 0.31 |
| Cr2O3 | 0.42 | 0.39 | 0.41 | 0.35 | 0.21 | 0.19 | 0.33 | 0.22 | 0.30 | 0.18 | 0.25 | 0.32 | 0.30 |
| LOI | 14.18 | 9.55 | 9.28 | 9.00 | 14.64 | 16.71 | 4.77 | 6.22 | 9.26 | 9.17 | 16.27 | 12.77 | 10.99 |
| Total | 99.27 | 98.39 | 98.06 | 97.27 | 98.64 | 98.42 | 98.31 | 98.50 | 97.74 | 98.32 | 101.97 | 98.05 | 98.58 |
| Mg# | 91.54 | 91.45 | 90.99 | 91.85 | 91.98 | 93.65 | 91.45 | 91.51 | 91.68 | 91.65 | 91.35 | 92.45 | 91.80 |
| % SERP | 80 | 78 | 55 | 70 | 85 | 85 | 17 | 35 | 85 | 60 | 93 | 85 | 69 |

Data (in wt% oxides) are from whole-rock analyses by XRF;
LOI = Loss on ignition between 150 deg. C. and 1030 deg. C.;
%SERP = percentage of serpentinization estimated from thin sections.

Table 5. (continued)

Major-element data for ultramafic rocks from Hole 779A

Harzburgites

| Core: | 4R-1 | 5R-2 | 5R-2 | 6R-1 | 8R-1 | 8R-1 | 9R-2 | 11R-1 | 12R-1 | 13R-1 | 13R-2 | 14R-2 |
|---|---|---|---|---|---|---|---|---|---|---|---|---|
| Interval (cm): | 27 - 30 | 34 - 37 | 40 - 43 | 18 - 20 | 45 - 48 | 57 - 60 | 52 - 54 | 14 - 18 | 38 - 42 | 2 - 5 | 52 - 54 | 139-141 |
| SiO2 | 33.64 | 36.46 | 35.12 | 37.57 | 38.35 | 29.39 | 35.45 | 36.49 | 36.81 | 32.18 | 38.62 | 38.08 |
| TiO2 | 0.00 | 0.00 | 0.00 | 0.00 | 0.00 | 0.00 | 0.00 | 0.00 | 0.00 | 0.00 | 0.00 | 0.00 |
| Al2O3 | 0.20 | 0.21 | 0.21 | 0.77 | 0.49 | 0.57 | 0.28 | 0.41 | 0.19 | 0.25 | 0.66 | 0.88 |
| Fe2O3 | 7.04 | 7.71 | 7.23 | 7.72 | 7.69 | 9.04 | 7.47 | 7.00 | 7.50 | 8.15 | 7.77 | 7.35 |
| MnO | 0.14 | 0.09 | 0.10 | 0.11 | 0.11 | 0.17 | 0.10 | 0.10 | 0.10 | 0.12 | 0.11 | 0.11 |
| MgO | 40.13 | 40.18 | 39.87 | 39.61 | 40.00 | 41.22 | 41.32 | 39.14 | 41.50 | 40.35 | 40.03 | 37.34 |
| CaO | 0.07 | 0.22 | 0.08 | 0.55 | 0.53 | 0.14 | 0.36 | 0.50 | 0.33 | 0.32 | 0.79 | 0.81 |
| Na2O | 0.00 | 0.00 | 0.00 | 0.00 | 0.00 | 0.00 | 0.00 | 0.00 | 0.00 | 0.00 | 0.00 | 0.00 |
| K2O | 0.00 | 0.02 | 0.00 | 0.01 | 0.01 | 0.00 | 0.01 | 0.01 | 0.01 | 0.00 | 0.00 | 0.02 |
| P2O5 | 0.00 | 0.00 | 0.00 | 0.00 | 0.00 | 0.00 | 0.00 | 0.00 | 0.00 | 0.00 | 0.00 | 0.00 |
| NiO | 0.31 | 0.29 | 0.28 | 0.28 | 0.29 | 0.32 | 0.31 | 0.28 | 0.29 | 0.30 | 0.29 | 0.28 |
| Cr2O3 | 0.24 | 0.19 | 0.24 | 0.26 | 0.37 | 0.41 | 0.22 | 0.24 | 0.21 | 0.33 | 0.27 | 0.43 |
| LOI | 16.66 | 14.62 | 16.35 | 12.42 | 11.01 | 17.41 | 14.03 | 14.83 | 12.33 | 16.87 | 11.28 | 13.82 |
| Total | 98.54 | 98.83 | 98.95 | 98.75 | 98.19 | 97.95 | 99.02 | 98.48 | 98.76 | 98.24 | 99.27 | 98.42 |
| Mg# | 91.16 | 91.88 | 91.62 | 91.04 | 91.16 | 90.03 | 91.64 | 91.72 | 91.64 | 90.75 | 91.08 | 90.96 |
| % SERP | 100 | 40 | 93 | 78 | 100 | 100 | 40 | 98 | 78 | 100 | 75 | 50 |

Data (in wt% oxides) are from whole-rock analyses by XRF;
LOI = Loss on ignition between 150 deg. C. and 1030 deg. C.;
%SERP = percentage of serpentinization estimated from thin sections.

Table 5. (continued)

**Major-element data for ultramafic rocks from Hole 779A**

**Harzburgites**

| Core: | 16R-2 | 17R-2 | 17R-3 | 22R-1 | 22R-1 | 26R-2 | 26R-3 | 28R-3 | average |
|---|---|---|---|---|---|---|---|---|---|
| Interval (cm): | 74 - 77 | 14 - 17 | 77 - 80 | 58 - 60 | 63 - 65 | 50 - 52 | 101-103 | 26 - 28 | Harzburgite |
| SiO2 | 38.7 | 40.20 | 37.37 | 29.13 | 38.61 | 39.61 | 37.09 | 35.53 | 36.26 |
| TiO2 | 0 | 0.00 | 0.00 | 0.00 | 0.00 | 0.00 | 0.00 | 0.00 | 0.00 |
| Al2O3 | 0.64 | 0.37 | 0.30 | 0.29 | 0.17 | 0.69 | 0.63 | 0.19 | 0.40 |
| Fe2O3 | 7.38 | 7.36 | 6.98 | 9.25 | 7.47 | 8.11 | 7.08 | 7.07 | 7.63 |
| MnO | 0.11 | 0.10 | 0.09 | 0.17 | 0.11 | 0.11 | 0.10 | 0.10 | 0.11 |
| MgO | 39.33 | 42.69 | 39.47 | 41.26 | 41.84 | 40.95 | 39.50 | 39.32 | 40.38 |
| CaO | 0.62 | 0.35 | 0.29 | 0.16 | 0.23 | 0.80 | 0.58 | 0.35 | 0.39 |
| Na2O | 0 | 0.00 | 0.00 | 0.00 | 0.00 | 0.00 | 0.00 | 0.00 | 0.00 |
| K2O | 0.03 | 0.01 | 0.01 | 0.00 | 0.01 | 0.00 | 0.00 | 0.00 | 0.01 |
| P2O5 | 0 | 0.00 | 0.00 | 0.00 | 0.00 | 0.00 | 0.00 | 0.00 | 0.00 |
| NiO | 0.28 | 0.32 | 0.30 | 0.33 | 0.30 | 0.29 | 0.28 | 0.29 | 0.30 |
| Cr2O3 | 0.32 | 0.28 | 0.26 | 0.57 | 0.42 | 0.29 | 0.24 | 0.25 | 0.30 |
| LOI | 11.46 | 6.81 | 15.40 | 16.93 | 10.01 | 8.57 | 13.32 | 15.63 | 13.28 |
| Total | 98.27 | 97.90 | 98.92 | 97.19 | 98.44 | 98.84 | 98.30 | 98.19 | 98.47 |
| Mg# | 91.35 | 92.00 | 91.81 | 89.84 | 91.73 | 90.91 | 91.70 | 91.68 | 91.29 |
| % SERP | 75 | 25 | 35 | 75 | 50 | 45 | 35 | 100 | 69 |

Data (in wt% oxides) are from whole-rock analyses by XRF;
LOI = Loss on ignition between 150 deg. C. and 1030 deg. C.;
%SERP = percentage of serpentinization estimated from thin sections.

inversely correlated with percentage of serpentinization (Fryer, Pearce, Stokking, et al., 1990).

Trace Elements

Trace element data are presented in Table 6. Compatible element abundances are predictably high in both the dunite and harzburgite samples: Cr values ranges from 1216 to 2917 ppm with a single high Cr value in sample 125-779A-22-1, 58-60 cm, a harzburgite which contains 3914 ppm. Ni values range from 2171 to 2541 ppm with the exception of a single high Ni value in sample 125-779A-15-2, 24-27 cm, a dunite which contains 3527 ppm. Cr and Ni do not correlate with one another nor with degree of serpentinization. Nb, Zr, Y, Rb and Ti are present at low or trace levels. Ce and Ba values are typically below detection limits, although four samples have Ba values of 16 ppm or greater. Sr, Zn, and V are slightly lower in the dunites (Sr less than 5 ppm; Zn less than 46 ppm; V = 8-42 ppm) than the harzburgites (Sr less than 21 ppm; Zn less than 63 ppm; V = 4-50 ppm). Dunite sample, 125-779A-24-1, 36-38 cm, has 21 ppm Sr. There is no significant correlation between geochemical parameters and depth below the seafloor (Fryer, Pearce, Stokking, et al., 1990).

Although the samples analyzed from Site 778 and 779 are generally similar, several element concentrations ($Al_2O_3$ and Ni ) are slightly less in Site 778 samples than in Site 779 samples (Tables 3 and 5), and others (MgO and CaO) are slightly greater.

Table 6.

**Trace-element data for ultramafic rocks from Hole 779A**

**Dunites**

| Core: | 3R-CC | 8R-1 | 10R-1 | 14R-1 | 14R-2 | 15R-2 | 16R-1 | 19R-2 | 22R-2 | 22R-3 | 24R-1 | 25R-1 | average |
|---|---|---|---|---|---|---|---|---|---|---|---|---|---|
| Interval (cm): | 13 - 15 | 90 - 93 | 40 - 43 | 74 - 77 | 21 - 24 | 24 - 27 | 19 - 23 | 97 - 99 | 18 - 20 | 55 - 57 | 36 - 38 | 85 - 87 | Dunite |
| Nb | tr | tr | tr | tr | tr | tr | tr | tr | tr | tr | tr | tr | tr |
| Zr | 1 | 1 | 1 | 0 | 0 | 1 | 1 | 1 | 1 | 1 | 1 | 1 | 1 |
| Y | nd | 0 | 2 | 1 | nd | nd | 0 | 1 | 1 | 0 | 0 | nd | 0 |
| Sr | 2 | 2 | 2 | 4 | 0 | 4 | 0 | nd | 1 | 4 | 21 | 3 | 4 |
| Rb | 1 | 0 | nd | 1 | 0 | 1 | 0 | nd | nd | 1 | nd | 0 | 0 |
| Zn | 31 | 36 | 35 | 34 | 22 | 33 | 37 | 33 | 31 | 32 | 46 | 33 | 34 |
| Cu | 1 | 2 | 7 | nd | 1 | nd | 5 | 4 | 2 | 3 | 2 | 3 | 2 |
| Ni | 2238 | 2208 | 2396 | 2446 | 2398 | 3527 | 2515 | 2520 | 2163 | 2382 | 2667 | 2486 | 2496 |
| Cr | 2903 | 2650 | 2796 | 2396 | 1144 | 1319 | 2236 | 1509 | 2024 | 1216 | 1688 | 2167 | 2004 |
| V | 25 | 22 | 42 | 22 | 12 | 11 | 32 | 13 | 29 | 8 | 23 | 8 | 21 |
| Ce | tr | tr | tr | tr | tr | tr | tr | tr | tr | tr | tr | tr | tr |
| Ba | tr | 13 | tr | tr | tr | nd | 13 | nd | 12 | tr | tr | nd | tr |

Data (in ppm) are from whole-rock analyses by XRF;
tr = below detection limit (<5 ppm for Nb; <10 ppm for Ba and Ce);
nd = not detected (background count was greater than sample count).

Table 6. (continued)

Trace-element data for ultramafic rocks from Hole 779A

Harzburgites

| Core: | 4R-1 | 5R-2 | 5R-2 | 6R-1 | 8R-1 | 8R-1 | 9R-2 | 11R-1 | 12R-1 | 13R-1 | 13R-2 | 14R-2 |
|---|---|---|---|---|---|---|---|---|---|---|---|---|
| Interval (cm): | 27 - 30 | 34 - 37 | 40 - 43 | 18 - 20 | 45 - 48 | 57 - 60 | 52 - 54 | 14 - 18 | 38 - 42 | 2 - 5 | 52 - 54 | 139-141 |
| Nb | tr | tr | tr | tr | tr | tr | tr | tr | tr | tr | tr | tr |
| Zr | 1 | 1 | 1 | 1 | 1 | 0 | 1 | 1 | 1 | nd | nd | 0 |
| Y | nd | 1 | 0 | 0 | 1 | 0 | 0 | nd | nd | 0 | 1 | 0 |
| Sr | 5 | 14 | 6 | 8 | 11 | 8 | 8 | 20 | 11 | 12 | 1 | 4 |
| Rb | 0 | 1 | nd | 0 | 0 | 0 | nd | nd | 1 | 0 | 0 | 1 |
| Zn | 44 | 32 | 49 | 35 | 38 | 63 | 36 | 36 | 31 | 56 | 30 | 39 |
| Cu | 2 | 2 | 4 | 1 | 3 | 3 | 1 | 1 | 2 | 1 | 6 | 10 |
| Nl | 2290 | 2203 | 2171 | 2302 | 2302 | 2541 | 2476 | 2181 | 2313 | 2391 | 2267 | 2185 |
| Cr | 1667 | 1278 | 1629 | 1752 | 2542 | 2841 | 1517 | 1632 | 1434 | 2256 | 1824 | 2917 |
| V | 15 | 21 | 19 | 29 | 29 | 41 | 15 | 24 | 20 | 16 | 31 | 50 |
| Ce | tr | nd | nd | nd | nd | tr | tr | nd | tr | tr | 15 | tr |
| Ba | tr | 20 | tr | 21 | tr | nd | nd | tr | 14 | tr | tr | 20 |

Data (in ppm) are from whole-rock analyses by XRF;
tr = below detection limit (<5 ppm for Nb; <10 ppm for Ba and Ce);
nd = not detected (background count was greater than sample count).

Table 6. (continued)

**Trace-element data for ultramafic rocks from Hole 779A**

**Harzburgites**

| Core: | 16R-2 | 17R-2 | 17R-3 | 22R-1 | 22R-1 | 26R-2 | 26R-3 | 28R-3 | average |
|---|---|---|---|---|---|---|---|---|---|
| Interval (cm): | 74 - 77 | 14 - 17 | 77 - 80 | 58 - 60 | 63 - 65 | 50 - 52 | 101-103 | 26 - 28 | Harzburgite |
| Nb | tr | tr | tr | tr | tr | tr | tr | tr | tr |
| Zr | 0 | 0 | 1 | 1 | 1 | 1 | 1 | 1 | 1 |
| Y | 0 | 1 | nd | 0 | 0 | 1 | nd | 0 | 0 |
| Sr | 1 | 1 | 1 | 6 | 1 | 1 | 21 | 28 | 8 |
| Rb | 1 | 1 | 1 | nd | 0 | nd | nd | nd | 0 |
| Zn | 31 | 30 | 32 | 57 | 37 | 35 | 36 | 37 | 39 |
| Cu | 3 | 4 | 3 | 2 | 3 | 7 | 2 | 1 | 3 |
| Nl | 2244 | 2502 | 2389 | 2571 | 2360 | 2308 | 2185 | 2251 | 2322 |
| Cr | 2166 | 1920 | 1786 | 3914 | 2888 | 1956 | 1616 | 1682 | 2061 |
| V | 31 | 32 | 21 | 23 | 28 | 30 | 24 | 4 | 25 |
| Ce | tr | tr | tr | tr | nd | nd | tr | nd | tr |
| Ba | tr | tr | 13 | nd | tr | tr | tr | 17 | tr |

Data (in ppm) are from whole-rock analyses by XRF;
tr = below detection limit (<5 ppm for Nb; <10 ppm for Ba and Ce);
nd = not detected (background count was greater than sample count).

## 3) SITE 780-----CONICAL SEAMOUNT SUMMIT SITE

### Principal Results

Site 780 (19°32.5'N, 146°39.2'E) is located on the western side of Conical Seamount near the summit, at a depth of 3083.4 mbsl (Figure 26) *Alvin* submersible studies had shown this area to be only partly sediment-covered and lie near active venting fields where chimney structures are forming (Fryer, et al., 1987; Fryer, et al., 1990).

The ultramafic clasts from the holes drilled at the summit are exclusively serpentinized harzburgite and are very uniform in both composition and degree of alteration. The rocks are moderately to highly altered (61% to 100%)and exhibit evidence of metamorphism characteristic of moderate temperature and pressure as described by Wicks (1979). The source, as for clasts at Sites 778 and 779, is a depleted, supra-subduction zone peridotite.

Rheological studies performed on board ship suggest the muds drilled at the summit are capable of supporting large clasts (maximum of 20 m diameter) and of transporting them during rise and protrusion of the relatively low density (1.5-2.0 g/cc for the matrix vs. 2.5-3.0 g/cc for the clasts) serpentine mud matrix of the flows that form the seamount. The presence of fluids with high pH, high alkalinity, and very low magnesium (Fryer and Mottl, in press) within a few meters of the seafloor precludes mixing between entrained fluids and seawater at shallow sub-bottom levels near the summit. The presence of these fluids at depth in the summit is interpreted to indicate an active egress of fluids through a central conduit (Fryer, Pearce, Stokking, et al., 1990). The more uniform degree of

alteration of the ultramafic clasts may reflect prolonged contact with conduit-related fluids.

## Petrography

The serpentinized and tectonized harzburgites are massive and range from gray, where relatively fresh, to bluish gray, where serpentinized (e.g. Interval 125-780C-18R-1, 36-45 cm, and 25-36 cm, respectively). The primary mineralogy of these rocks is olivine (75%-90%), orthopyroxene (10%-25%), chromium-spinel (trace to 2%), and clinopyroxene (trace to 2%) (Table 2). Clinopyroxene is present as exsolution lamellae on (100) in orthopyroxene and as anhedral crystals (less than 1 mm), typically closely related to orthopyroxene.

The harzburgites display penetrative deformation. Typically, orthopyroxene crystals are 1 to 4 mm in diameter and range from equant to asymmetric-elongate. Kink-banding is common, thin clinopyroxene exsolution lamellae on (100) are bent, and cleavage surfaces and extinction are wavy. Elongate crystals (less than 5-mm long) and kink-banding (sometimes showing fine lamellae) characterize some of the olivine morphologies. Microgranular (less than 0.5 mm equant crystals) fabrics indicative of recrystallization under temperatures greater than 300$^{o}$C are also present. Chromium-spinel crystals range from equant (0.5 mm in size) to elongated shapes (up to 2 mm long). Some of the elongate spinels define a lineation parallel to the elongate olivine and orthopyroxene.

The degree of serpentinization varies from 50%-100%, with the olivine and the orthopyroxene replaced by mesh-textured serpentine (chrysotile-rich) and bastite, respectively. In these strongly serpentinized samples, most of the chromium-spinel appears to be fresh. Antigorite and

brucite may also be present. The harzburgite clasts are cut by numerous veins of serpentine showing a multistage history of filling.

The serpentinized and tectonized dunites are greenish dark-gray, are generally massive, and sometimes grade to harzburgite. The primary mineralogy consists of olivine (90%-99%), orthopyroxene (1%-9%), and spinel (trace to 1%) (Table 2). Most dunites are extensively (90%-100%) serpentinized and show mesh textures and are cut by numerous serpentine-rich veins. Some dunite samples are rich in antigorite (based on the presence of the bladed-textured serpentine) and brucite (based on characteristic yellow birefringence color). Microgranulation of relict olivine, kink-banding of orthopyroxene and olivine, and asymmetric elongation of spinel are evidence of penetrative deformation. Other secondary minerals include magnetite, which replaces chromium-spinel and is found in serpentine veins, and up to 5% chlorite, clays (after serpentine) and talc (Fryer, Pearce, Stokking, et al., 1990).

## Geochemistry

Six of the ultramafic clasts (five harzburgite, one dunite) from Site 780 were selected for shipboard geochemical (XRF) analysis. The compositions of the ultramafic rocks are similar (Tables 7 and 8) and deviate very little from the average harzburgite values (Fryer, Pearce, Stokking, et al., 1990).

### Major Elements

LOI (loss on ignition) of these samples ranges from 5.28 to 12.31 wt%. Concentrations of major element oxides are similar in the single dunite sample (125-780C-8R-1, 98-101 cm) and the harzburgites (Table 7). $SiO_2$ ranges from 37.76 to 40.70 wt%, and MgO ranges from 39.13 to 42.94 wt%.

Table 7.

**Major-element data for ultramafic rocks from Hole 780C**

| | Harzburgites | | | | | | Dunite |
|---|---|---|---|---|---|---|---|
| Core: | 6R-1 | 10R-1 | 16R-1 | 18R-1 | 18R-1 | avg. | 8R-1 |
| Interval (cm): | 61 - 62 | 13 - 16 | 53 - 59 | 54 - 57 | 58 - 61 | harz. | 98-101 |
| SiO2 | 40.70 | 38.42 | 37.76 | 38.56 | 38.85 | 38.86 | 38.43 |
| TiO2 | 0.00 | 0.00 | 0.00 | 0.00 | 0.00 | 0.00 | 0.00 |
| Al2O3 | 0.47 | 0.60 | 0.54 | 0.63 | 0.66 | 0.58 | 0.65 |
| Fe2O3 | 7.91 | 7.45 | 7.44 | 7.80 | 7.81 | 7.68 | 7.84 |
| MnO | 0.11 | 0.11 | 0.11 | 0.11 | 0.11 | 0.11 | 0.11 |
| MgO | 42.94 | 39.04 | 39.97 | 39.13 | 38.87 | 39.99 | 39.78 |
| CaO | 0.60 | 0.79 | 0.69 | 0.86 | 0.89 | 0.77 | 0.50 |
| Na2O | 0.00 | 0.00 | 0.00 | 0.00 | 0.00 | 0.00 | 0.00 |
| K2O | 0.00 | 0.02 | 0.01 | 0.00 | 0.00 | 0.01 | 0.01 |
| P2O5 | 0.00 | 0.00 | 0.03 | 0.00 | 0.00 | 0.01 | 0.00 |
| NiO | 0.29 | 0.28 | 0.29 | 0.29 | 0.28 | 0.29 | 0.29 |
| Cr2O3 | 30.24 | 0.31 | 0.31 | 0.28 | 0.34 | 0.30 | 0.34 |
| LOI | 5.28 | 12.31 | 12.06 | 11.13 | 11.12 | 10.38 | 11.90 |
| Total | 98.55 | 99.31 | 98.60 | 98.78 | 98.92 | 98.83 | 99.84 |
| Mg# | 91.49 | 91.21 | 91.41 | 90.86 | 90.79 | 91.16 | 90.95 |
| % SERP | 65 | 65 | 70 | 75 | 75 | 70 | 55 |

Data (in wt% oxides) are from whole-rock analyses by XRF;
LOI = loss on ignition between 150 deg. C. and 1030 deg. C.;
%SERP = percentage of serpentinization as estimated from thin sections.

$SiO_2$ and MgO are both inversely correlated with LOI. $Al_2O_3$ ranges from 0.47 to 0.65 wt%, and $Fe_2O_3$ ranges from 7.44 to 7.91 wt%. Mg# is high, ranging from 90.86 to 91.49. $Na_2O$, $K_2O$, and $P_2O_5$ are low in all samples; $K_2O$ and $P_2O_5$ reach 0.02 and 0.03 wt%, respectively; $Na_2O$ is below the detection limit (less than 0.01 wt%) (Fryer, Pearce, Stokking, et al., 1990).

Trace Elements

Trace element data are presented in Table 8. Predictably, the compatible elements have a high concentration in all samples; Cr ranges from 1620 to 2303 ppm, and Ni ranges from 2188 to 2319 ppm. Average concentration of Ni (harzburgite: 2261 ppm, dunite: 2280 ppm) is slightly lower in samples from Site 780 than for samples from Sites 778 (harzburgite: 2644 ppm) and 779 (harzburgite: 2320 ppm, dunite: 2486 ppm). Cr and Ni do not correlate with one another nor with degree of serpentinization. Nb, Zr, Y, Rb, and Ti are all present at low or trace levels. Ce and Ba values are typically below detection limits, although two samples have Ba concentrations greater than 13 ppm. Sr reaches a maximum of 11 ppm and V ranges from 23 to 41 ppm. Sr and V concentrations are similar to those in Sites 778 and 779. Zn ranges from 32 to 35 ppm with a single high concentration (Sample 125-780C-16X-1, 53 to 59 cm) of 45 ppm. Zn averages 36 ppm for harzburgite and 32 ppm for dunite in samples from Site 780, which is slightly lower than the average concentrations for Sites 778 (harzburgite: 42 ppm) and 779 (harzburgite: 39 ppm, dunite: 34 ppm). There is no significant correlation between geochemical parameters and depth below the seafloor.

The samples analyzed from Site 780 are, therefore, quite similar to those from Sites 778 and 779. The few differences between the chemistry of

Table 8.

Trace-element data for ultramafic rocks from Hole 780C

| | Harzburgites | | | | | | Dunite |
|---|---|---|---|---|---|---|---|
| Core: | 6R-1 | 10R-1 | 16R-1 | 18R-1 | 18R-1 | avg. | 8R-1 |
| Interval (cm): | 61 - 62 | 13 - 16 | 53 - 59 | 54 - 57 | 58 - 61 | harz. | 98-101 |
| Nb | tr | tr | tr | tr | tr | tr | tr |
| Zr | 0 | 1 | 1 | 1 | 1 | 1 | 1 |
| Y | nd | 0 | 0 | 1 | 1 | 0 | 0 |
| Sr | 3 | 9 | 11 | nd | 0 | 5 | 6 |
| Rb | 0 | 1 | 1 | nd | 0 | 0 | 0 |
| Zn | 33 | 35 | 45 | 33 | 33 | 36 | 32 |
| Cu | 3 | 2 | 8 | 10 | 12 | 7 | 1 |
| Ni | 2319 | 2188 | 2264 | 2318 | 2207 | 2259 | 2280 |
| Cr | 1620 | 2103 | 2126 | 1907 | 2303 | 2012 | 2295 |
| V | 25 | 24 | 30 | 25 | 33 | 27 | 41 |
| Ce | nd | nd | tr | nd | tr | tr | nd |
| Ba | tr | tr | tr | nd | tr | 13 | |

Data (in ppm) are from whole-rock analyses by XRF;
tr = below detection limit (<5 ppm for Nb; <10 ppm for Ba and Ce);
nd = not detected (background count was greater than sample count).

the three sites are noted above, but the smaller data sets for 778 (10 samples) and 780 (6 samples) relative to 779 (32 samples) may be the cause of these distinctions (Fryer, Pearce, Stokking, et al., 1990).

## SHORE-BASED STUDIES

### METHODS

The samples used for the onshore portion of this study were those ultramafic clasts studied for major and trace element analyses by XRF on board ship. Sample selection on the ship was made at any indication of a lithology change (e.g., color, lineation, degree of alteration and metamorphism, or mineralogy). Thus, these samples are representative of the different lithologic types and their distribution in the cores.

X-ray diffraction (XRD) analysis of selected samples was performed to clarify questions regarding the presence and mineralogy of several major and minor phases. All analyses were performed using the University of Hawaii X-ray diffractometer, integrated with a Data General data collection system interfaced with an Apple Macintosh SE computer. The XRD utilizes a solid-state Ge detector and a Cu K-alpha radiation source; the computer strips K-alpha-2 using only the K-alpha-1 emission. The instrument was run at $1^{o}$ from $2^{o}$ to $70^{o}$ 2 theta. Tube current was at 40 mA and voltage at 45kV. Crystal slits and settings were used. The peaks were identified with the Scintag Pad V Peakfinder program.

In Tables 9, 10, 11, and 12 a given mineral is considered definitely present (●) if all three main peaks are present, probably present (Ø) if two of the main peaks are present, possibly present (o) if one of the main peaks is

present, probably absent if the main peaks present were ambiguous, and definitely absent if none of the main peaks are present.

## RESULTS

The samples are grouped into four categories for discussion of the nature of alteration and metamorphism. Group 1 are those samples which are freshest (less than 45% secondary minerals based on thin section inspection). Group 2 are 46%-65% altered and metamorphosed and group 3 are 66%-89% altered and metamorphosed. Group 4 consists of ultramafic clasts in which more than 90% of the original minerals are altered or metamorphosed.

Group 1 samples are the six freshest ultramafic clasts analyzed. Samples 779A-16R-1, 19-23 cm, #3 and 779A-19R-2, 97-99 cm, #13b are dunite and the rest (779A-16R-2, 74-77 cm, #9, 779A-17R-2, 14-17 cm, #3, 779A-17R-3, 77-80 cm, #8b, 779A-26R-2, 50-52 cm, #2b) are harzburgite (Table 9). Although the patterns in this group are complex (Figure 27), most of the peaks belong to the primary mineralogy.

Olivine is definitely present in five of the samples and probably present in sample 779A-16R-1, 19-23 cm, #3. This sample is missing the second major peak at 3.88Å but contains most of the other major and minor peaks. The patterns of the samples were compared with patterns for fayalite, hortonolite, hyalosiderite, and forsterite. Forsterite is the most common olivine present based on the presence of the 5.10Å (Fo-50) and 3.73Å (Fo-10) peaks.

Orthopyroxene is a major phase in all the harzburgite samples as well as a minor phase in one of the dunite samples (779A-16R-1,19-23 cm, #3).

Table 9.

**Mineralogy of group 1 (<45% altered/metamorphosed) ultramafic rocks by X-ray diffraction analysis**

| Sample site-core | interval | p # | rock name | ol | opx | cpx | sp | C | L | A | br | mt | talc | magn | cal | arag | chl | clay | amph | hem | il | coal |
|---|---|---|---|---|---|---|---|---|---|---|---|---|---|---|---|---|---|---|---|---|---|---|
| 779A-16R-1 | 19-23 | 3 | D20 | Ø | Ø | Ø | o | ● | ● | ● | ● | o | Ø | | o | | ● | o | o | o | o | |
| 779A-16R-2 | 74-77 | 9 | H37 | ● | ● | Ø | o | ● | ● | Ø | ● | o | Ø | | o | | o | o | | | | o |
| 779A-17R-2 | 14-17 | 3 | H36 | ● | ● | Ø | | ● | ● | o | ● | o | | | o | | o | | | | o | |
| 779A-17R-3 | 77-80 | 8b | H36 | ● | Ø | Ø | o | ● | ● | | ● | o | o | | o | o | o | Ø | | | o | |
| 779A-19R-2 | 97-99 | 13b | D38 | ● | | o | o | ● | ● | ● | ● | o | | | | | o | | | | | |
| 779A-26R-2 | 50-52 | 2b | H36 | ● | Ø | ● | o | ● | ● | | ● | o | | | o | | | | | | Ø | |

D=dunite; H=harzburgite; ol=olivine; opx=orthopyroxene; cpx=clinopyroxene; sp=spinel; C=chrysotile; L=lizardite; A=antigorite; br=brucite; mt=magnetite; magn=magnesite; cal=calcite; arag=aragonite; chl=chlorite; clay=clay minerals; amph=amphibole; hem=hematite; il=ilmenite; coal=coalingite; (numbers under rock name correspond to the deg. of secondary mineralogy), (●=definitely present, Ø=probably present, o=possibly present).

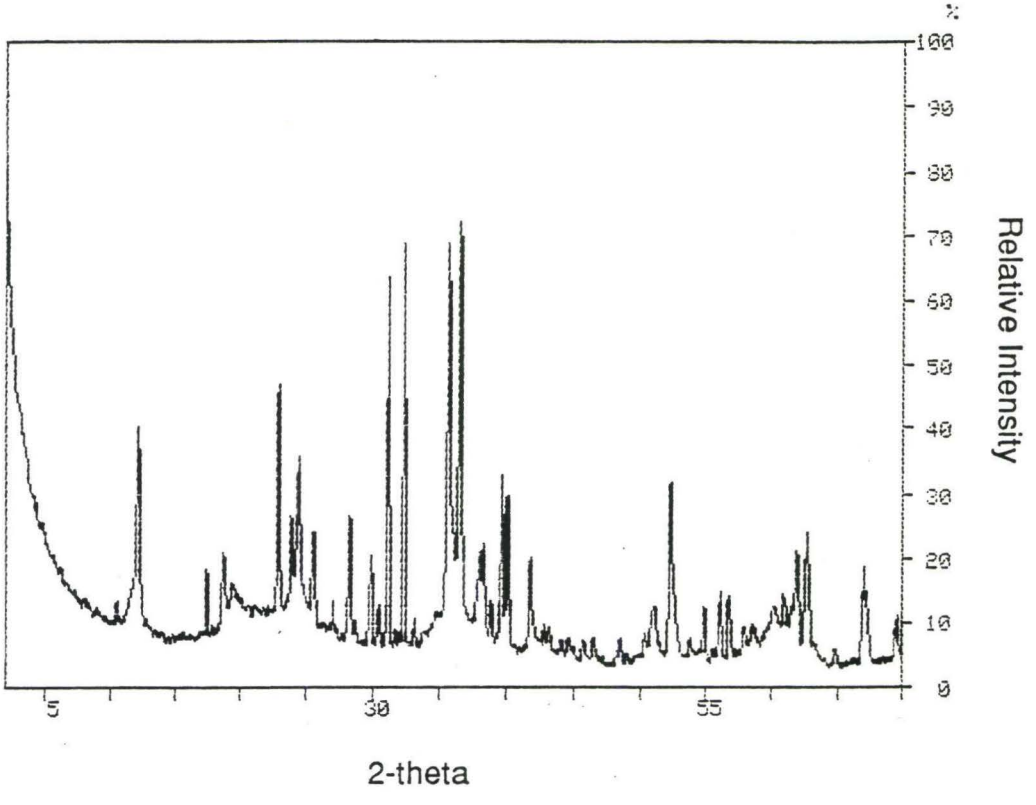


Figure 27. Representative X-ray diffraction pattern of group 1 samples. This is sample 125-779A-17R-2, 14-17 cm, #3; a harzburgite which is 36% altered and metamorphosed.

The other dunite (779A-19R-2, 97-99 cm, #13b) shows no evidence of orthopyroxene. The samples were compared with the patterns for enstatite, bronzite, hypersthene, eulite, and orthoferrosilite. Bronzite is the most common orthopyroxene present. The samples usually have the second major peak of the orthopyroxenes at 3.17Å , but rarely have the third major peak at 3.15Å.

Although clinopyroxene is a relatively minor phase (~0-2 modal %) in these clasts, it is definitely present in sample 779A-26R-2, 50-52 cm, #2b and possibly present in the other five samples. Clinoenstatite is the most common clinopyroxene present. Usually the major peaks of clinopyroxene at 2.99Å and 2.94Å are present, but these peaks also overlap with the forsterite and the bronzite peaks respectively. Spinel also is possibly a minor phase in these samples (~1 modal %).

Serpentine constitutes the bulk of the secondary minerals in these rocks. Lizardite and chrysotile are definitely present in all the samples based on the diagnostic peaks at 7.27Å (for lizardite and chrysotile), 3.89Å (for lizardite), 1.79Å (for lizardite), 2.095Å (for chrysotile), and 1.644Å (for chrysotile). Antigorite is only definitely present in two of the samples (based on the diagnostic peaks at 1.779Å, 1.558-1.56Å, and a doublet between 3.53-3.66Å. Antigorite is definitely absent in 779A-17R-3, 77-80 cm, #8b because the only diagnostic peak detected shows a relative intensity much greater than 2. Brucite is definitely present in all the samples based on the presence of the 4.77Å peak, which is the only main peak not shared with serpentine. Magnetite is possibly present in the samples, but the low modal percentage of this mineral causes some of the main peaks to be swamped by the noise. Talc may be a very minor phase and only 779A-16R-1, 19-23 cm, #3 has the main peak (9.34Å).

Although magnesite was expected, tentative identification can be made in only two samples. In these two, only the $I/I_1$=45 peak is present. This peak is shared with chrysotile ($I/I_1$=20) and therefore, the presence of magnesite is suspect. Calcite is possibly present, but the 3.035Å ($I/I_1$=100) peak is missing in most of the samples. Aragonite appears possibly present in only one sample. Sample 779A-17R-3, 77-80 cm, #8b has the second main peak for aragonite (1.98Å, I/I1=65) and two minor peaks, but their intensities are too low relative to the second main peak.

The presence of chlorite could not be verified because the ~14.0Å diagnostic peak of the chlorites is lacking. The 7.21Å peak of the chlorites is usually present but tends to be swamped by the main serpentine peak (7.26Å-7.30Å). The 4.77Å peak is also usually present, but is also shared by brucite. Therefore, the ~14.0Å peak is critical for identification. Sample 779A-16R-1, 19-23 cm, #3 is believed to contain clinochlore-Ib because it has the first five peaks (including the 14.3 Å peak).

Group 1 clasts are relatively unaltered; therefore, clays and amphiboles are not present to any great degree. Hematite, ilmenite, and coalingite also were not found in most of the samples. The XRD analyses of group 1 agree well with the petrographic descriptions of the samples.

Group 2 has 13 samples with fairly uniform primary mineralogy (Table 10 and Figure 28). Olivine and orthopyroxene are the dominant primary phases with minor amounts of clinopyroxene and spinel. Forsterite is the dominant olivine phase in all the patterns. The orthopyroxene ranges from enstatite to bronzite. Clinopyroxene can be identified as possibly either augite, clinoenstatite, hedenburgite, or diopside, depending on the specific pattern. Spinel is definitely present in only four samples (either spinel, syn-

Table 10.

**Mineralogy of group 2 (46%-65% altered/metamorphosed) ultramafic rocks by X-ray diffraction analysis**

| Sample site-core | interval | p # | rock name | ol | opx | cpx | sp | C | L | A | br | mt | talc | magn | cal | arag | chl | clay | amph | hem | il | coal |
|---|---|---|---|---|---|---|---|---|---|---|---|---|---|---|---|---|---|---|---|---|---|---|
| 779A-8R-1 | 90-93 | 8b | STD53 | ● | | o | ● | ● | o | ● | ● | Ø | o | | | | Ø | | | o | | |
| 779A-9R-2 | 52-54 | 4b | STH50 | ● | Ø | Ø | o | Ø | o | Ø | ● | o | Ø | | o | | o | | | | | |
| 779A-10R-1 | 40-43 | 5 | STD56 | ● | | Ø | Ø | Ø | Ø | Ø | ● | ● | o | | | | ● | | o | | | o |
| 779A-13R-2 | 50-54 | 1 | SH60 | ● | ● | Ø | Ø | ● | ● | Ø | ● | Ø | Ø | o | o | o | ● | o | ● | Ø | | |
| 779A-14R-1 | 74-77 | 5a | SD57 | ● | ● | Ø | o | ● | ● | ● | ● | Ø | Ø | | o | | ● | o | o | | | |
| 779A-14R-2 | 139-141 | | SH49 | ● | ● | O | ● | ● | ● | ● | ● | Ø | Ø | | Ø | o | Ø | | Ø | | | |
| 779A-22R-1 | 63-65 | 11 | SH52 | ● | Ø | Ø | ● | ● | ● | | ● | Ø | o | | | o | o | | | | | o |
| 779A-22R-2 | 53-57 | 7 | SD61 | ● | | o | o | Ø | ● | o | ● | o | Ø | | o | | o | | | | | |
| 779A-26R-3 | 101-103 | 3b | SH51 | ● | Ø | Ø | Ø | Ø | ● | o | ● | o | Ø | o | o | o | o | | | o | | |
| 780C-6R-1 | 61-62 | 7a | SH63 | ● | Ø | Ø | Ø | ● | ● | Ø | ● | Ø | o | o | o | o | o | o | o | | | |
| 780C-8R-1 | 98-101 | 10 | SD61 | ● | o | Ø | o | ● | ● | o | ● | Ø | ● | | o | | ● | o | o | | | |
| 780C-10R-1 | 13-16 | 2 | SH63 | ● | Ø | Ø | o | ● | ● | | ● | Ø | Ø | Ø | o | o | o | | Ø | ● | Ø | o |
| 780C-16R-1 | 53-59 | 7 | SH65 | ● | Ø | Ø | ● | ● | ● | Ø | ● | Ø | Ø | | Ø | | o | | o | | | |

SD=serpentinized dunite; SH=serpentinized harzburgite; STH=serpentinized tectonized harzburgite; STD serpentinized tectonized dunite; ol=olivine; opx=orthopyroxene; cpx=clinopyroxene; sp=spinel; C=chrysotile; L=lizardite; A=antigorite; br=brucite; mt=magnetite; magn=magnesite; cal=calcite; arag=aragonite; chl=chlorite; clay=clay minerals; amph=amphibole; hem=hematite; il=ilmenite; coal=coalingite; (numbers under rock name correspond to the degree of secondary mineralogy); (●=definitely present, Ø=probably present, o=possibly present).

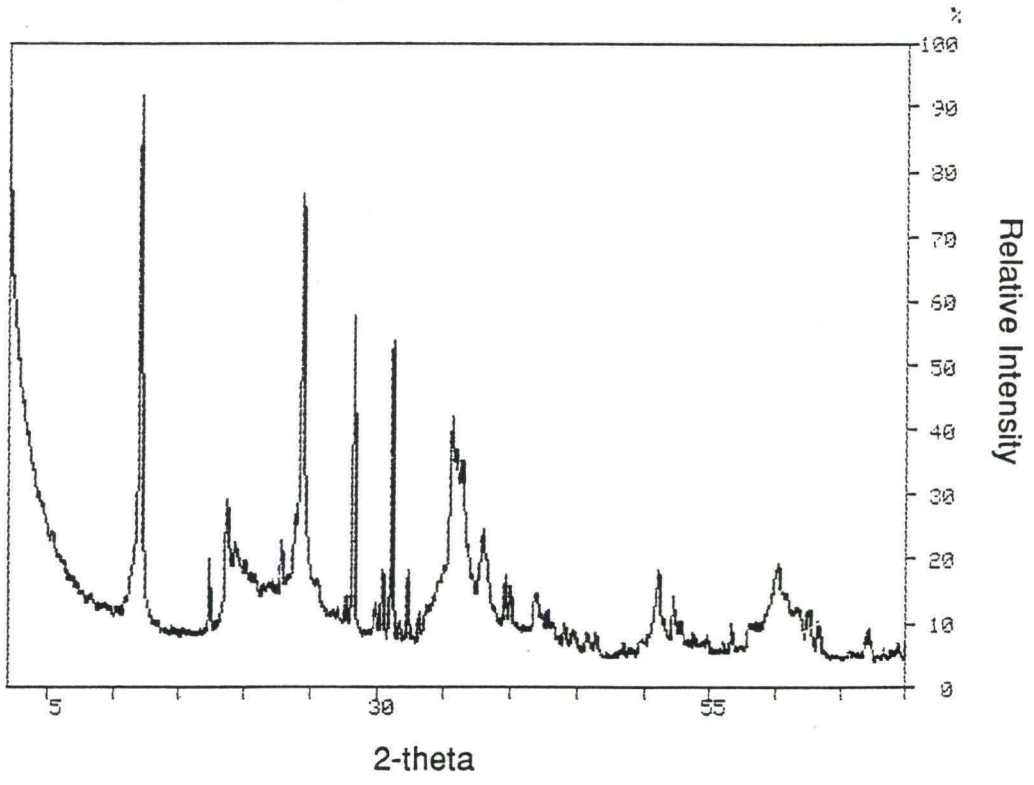


Figure 28. Representative X-ray diffraction pattern of group 2 samples. This is sample 125-780C-10R-1, 13-16 cm, #2; a serpentinized harzburgite which is 63% altered and metamorphosed.

Table 11.

**Mineralogy of group 3 (66%-89% altered/metamorphosed) ultramafic rocks by X-ray diffraction analysis**

| Sample site-core | interval | p # | rock name | ol | opx | cpx | sp | C | L | A | br | mt | talc | magn | cal | arag | chl | clay | amph | hem | il | coal |
|---|---|---|---|---|---|---|---|---|---|---|---|---|---|---|---|---|---|---|---|---|---|---|
| 779A-3R-CC | 13-15 | 2 | SD80 | ● | ● | Ø | o | | ● | | ● | Ø | ● | | | | ● | o | o | o | | |
| 779A-5R-2 | 34-37 | 3 | SH80 | ● | ● | ● | o | Ø | ● | o | ● | Ø | Ø | | | | o | o | | o | | |
| 779A-12R-1 | 38-42 | 6 | SH80 | ● | ● | Ø | Ø | Ø | Ø | o | ● | Ø | Ø | | | | o | o | | | | |
| 779A-14R-2 | 21-24 | 3 | SD76 | ● | o | | o | ● | ● | | ● | o | ● | | | | o | | | | | |
| 779A-15R-2 | 24-27 | | SD89 | ● | o | o | o | o | ● | o | ● | o | Ø | | | | | | | | | |
| 779A-22R-2 | 18-20 | | SD85 | ● | o | ● | o | ● | ● | o | ● | Ø | o | | o | | Ø | | | o | | Ø |
| 779A-25R-1 | 85-87 | | SD79 | ● | o | Ø | o | ● | ● | | ● | o | Ø | | | | | | | | | |
| 780C-18R-1 | 54-57 | 2a | SH69 | ● | Ø | ● | Ø | ● | ● | o | ● | Ø | Ø | o | Ø | | o | | o | | | |
| 780C-18R-1 | 58-61 | 2a | SH69 | ● | Ø | Ø | o | ● | ● | o | ● | Ø | ● | | o | | o | o | o | o | | |

SD=serpentinized dunite; SH=serpentinized harzburgite; STH=serpentinized tectonized harzburgite; STD=serpentinized tectonized dunite ol=olivine; opx=orthopyroxene; cpx=clinopyroxene; sp=spinel; C=chrysotile; L=lizardite; A=antigorite; br=brucite; mt=magnetite; magn=magnesite; cal=calcite; arag=aragonite; chl=chlorite; clay=clay minerals; amph=amphibole; hem=hematite; il=ilmenite; coal=coalingite; (numbers under rock name correspond to the deg. of secondary mineralogy); (●=definitely present, Ø=probably present, o=possibly present).

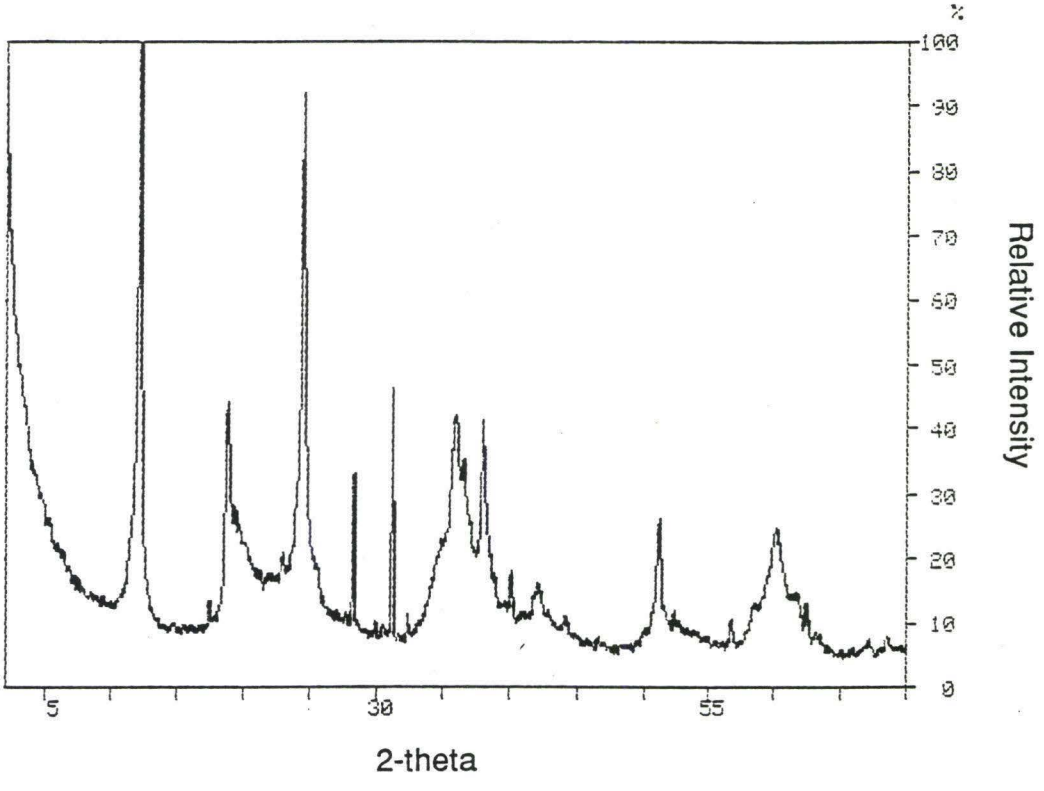


Figure 29. Representative X-ray diffraction pattern of group 3 samples. This is sample 125-779A-12R-1, 38-42 cm, #2; a serpentinized harzburgite which is 80% altered and metamorphosed.

or chromite-Al), but ranges from probably present to possibly present in the other samples.

The secondary mineralogy consists predominantly of serpentine. Brucite is present in all of the samples, based on the occurrence of the 4.77Å peak. Magnetite varies from possibly present to definitely present in all samples as does talc (although talc is definitely present in sample 780C-8R-1, 98-101 cm, #10). Most samples lack magnesite although it is possibly present in four of the samples. Calcite is possibly present in many of the samples.

Chlorite group minerals are definitely to possibly present in all the samples. Clinochlore-Ib, clinochlore-IIb, and clinochlore-Cr are all found separately in different patterns. There is little evidence for any of the clays, except in four samples (779A-13R-2, 50-54 cm, #1; 779A-14R-1, 74-77 cm, #5a; 780C-6R-1, 61-62 cm, #7a; 780C-8R-1, 98-101 cm, #10) where montmorillonite is possibly present. The identification of amphibole phases was difficult because their peaks are shared with olivine and orthopyroxene. The required ~8.00Å peak that indicates the possible presence of an amphibole, usually actinolite, tremolite, hornblende, or magnesiohornblende was not found Hematite, ilmenite, and coalingite are generally absent in most samples.

There are nine group 3 samples (Table 11, Figure 29). Forsterite is definitely present in all nine samples, whereas orthopyroxene and clinopyroxene vary from possibly present to definitely present. Hypersthene is found in three samples, (779A-3R-CC, 13-15 cm, #2; 779A-5R-2, 34-37 cm, #3; 779A-12R-1, 38-42 cm, #6). Clinopyroxene can be identified as augite, (779A-5R-2, 34-37 cm, #3 and 780C-18R-1, 54-57 cm, #2a), and

hedenburgite, (779A-22R-2, 18-20 cm). The spinel phase is usually chromite-Al and is probably present in all samples.

The secondary mineralogy is dominated by serpentine. Where possible, the specific serpentine mineral has been identified. Brucite is definitely present in all the samples (based on the presence of the 4.77Å peak). Magnetite and talc range from possibly to definitely present, but are present in minor amounts at most.

Magnesite, calcite, and aragonite are mostly absent. Only one sample (780C-18R-1, 54-57 cm, #2a) probably contains calcite. Chlorite is possibly present in all samples except for 779A-25R-1, 85-87 cm and 779A-15R-2, 24-27 cm. The chlorite has been identified as either clinochlore-Ib, clinochlore-IIb, or clinochlore-Cr. The clay that is possibly present in some of these samples is montmorillonite (MPDF #13-259). Amphibole is possibly present in three samples and is tentatively identified as either actinolite or tremolite. Hematite is possibly present in only some of the samples. Ilmenite and coalingite are absent in all samples except 779A-22R-2, 18-20 cm which probably contains very minor coalingite.

Group 4 represents nine of the most altered and metamorphosed (>90%) ultramafic samples (Table 12 and Figure 30). The peaks indicative of the primary mineralogy are overwhelmed by the serpentine and clay peaks. However, olivine, orthopyroxene, and clinopyroxene are possibly to definitely present in these samples. Spinel is possibly to definitely present .

Serpentine dominates the samples. Chrysotile and antigorite are present in greater amounts in the samples of this group. Brucite is probably present in all but three samples (778A-12R-2, 43-45 cm; 779A-28R-3, 26-28 cm, #2a; 778A-3R-CC, 1-7 cm). Magnetite is possibly to definitely present in all the samples. Talc is probably present in most samples and appears

Table 12.

**Mineralogy of group 4 (>90% altered/metamorphosed) ultramafic rocks by X-ray diffraction analysis**

| Sample site-core | interval | p # | rock name | ol | opx | cpx | sp | C | L | A | br | mt | talc | magn | cal | arag | chl | clay | amph | hem | il | coal | sm-k | kao | gr | cron | ch-lb | sjog |
|---|---|---|---|---|---|---|---|---|---|---|---|---|---|---|---|---|---|---|---|---|---|---|---|---|---|---|---|---|
| 778A-2R-1 | 89-92 | 7 | S | ● | o | Ø | o | Ø | Ø | o | o | o | o | o | o | Ø | o | | | Ø | | | | | | | | |
| 778A-3R-CC | 1 - 7 | | S | ● | Ø | ● | o | ● | ● | ● | | Ø | o | o | | | o | o | o | | | | o | o | | | | |
| 778A-7R-CC | 7 - 13 | | S | Ø | o | Ø | ● | ● | Ø | ● | Ø | ● | Ø | Ø | o | | Ø | o | | o | | Ø | | | | | | |
| 778A-12R-2 | 43-45 | | SH98 | o | o | Ø | ● | ● | | ● | | ● | o | o | o | | Ø | | o | o | o | | o | | ø | | o | |
| 778A-12R-2 | 73-75 | | SH99 | o | o | Ø | Ø | ● | | ● | o | ● | Ø | o | o | | ● | | | o | | | o | | Ø | | o | |
| 779A-5R-2 | 40-43 | 3 | SH96 | Ø | Ø | Ø | Ø | o | o | ● | Ø | o | Ø | | | | o | o | | | Ø | Ø | ● | | Ø | o | Ø | o |
| 779A-8R-1 | 57-60 | 5b | SH98 | Ø | o | Ø | | ● | o | ● | ● | o | Ø | | | | Ø | o | | | | ● | o | | Ø | | | |
| 779A-11R-1 | 14-18 | 3 | SH97 | Ø | o | Ø | o | ● | o | ● | Ø | o | Ø | | | | | o | | | o | | o | | Ø | | | |
| 779A-28R-3 | 26-28 | 2a | SH98 | ● | o | Ø | o | ● | | ● | | o | Ø | o | o | | Ø | o | o | | | | ● | Ø | Ø | o | o | |

S=serpentinite; SH=serpentinized harzburgite; ol=olivine; opx=orthopyroxene; cpx=clinopyroxene; sp=spinel; C=chrysotile; L=lizardite; A=antigorite; br=brucite; mt=magnetite; magn=magnesite; cal=calcite; arag=aragonite; chl=chlorite; clay=clay minerals; amph=amphibole; hem=hematite; il=ilmenite; coal=coalingite; sm-k=smectite-kaolinite; kao=kaolinite; ch-lb=chamosite-lb; cron=cronstedite; sjog=sjogrenite; gr=greenalite; (numbers under rock name correspond to the degree of secondary mineralogy); (●=definitely present, Ø=probably present, o=possibly present).

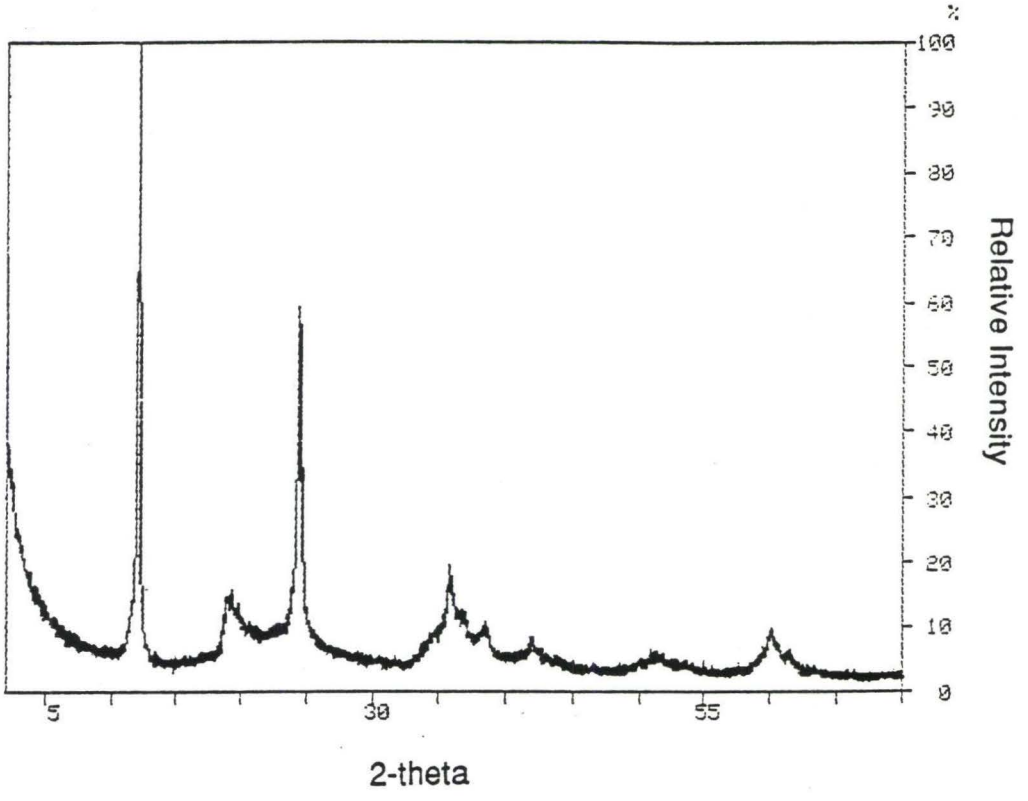


Figure 30. Representative X-ray diffraction pattern of group 4 samples. This is sample 125-779A-28R-3, 26-28 cm, #2a; a serpentinized harzburgite which is 98% altered and metamorphosed.

more common in this group than in the other groups. Calcite is possibly present in over half the samples.

The amount of chlorite in each sample is greater than in the other groups. The chlorite varies from clinochlore-Ib, clinochlore-IIb, and clinochlore-Cr. Montmorillonite is possibly present in most samples. Actinolite is probably present in three samples. Hematite, ilmenite, and coalingite are also much more common in this group. Coalingite is definitely present in 779A-8R-1, 57-60 cm, #5b.

Other secondary minerals present include smectite-kaolinite (MPDF #29-1490) and chamosite-Ib. Greenalite, from the serpentine mineral group, is also probably present in all the samples. The identification of the secondary mineral peaks is much more uncertain because of the pervasive alteration.

As alteration and metamorphism takes place there is a general increase in the presence of the secondary minerals (clays, amphiboles, serpentine, and chlorite). Lizardite is more prominent in groups 1, 2, 3, and less in group 4. Antigorite shows the opposite trend and is most prevalent in group 4. The definite presence of olivine and orthopyroxene decreases with an increase in degree of alteration and metamorphism.

## DISCUSSION

The ultramafic rocks recovered in the holes drilled on Conical Seamount are variably altered and metamorphosed harzburgite and dunite. Stratigraphic relationships between the rocks within the holes are difficult to discern. However, it is possible to determine gross variations between the degree of alteration and metamorphism of the rocks within each hole. The

Table 13.

Variation in Mineralogy of ultramafic rocks with depth in ODP Leg 125 Drill Holes

| Sample | | | rock | | Serpentine Grp | | | | | Layered Grp | | | | | | | | Sjog Grp | | Carbonate Grp | | | Others | | | | | Opaques | | |
|---|---|---|---|---|---|---|---|---|---|---|---|---|---|---|---|---|---|---|---|---|---|---|---|---|---|---|---|---|---|---|
| site-core | Interval | p # | name | alteration | C | L | A | G | cron | talc | br | chl | ch-lb | clay | sm-k | kao | coal | sjog | cal | arag | magn | ol | opx | cpx | sp | amph | mt | hem | il |
| 778A-1R | | | | | | | | | | | | | | | | | | | | | | | | | | | | | | |
| 778A-2R | 89-92 | 7 | S | 4 | Ø | Ø | o | | | o | o | o | | | | | | | | Ø | o | ● | o | Ø | o | | o | Ø | |
| 778A-3R-CC | 1- 7 | | S | 4 | ● | ● | ● | | | o | | o | | o | o | o | | | o | | o | ● | Ø | ● | o | o | Ø | | |
| 778A-4R | | | | | | | | | | | | | | | | | | | | | | | | | | | | | | |
| 778A-5R | | | | | | | | | | | | | | | | | | | | | | | | | | | | | | |
| 778A-6R | | | | | | | | | | | | | | | | | | | | | | | | | | | | | | |
| 778A-7R-CC | 7- 13 | | S | 4 | ● | Ø | ● | | | Ø | Ø | Ø | | o | | | Ø | | o | | Ø | Ø | Ø | o | Ø | ● | | ● | o | |
| 778A-8R | | | | | | | | | | | | | | | | | | | | | | | | | | | | | | |
| 778A-9R | | | | | | | | | | | | | | | | | | | | | | | | | | | | | | |
| 778A-10R | | | | | | | | | | | | | | | | | | | | | | | | | | | | | | |
| 778A-11R | | | | | | | | | | | | | | | | | | | | | | | | | | | | | | |
| 778A-12R-2 | 43-45 | | SH98 | 4 | ● | | ● | Ø | | o | | Ø | o | | o | | | | o | | o | o | o | o | Ø | ● | o | ● | o | o |
| 778A-12R-2 | 73-75 | | SH99 | 4 | ● | | ● | Ø | | Ø | o | ● | o | | o | | | | o | | o | o | o | o | Ø | Ø | | ● | o | |

Table 13. (continued)

Variation in Mineralogy of ultramafic rocks with depth in ODP Leg 125 Drill Holes

| Sample site-core | Interval | p # | rock name | alt. | Serpentine Grp C | L | A | G | cron | Layered Grp talc | br | chl | ch-lb | clay | sm-k | kao | Sjog Grp coal | sjog | Carbonate Grp cal | arag | magn | Others ol | opx | cpx | sp | amph | Opaques mt | hem | il |
|---|---|---|---|---|---|---|---|---|---|---|---|---|---|---|---|---|---|---|---|---|---|---|---|---|---|---|---|---|---|
| 779A-1R | | | | | | | | | | | | | | | | | | | | | | | | | | | | | |
| 779A-2R | | | | | | | | | | | | | | | | | | | | | | | | | | | | | |
| 779A-3R-CC | 13- 15 | 2 | SD80 | 3 | | ● | | | | ● | ● | ● | | o | | | | | | | | ● | ● | Ø | o | o | Ø | o | |
| 779A-4R | | | | | | | | | | | | | | | | | | | | | | | | | | | | | |
| 779A-5R-2 | 34-37 | 3 | SH80 | 3 | Ø | ● | o | | | Ø | ● | o | | o | | | | | | | | ● | ● | ● | o | | Ø | o | |
| 779A-5R-2 | 40-43 | 3 | SH96 | 4 | o | o | ● | Ø | o | Ø | Ø | o | Ø | o | ● | | Ø | o | | | | Ø | Ø | Ø | Ø | | o | | Ø |
| 779A-6R | | | | | | | | | | | | | | | | | | | | | | | | | | | | | |
| 779A-7R | | | | | | | | | | | | | | | | | | | | | | | | | | | | | |
| 779A-8R-1 | 57-60 | 5b | SH98 | 4 | ● | o | ● | Ø | | Ø | ● | Ø | | o | o | | ● | | | | | Ø | o | Ø | | | o | | |
| 779A-8R-1 | 90-93 | 8b | STD53 | 2 | ● | o | ● | | | o | ● | Ø | | | | | | | | | | ● | | o | ● | | Ø | o | |
| 779A-9R-2 | 52-54 | 4b | STH50 | 2 | Ø | o | Ø | | | Ø | ● | o | | | | | | | o | | | ● | Ø | Ø | o | | o | | |
| 779A-10R-1 | 40-43 | 5 | STD56 | 2 | Ø | Ø | Ø | | | o | ● | ● | | | | | o | | | | | ● | | Ø | Ø | o | ● | | |
| 779A-11R-1 | 14-18 | 3 | SH97 | 4 | ● | o | ● | Ø | | Ø | Ø | | | o | o | | | | | | | Ø | o | Ø | o | | o | | o |
| 779A-12R-1 | 38-42 | 6 | SH80 | 3 | Ø | Ø | o | | | Ø | ● | o | | o | | | | | | | | ● | ● | Ø | Ø | | Ø | | |
| 779A-13R-2 | 50-54 | 1 | SH60 | 2 | ● | ● | Ø | | | Ø | ● | ● | | o | | | | | o | o | o | ● | ● | Ø | Ø | ● | Ø | Ø | |
| 779A-14R-1 | 74-77 | 5a | SD57 | 2 | ● | ● | ● | | | Ø | ● | ● | | o | | | | | o | | | ● | ● | Ø | o | o | Ø | | |
| 779A-14R-2 | 21-24 | 3 | SD76 | 3 | ● | ● | | | | ● | ● | o | | | | | | | | | | ● | o | | o | | o | | |
| 779A-14R-2 | 139-141 | | SH49 | 2 | ● | ● | ● | | | Ø | ● | Ø | | | | | | | Ø | o | | ● | ● | ● | ● | Ø | Ø | | |
| 779A-15R-2 | 24-27 | | SD89 | 3 | o | ● | o | | | Ø | ● | | | | | | | | | | | ● | o | o | o | | o | | |
| 779A-16R-1 | 19-23 | 3 | D20 | 1 | ● | ● | ● | | | Ø | ● | ● | | o | | | | | o | | | Ø | Ø | Ø | o | o | o | o | o |
| 779A-16R-2 | 74-77 | 9 | H37 | 1 | ● | ● | Ø | | | Ø | ● | o | | o | | | o | | o | | | ● | ● | Ø | o | | o | | |
| 779A-17R-2 | 14-17 | 3 | H36 | 1 | ● | ● | o | | | | ● | o | | | | | | | o | | | ● | ● | Ø | | | o | | o |

Table 13. (continued)

Variation in Mineralogy of ultramafic rocks with depth in ODP Leg 125 Drill Holes

| Sample site-core | Interval | p # | rock name | alt. | Serpentine Grp C | L | A | G | cron | Layered Grp talc | br | chl | ch-lb | clay | sm-k | kao | Sjog Grp coal | sjog | Carbonate Grp cal | arag | magn | Others ol | opx | cpx | sp | amph | Opaques mt | hem | il |
|---|---|---|---|---|---|---|---|---|---|---|---|---|---|---|---|---|---|---|---|---|---|---|---|---|---|---|---|---|---|
| 779A-17R-3 | 77-80 | 8b | H36 | 1 | ● | ● | | | | o | ● | o | | Ø | | | | | o | o | | ● | Ø | Ø | o | | o | | o |
| 779A-19R-2 | 97-99 | 13b | D38 | 1 | ● | ● | ● | | | | ● | o | | | | | | | | | | ● | | o | o | | o | | |
| 779A-20R | | | | | | | | | | | | | | | | | | | | | | | | | | | | | |
| 779A-21R | | | | | | | | | | | | | | | | | | | | | | | | | | | | | |
| 779A-22R-1 | 63-65 | 11 | SH52 | 2 | ● | ● | | | | o | ● | o | | | | | o | | | o | | ● | Ø | Ø | ● | | Ø | | |
| 779A-22R-2 | 18-20 | | SD85 | 3 | ● | ● | o | | | o | ● | Ø | | | | | Ø | | o | | | ● | o | ● | o | | Ø | o | |
| 779A-22R-2 | 53-57 | 7 | SD61 | 2 | Ø | ● | o | | | Ø | ● | o | | | | | | | o | | | ● | | o | o | | o | | |
| 779A-23R | | | | | | | | | | | | | | | | | | | | | | | | | | | | | |
| 779A-24R | | | | | | | | | | | | | | | | | | | | | | | | | | | | | |
| 779A-25R-1 | 85-87 | | SD79 | 3 | ● | ● | | | | Ø | ● | | | | | | | | | | | ● | o | Ø | o | | o | | |
| 779A-26R-2 | 50-52 | 2b | H36 | 1 | ● | ● | | | | | ● | | | | | | | | o | | | ● | Ø | ● | o | | o | | Ø |
| 779A-26R-3 | 101-103 | 3b | SH51 | 2 | Ø | ● | o | | | Ø | ● | o | | | | | | | o | o | o | ● | Ø | Ø | Ø | | o | o | |
| 779A-27R | | | | | | | | | | | | | | | | | | | | | | | | | | | | | |
| 779A-28R-3 | 26-28 | 2a | SH98 | 4 | ● | | ● | Ø | o | Ø | | Ø | o | o | ● | Ø | | | o | | o | ● | o | Ø | Ø | o | o | | |

Table 13. (continued)

Variation in Mineralogy of ultramafic rocks with depth in ODP Leg 125 Drill Holes

| Sample site-core | Interval | p # | rock name | alt. | Serpentine Grp C | L | A | G | cron | Layered Grp talc | br | chl | ch-lb | clay | sm-k | kao | Sjog Grp coal | sjog | Carbonate Grp cal | arag | magn | Others ol | opx | cpx | sp | amph | Opaques mt | hem | il |
|---|---|---|---|---|---|---|---|---|---|---|---|---|---|---|---|---|---|---|---|---|---|---|---|---|---|---|---|---|---|
| 780C-1R | | | | | | | | | | | | | | | | | | | | | | | | | | | | | |
| 780C-2R | | | | | | | | | | | | | | | | | | | | | | | | | | | | | |
| 780C-3R | | | | | | | | | | | | | | | | | | | | | | | | | | | | | |
| 780C-4R | | | | | | | | | | | | | | | | | | | | | | | | | | | | | |
| 780C-5R | | | | | | | | | | | | | | | | | | | | | | | | | | | | | |
| 780C-6R-1 | 61-62 | 7a | SH63 | 2 | ● | ● | Ø | | | o | ● | o | | o | | | | | o | o | o | ● | Ø | Ø | Ø | o | Ø | | |
| 780C-7R | | | | | | | | | | | | | | | | | | | | | | | | | | | | | |
| 780C-8R-1 | 98-101 | 10 | SD61 | 2 | ● | ● | o | | | ● | ● | ● | | o | | | | | o | | | ● | o | Ø | o | o | Ø | | |
| 780C-9R | | | | | | | | | | | | | | | | | | | | | | | | | | | | | |
| 780C-10R-1 | 13-16 | 2 | SH63 | 2 | ● | ● | | | | Ø | ● | o | | | | | o | | o | o | Ø | ● | Ø | Ø | o | Ø | Ø | ● | Ø |
| 780C-11R | | | | | | | | | | | | | | | | | | | | | | | | | | | | | |
| 780C-12R | | | | | | | | | | | | | | | | | | | | | | | | | | | | | |
| 780C-13R | | | | | | | | | | | | | | | | | | | | | | | | | | | | | |
| 780C-14R | | | | | | | | | | | | | | | | | | | | | | | | | | | | | |
| 780C-15R | | | | | | | | | | | | | | | | | | | | | | | | | | | | | |
| 780C-16R-1 | 53-59 | 7 | SH65 | 2 | ● | ● | Ø | | | Ø | ● | o | | | | | | | Ø | | | ● | Ø | Ø | ● | o | Ø | | |
| 780C-17R | | | | | | | | | | | | | | | | | | | | | | | | | | | | | |
| 780C-18R-1 | 54-57 | 2a | SH69 | 3 | ● | ● | o | | | Ø | ● | o | | | | | | | Ø | | o | ● | Ø | ● | Ø | o | Ø | | |
| 780C-18R-1 | 58-61 | 2a | SH69 | 3 | ● | ● | o | | | ● | ● | o | | o | | | | | o | | | ● | Ø | Ø | o | o | Ø | o | |

SH=serpentinized harzburgite; SD=serpentinized dunite; C=chrysotile; L=lizardite; A=antigorite; G=greenalite; cron=cronstedite; br=brucite; chl=chlorite; ch-lb=chamosite-lb; clay=clay minerals; sm-k=smectite-kaoloinite; kao=kaolinite; coal=coalingite; sjog=sjogrenite; cal=calcite; arag=aragonite; magn=magnesite; ol=olivine; opx=orthopyroxene; cpx=clinopyroxene; sp=spinel; amph=amphibole; mt=magnetite; hem=hematite; il=ilmenite; (numbers under rock name correspond to the degree of secondary mineralogy); (●=definitely present, Ø=probably present, o=possibly present); (1=freshest, 2=slightly altered, 3=moderately altered, 4=heavily altered).

stratigraphic summary of the mineralogy of the ultramafic rocks from these three sites is given in Table 13.

The serpentinized harzburgite samples from Site 778 are all highly altered and metamorphosed and are very uniform in composition. The principal stratigraphic variation observed is in the talc and chlorite content of the samples. Toward the bottom of the hole (cores 7 and 12, about 49-98 mbsf) XRD analyses show a greater abundance of talc and chlorite. Examinations of fluid compositions and serpentine muds in which the ultramafic clasts are entrained provide strong evidence that water/rock reactions are occurring *in situ* in the seamount (Fryer, Pearce, Stokking et al., 1990; Fryer and Mottl, in press).

The probable presence of the sjogrenite group mineral, coalingite [$Mg_{10}Fe_2(CO_3)(OH)_{24}\cdot 2H_2O$], in the sample from core 7 suggests that some of the rocks have interacted with the slab derived pore fluids (Mottl, in press) associated with the serpentine mudflows on this seamount. The sjogrenite group minerals are prevalent in the serpentine muds analyzed from the flank sites (Fryer and Mottl, in press). On land, these minerals form in the weathering zone of serpentinite bodies exposed, primarily as alteration products of brucite (Mumpton et al., 1965), and thus are interpreted to form by the reaction of serpentinized ultramafics with groundwater (fresh water not seawater) (Fryer and Mottl, in press). Possibly the presence of talc and chlorite in rocks at this depth in the core is further evidence of interaction with the pore fluids.

Mineralogic variations in Hole 779A are also very subtle. The only striking mineralogical distinction which can be drawn among any group of samples from this hole is the greater degree of freshness of the samples in the interval from cores 16 through 19 (135-169 mbsf). According to Fryer

and Mottl (in press) the serpentine muds from this interval are more diverse mineralogically and contain antigorite, unusual in muds from Conical Seamount and suggestive of a less altered serpentine protolith.

The uniformity of both the composition and the texture of the samples from this hole suggests that a relatively restricted region in the supra-subduction zone mantle is the source for the rocks that comprise the clasts in the serpentine mudflows on the southeast flank of Conical Seamount. The range of metamorphism to which the source region was subjected is very low- to medium-grade.

Hole 780C at the summit site contains harzburgite and dunite samples indistinguishable from those at Sites 778 and 779, except that they exhibit a greater uniformity of the amount of alteration (61%-69%). Rheological studies of the summit muds indicate that the rocks are carried upward with the rising muds and are either protruded and become part of the flows that blanket the seamount, or may settle back into the conduit during periods of quiescence between eruptions (Fryer and Mottl, in press). The rocks recovered from this site probably are from recent intrusions of muds containing ultramafic clasts, which have derived from a single source.

The ultramafic clasts in the serpentine muds of Conical Seamount represent a depleted supra-subduction zone mantle affected by very low- to medium-grade metamorphism. The source region is likely to be relatively small because of the uniformity of composition of the rocks. Alteration and metamorphism has probably taken place as a consequence of interaction with fluids generated by dehydration of the subducted slab. The water/rock interaction probably take place both in the source region and in the body of the edifice. Subtle variations in mineral content of the rocks are consistent

with interpretations of the periodicity of activity associated with formation of serpentine mudflows.

## DISCUSSION: CONDITIONS OF METAMORPHISM

The temperature and pressure conditions of the very low- to medium-grade metamorphism represented by the ultramafic rocks from Conical Seamount are complex. Serpentinization of ultramafic rocks composed mainly of forsterite, Mg-rich pyroxenes and amphiboles depends on the availability of water. Serpentinization is a complex process and it can occur as either a retrograde (taking place in a falling temperature/pressure environment) or a prograde (taking place in a rising temperature/pressure environment) event. It is generally agreed, based on field work, petrographic evidence, and laboratory experiments, that antigorite is stable in the high temperature-pressure range of serpentinization (~200$^{o}$C - 600$^{o}$C) (Figure 31; note that there is very little pressure dependence in any of the curves) and chrysotile and lizardite are stable in the lower temperature-pressure range of serpentinization (0$^{o}$C - 200$^{o}$C) in prograde events (Coleman, 1971; Moody, 1976; Bonatti et al., 1984). Formation of antigorite requires less water than does that of lizardite or chrysotile because the structure of antigorite accommodates less $Mg(OH)_2$ than does that of either lizardite or chrysotile (Whittaker and Wicks, 1970; Moody, 1976). Therefore, the generally higher temperature (200$^{o}$C$^{+}$) characteristic of antigorite formation is attributed by Moody (1976) to the greater degree of dehydration of the host rock and a concomitant lower activity of water as temperatures rise. Based solely on laboratory experiments, the different temperature-pressure stability conditions for chrysotile relative to lizardite cannot be distinguished (Bonatti, et al., 1984). Textural relationships between these phases in thin section can shed light on the relative

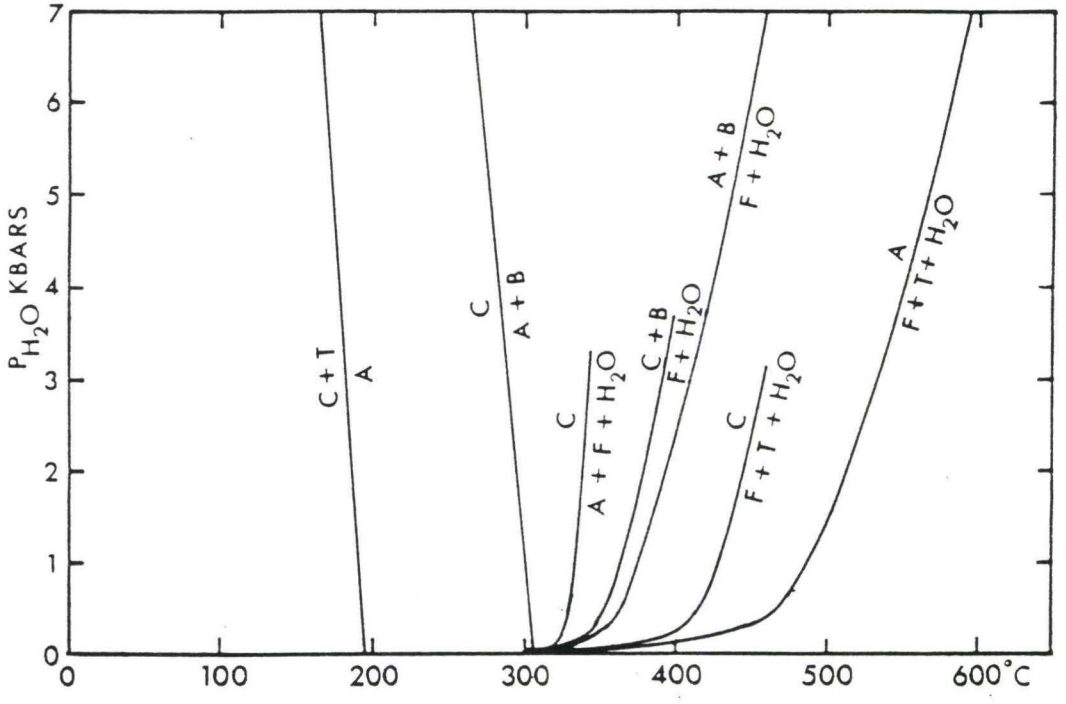


Figure 31. Temperature-pressure (PH2O = Ptotal) diagram for serpentinites. A = antigorite; B = brucite; C = chrysotile; F = forsterite; T = talc (Wicks, 1979).

sequence of their formation, but still cannot be used to determine temperature-pressure history.

Wenner and Taylor (1971) were able to estimate formation temperatures of serpentine minerals in prograde events in oceanic ultramafic rocks based on $^{18}O/^{16}O$ fractionation between coexisting serpentine and magnetite. Approximate equilibrium temperatures are 125°C for lizardite, 180°C for chrysotile, and 220°C to 460°C for antigorite (Wenner and Taylor, 1971). The most common serpentine textures in the medium to high temperature range of serpentinization (220°C to 600°C) are antigorite ± magnetite in interpenetrating configurations that form either through the recrystallization of lizardite ± chrysotile pseudomorphic textures (formed at lower temperatures), or less frequently through the serpentinization of previously unserpentinized primary minerals (Wicks, 1979). According to Wicks (1979) antigorite textures represent fairly intense metamorphism and form up to 510°C at 2 kbar water pressure. Thus, the reported range of antigorite formation at 2 kbars spans about 220°C (Wenner and Taylor, 1971) to 510°C (Wicks, 1979; see also Figure 31). The reported range of chrysotile formation spans about 180°C (Wenner and Taylor, 1971) to 440°C at 2 kbars (Wicks, 1979; see also Figure 31). The reported range of lizardite formation spans about 120°C (Wenner and Taylor, 1971) to 375°C (Wicks, 1979; not shown on Figure 31).

According to Wicks (1979), at temperatures below approximately 375°C at 2 kbar water pressure, lizardite with or without chrysotile replaces olivine, pyroxene, amphibole, chlorite, and talc. A common mineral assemblage of serpentinization below 375°C is lizardite ± chrysotile ± magnetite, where lizardite ± chrysotile form mesh-textured pseudomorphs after olivine and form bastite after pyroxenes and the magnetite is a common

by-product of the serpentinization of the olivine (Wicks, 1979). Lizardite ± chrysotile have been reported as replacing pre-existing antigorite in a lower temperature-pressure regime than is observed for antigorite formation (Coleman, 1971; Mumpton and Thompson, 1975). However, antigorite can persist into a retrograde metamorphic regime (Mumpton and Thompson, 1975). The texture of the common very low grade (120°C - 180°C) serpentinite containing lizardite ± chrysotile is pseudomorphism of the pre-existing primary minerals (Winkler, 1976; Wicks, 1979). Wicks (1979) also notes that serpentine phases can persist metastably within broad temperature/pressure ranges. Thus, although these criteria (Wicks, 1979) can help determine the grade of metamorphism of the rocks in this study, without further detailed analysis the metamorphic grade of the rocks can only be constrained to very low- to medium-grade, i. e., 120°C - 600°C.

Brucite is produced by serpentinization with the temperature range of approximately 250°C to 450°C (Wicks, 1979) (Figure 31). The mineral assemblage then becomes lizardite ± chrysotile ± brucite ± antigorite ± magnetite. Brucite is difficult to determine petrographically because it often occurs as fine grains intimately associated with the lizardite. It is easier to identify in veins. The importance of brucite is that it may define a lower temperature of serpentinization than the presence of antigorite alone or antigorite and chrysotile (Moody, 1976; Wicks, 1979).

Although mineral assemblages alone can be used to determine the range of temperature-pressure conditions in rocks which have undergone prograde events, it is extremely difficult to use them to determine the range for retrograde events. Detailed textural analyses by spectral reflectance, electron microscopy, or microbeam X-ray diffraction are needed in order to

further define the intricate mineralogical interrelationships which may indicate the metamorphic history.

As stated earlier, the low percentage of brucite in the petrographic tables (Tables 1 and 2) results from the difficulty of identifying it optically. Fine-grained brucite is usually intimately intergrown with the serpentine and their petrographic characteristics (low-moderate relief and birefringence) are very similar. Brucite is usually identified optically when it occurs as veins crosscutting the serpentine and showing characteristic first order yellow interference colors. Shore-based X-ray diffraction results indicate that brucite is definitely present in a majority of the samples.

There are several different alteration assemblages observed in this study. Twenty seven samples (of the thirty seven samples studied by x-ray diffraction) contain the assemblage chrysotile + lizardite + magnetite + brucite + antigorite. Six samples contain chrysotile + lizardite + magnetite + brucite. Two samples contain the assemblage chrysotile + magnetite.+ antigorite. One sample contains chrysotile + lizardite + magnetite + antigorite. One sample contains chrysotile + magnetite + antigorite + brucite. One sample contains lizardite + magnetite + brucite. There are only three samples which contain antigorite in the absence of brucite. These samples are all extremely serpentinized (i. e. > 98%).

Talc is present to some degree in most of the samples analyzed by x-ray diffraction. The occurrence of talc in the same thin sections that have brucite is an apparent contradiction because the stability fields of these two minerals do not overlap. By knowing which one of these two mineral phases developed first it would be possible to discuss the history of the rock. Unfortunately, it is extremely difficult to discern the brucite and its

interrelationship with talc in thin section. We can say that the rocks are in disequilibrium on a relatively fine scale (cm in size).

The vast majority of thin sections studied demonstrate a pseudomorphic mesh and bastitic texture of lizardite and chrysotile after olivine and orthopyroxene, suggesting recrystallization between 125°C and about 500°C. Rocks containing antigorite indicate formation at a higher temperature between 200°C and 600°C. Brucite can only be observed petrographically as large cross-cutting veins in both types of the above-mentioned rocks. In almost all rocks analyzed by X-ray diffraction from Sites 779 and 780, brucite is definitely present. However, in the samples from Site 778, brucite is less prevalent, and these generally contain more antigorite. Brucite forms within a temperature range of 250°C to 450°C and thus the last metamorphic event must have occurred within the temperature range of brucite formation.

Some rocks are characterized by tectonized fabrics including neoblastic recrystallization of olivine, elongation of mineral grains, and excessive wavy extinction and kink-banding. It is impossible to determine the type of metamorphism which has occurred because the texture has been obliterated.

The lesser amount of brucite and the greater abundance of antigorite in rocks from Site 778 may indicate a higher temperature of metamorphism. The importance of the widespread occurrence of brucite and antigorite is that based on temperature constraints (Fryer and Fryer, 1987; Fryer, et al., 1989) the metamorphism of these rocks would have to be constrained to a very early stage in the evolution of the Mariana subduction system. Thermal models constructed by Fryer et al. (1989) require the upper temperature limit

of the region of the forearc in which Conical Seamount is located to cool to less than 200$^{o}$C within a few million years from the beginning of subduction.

# CONCLUSIONS

Several important factors based on these studies and related work have changed concepts of processes active at non-accretionary convergent margins. Evidence suggests that mobilization of the forearc mantle wedge by serpentinization and diapiric intrusion is an important phenomenon in the region between the outer-arc high and the trench. Emplacement of large serpentine seamounts is a common occurrence in the outer half of the Mariana forearc (Fryer, et al., 1985). One such seamount, Conical Seamount, is an actively "erupting" serpentine seamount, and exhibits characteristics of mud volcanoes. This seamount is composed of unconsolidated serpentine mud flows that have entrained serpentinized ultramafic and metamorphosed mafic rocks (very low- to medium-grade). The extent of metamorphism in the dive and drill samples is variable, but all of the ultramafic samples recovered are serpentinized to some degree. Most of the rocks studied from this seamount are harzburgites with very small proportions of clinopyroxene and low contents of alumina. This indicates a highly depleted mantle rock that represents the residue from a high degree of partial melting or more than one melting event.

The nature and magnitude of fluid flow within the forearc at non-accretionary margins are still poorly understood. In the Mariana region, the hydration of the crust and upper mantle of the forearc wedge is probably facilitated by the escape of fluids from the subducting Pacific Plate. Large regions beneath the forearc lie within the chlorite, greenschist and blueschist stability fields. Widespread metamorphism of the forearc wedge might explain the apparent capacity of the forearc regions to accommodate the potentially large volumes of fluid driven off a descending slab over

millions of years of subduction (Fryer and Fryer, 1987; Saboda et al., 1987; Fryer, et al., 1990). Serpentine protrusions may be able to entrain deep-seated fluids during formation and ascent and to lose these fluids during protrusion of the serpentine flow onto the surface. Conical Seamount provides samples of these escaping fluids and associated metamorphosed clasts from the deep forearc through which changes in the pressure-temperature regimes can be traced.

## BIBLIOGRAPHY

Bloomer, S., (1982), Structure and Evolution of the Mariana Trench, Petrologic and Geochemical Studies, Ph.D. Dissertation, Univ. Calif, San Diego.

Bloomer, S.H., and J.W. Hawkins, (1983), Gabbroic and ultramafic rocks from the Mariana Trench: An island arc ophiolite, in The Tectonic and Geologic Evolution of Southeast Asian Seas and Islands. Part 2. Geophys. Monogr. Ser., 27, edited by D.E. Hayes, AGU, Washington, D.C., 294-317.

Bonatti, E., J.R. Lawrence, and N. Morandi, (1984), Serpentinization of oceanic peridotites: temperature dependence of mineralogy and boron content, EPSL, 70, 88-94.

Carlson, C., (1984), Stratigraphic and structural significance of foliate serpentine breccias, Wilbur Springs, Society of Economic Paleontologists and Mineralogists, Field Trip Guidebook, no. 3, 108-112.

Coleman, R.G., (1957), Mineralogy and Petrology of the New Idria District, California, PhD Thesis, Stanford University, Stanford, California.

Coleman, R.G., (1961), Jadeite deposits of the Clear Creek area, New Idria District, San Benito County, California, J. Petrology, 2, 209-247.

Coleman, R.G., (1971), Petrologic and geophysical nature of serpentinites, Geol. Soc. Am. Bull., 82, 897-918.

Coleman, R.G., (1980), Tectonic Inclusions in Serpentinites, Arch. du Sci. Geneve, 33, 89-102.

Coleman, R.G., (1986), Field Trip Guide Book to New Idria Area, California, 14th General Meeting of the International Mineralogical Association, Stanford University, Stanford, California.

Evans, B.W., (1977), Metamorphism of Alpine Peridiotite and Serpentinite, Ann. Rev. Earth Planet. Sci., 5, 397-447.

Fryer, G., P. Fryer, and K. Saboda, (1989), Thermal metamorphic evolution of the Mariana forearc, EOS, Abstract Trans. Am. Geophys. Union, 70:43 , 1381.

Fryer, P. , E. L. Ambos, and D. M. Hussong, (1985), Origin and emplacement of Mariana forearc seamounts, Geology, 13, 774-777.

Fryer, P., and G. Fryer, (1987), Origins of nonvolcanic seamounts in a forearc environment, in Seamounts, Islands, and Atolls, Geophys. Monogr. Ser., 43, edited by B.H. Keating, P. Fryer, R. Batiza, and G.W. Boehlert, AGU, Washington, D.C., 61-72.

Fryer, P., J. Haggerty, B. Tilbrook, K. L. Saboda, L. E. Johnson, P. Sedwick, S. Y. Newsom, G. McMurtry, D. E. Karig, S. Uyeda, T. Ishii and D.

Stakes, *Alvin* Observations of Two Serpentine Seamounts on the Mariana Convergent Margin, EPSL, in press.

Fryer, P. , J. Haggerty, B. Tilbrook, P. Sedwick, L. E. Johnson, K. L. Saboda, S. Y. Newsom D. E. Karig, S. Uyeda, and T. Ishii, Results of studies of Mariana forearc serpentinite diapirism, (1987), EOS, Abstract Trans. Am. Geophys. Union, 68:44 , 1534.

Fryer, P., and D.M. Hussong, (1982), Seafloor spreading in the Mariana Trough: Results of Leg 60 drill site selection surveys, in Initial Reports of the Deep-Sea Drilling Project, edited by D.M. Hussong and S. Uyeda, U.S. Govt. Printing Off., Washington, D.C., 60, 45-55.

Fryer, P., and M. Mottl, Lithology, Mineralogy, and Origin of Serpentine Muds recovered from Conical and Torishima forearc seamounts: Results of Leg 125 Drilling, Proceedings of the Ocean Drilling Program: Scientific Reports, College Station, Texas, 125, in press.

Fryer, P., J. A. Pearce, L. B. Stokking, et al. (1990), in Proceedings of the Ocean Drilling Program: Initial Reports, College Station, Texas, 125.

Fryer, P., K.L. Saboda, L.E. Johnson, M.E. Mackay, G.F. Moore, and P. Stoffers. (1990), Conical Seamount: SeaMarc II, *Alvin* submersible, and seismic reflection studies, in Proceedings of the Ocean Drilling Program: Initial Reports, College Station, Texas, 125, 69-80.

Fryer, P., and N.C. Smoot, (1985), Morphology of ocean plate seamounts in the Mariana and Izu-Bonin subduction zone, Marine Geology, 64, 77-94.

Haggerty, J. A., (1987a), Cold-water, deep-sea chimneys from the Mariana forearc serpentintite seamounts, EOS, Abstract Trans. Am. Geophys. Union, 68:44, 1534.

Haggerty, J.A. (1987b), Petrology and geochemistry of neogene sedimentary rocks from the Mariana forearc seamounts, in Seamounts, Islands, and Atolls, Geophys. Monogr. Ser., 43, edited by B.H. Keating, P. Fryer, R. Batiza, and G.W. Boehlert, AGU, Washington, D.C., 175-186.

Hsui, A.T., and S. Youngquist, (1985), A dynamic model of the curvature of the Mariana Trench, Nature, 318, (6045), 455-457.

Hussong, D. M. and P. Fryer, (1981), Structure and Tectonics of the Mariana Arc and Forearc: Drillsite selection surveys Leg 60, in Initial Reports of the Deep-Sea Drilling Project, edited by D.M. Hussong and S. Uyeda, U.S. Govt. Printing Off.,Washington, D.C., 60, 33-44.

Hussong, D. M. and P. Fryer, (1985), Forearc tectonics in the northern Mariana arc, in Formation of Active Ocean Margins, edited by N. Nasu, Terra Scientific Publishing Company, Tokyo, 273-290.

Hussong, D.M. and S. Uyeda, (1982), Tectonic processes and history of the Mariana arc: A synthesis of the results of Deep Sea Drilling Program Project Leg 60, in Initial Reports of the Deep-Sea Drilling Project, edited by D.M. Hussong and S. Uyeda, U.S. Govt. Printing Off.,Washington, D.C., 60, 909-929.

Ishii, T., Petrological studies of peridotites from serpentinite diapiric seamounts in the Izu-Bonin and Mariana forearcs, Proceedings of the Ocean Drilling Program: Scientific Reports, College Station, Texas, 125, in press.

Johnson, L.E., (1990), Mariana forearc mafic crustal complex: a pre-emplacement analog to the Coast Range ophiolite, California, EOS Abstract Trans. Am. Geophys. Union, 71, 1648.

Johnson, L.E., and P. Fryer, (1987), The first evidence for MORB-like lavas from the outer Mariana forearc: Geochemistry, Petrography, and Tectonic Implications, EPSL, 100, 304-316.

Johnson, L.E., and P. Fryer, (1988), Oceanic plate material on the Mariana forearc, EOS Abstract Trans. Am. Geophys. Union, 69,1471.

Karig, D.E., (1971), Structural history of the Mariana island arc system, Geol. Soc. Am. Bull., 83, 323-344.

Karig, D.E. and B. Ranken, (1983), Marine geology of the forearc region, southern Mariana island arc, in The Tectonic and Geologic

Evolution of Southeast Asian Seas and Islands. Part 2, Geophys. Monogr. Ser., 27, edited by D.E. Hayes, AGU, Washington, D.C., 266-280.

LaGabrielle, Y., H. Whitechurch, J. Marcoux, T. Juteau, I. Reuben, and F. Guillocheau, (1986), Obduction related ophiolitic polymict breccias covering the ophilites of Antalya (S.W. Turkey), Geology, 14, 734-737.

LaTraille, S.L., and D.M. Hussong. (1980), Crustal structure across the Mariana island arc, in The Tectonic and Geologic Evolution of Southeast Asian Seas and Islands. Part 1, Geophys. Monogr. Ser., 23, edited by D.E. Hayes, AGU, Washington, D.C., 209-222.

Lockwood, J. P., (1971). Sedimentary and gravity slide emplacement of serpentinite, Geol. Soc. Am. Bull., 82, 919-936.

McCabe, R., and S. Uyeda, (1983), Hypothetical model for the bending of the Mariana arc, in The Tectonic and Geologic Evolution of Southeast Asian Seas and Islands. Part 2, Geophys. Monogr. Ser., 27, edited by D.E. Hayes, AGU, Washington, D.C., 291-293.

Michael, P.J., and E. Bonatti, (1985), Petrology of ultramafic rocks from Sites 556, 558, and 560, in the North Atlantic,in Initial Reports of the Deep-Sea Drilling Project, edited by H. Bougault and S.C. Conde et al., U.S. Govt. Printing Off.,Washington, D.C., 82, 523-528.

Mineral Powder Diffraction File: Group Data Book, (1983), JCPOS Internation Centre for Diffraction Data, Swarthmore, Penn.

Moody, J.B., (1976), Serpentinization : A review, Lithos, 9, 125-138.

Mottl, M.J., Pore waters from serpentinite seamounts in the Mariana and Izu-Bonin forearcs, ODP Leg 125: evidence for volatiles from the subducting slab, submitted to Proceedings of the Ocean Drilling Program: Scientific Reports. College Station, Texas, 125, in press.

Mrosowski, C.L., D.E. Hayes, and B. Taylor, (1982), Multichannel seismic reflection surveys of Leg 60 Sites, Deep Sea Drilling Project.,in Initial Reports of the Deep-Sea Drilling Project. edited by D.M. Hussong and S. Uyeda, U.S. Govt. Printing Off.,Washington, D.C., 60, 57-71.

Mumpton, F.A., H.W. Jaffe, and C. S. Thompson, (1965), Coalingite, a new mineral from the New Idria serpentinite, Fresno and San Benito Counties, California, Am. Min., 50, 1893-1913.

Mumpton, F.A., C.S. Thompson, (1975), Mineralogy and origin of the Coalinga asbestos deposit, Clays Clay Min., 23, 131-144.

Phipps, S. P., (1984), Ophilitic olistostromes in the basal Great Valley sequences, Napa County, northern California Coast Ranges, Geol. Soc. Amer. Spec. Pap., 198, 103-125.

Saboda, K.L., P. Fryer, and G. Fryer, (1987), Preliminary studies of metamorphic rocks collected during Alvin studies of Mariana forearc seamounts, EOS Abstract Trans. Am. Geophys. Union, 68:44, 1534.

Uyeda, S., and H. Kanamori, (1979), Back-arc openinig and the mode of subduction, J. Geophys. Res., 84, 1049-1061.

Wenner, D.B. and H.P. Taylor Jr., (1971), Temperatures of serpentinization of ultramafic rocks based on $^{18}O/^{16}O$ fractionation between coexisting serpentine and magnetite, Contrib. Mineralogy and Petrology, 32, 165-185.

Whittaker, E.J.W. and F.J. Wicks, (1970), Chemical differences among the serpentine polymorphs: a discussion, Am. Min., 55, 1025-1047.

Wicks, F. J., (1979), Mineralogy, chemistry and crystallography of chrysotile asbestos, in Short Course Handbook Mineralogical Techniques of Asbestos Determination, edited by R.L. Ledoux, Mineralogical Association of Canada, Quebec, 4, 35-78.

Wicks, F. J., and E.J.W. Whittaker, (1977), Serpentine textures and serpentinization, Can. Min., 15, 459-488.

Wicks, F. J., and J. Zussman, (1975), Microbeam X-ray diffraction patterns of serpentine minerals, Can. Min., 13, 244-258.

Winkler, H.G.F., (1976), Petrogenesis of Metamorphic Rocks, Springer-Verlag, New York, pages 64-95.

# DATE DUE

| | | | |
|---|---|---|---|
| OCT 18 1996 | | | |
| NOV 2 4 1993 | | | |
| | | | |
| | | | |
| | | | |
| | | | |
| | | | |
| | | | |
| | | | |
| | | | |
| | | | |
| | | | |
| | | | |
| | | | |
| | | | |
| | | | |
| | | | |